

**NUMERICAL INVESTIGATION OF  
STAGNATION POINT FLOW OF NON-  
NEWTONIAN FLUID WITH THERMAL  
RADIATION**

**By**

**MAJID RAZZAQ**



**NATIONAL UNIVERSITY OF MODERN LANGUAGES**

**ISLAMABAD**

**July, 2023**

**NUMERICAL INVESTIGATION OF STAGNATION POINT  
FLOW OF NON-NEWTONIAN FLUID WITH THERMAL  
RADIATION**

**By**

**MAJID RAZZAQ**

MSMATH, National University of Modern Languages, Islamabad, 2023

A THESIS SUBMITTED IN PARTIAL FULFILMENT OF  
THE REQUIREMENTS FOR THE DEGREE OF

**MASTER OF SCIENCE**

In Mathematics

To

FACULTY OF ENGINEERING & COMPUTER SCIENCE



NATIONAL UNIVERSITY OF MODERN LANGUAGES ISLAMABAD

© Majid Razzaq, 2023



## THESIS AND DEFENSE APPROVAL FORM

The undersigned certify that they have read the following thesis, examined the defense, are satisfied with overall exam performance, and recommend the thesis to the Faculty of Engineering and Computer Sciences for acceptance.

**Thesis Title:** Numerical Investigation of Stagnation Point Flow of Non-Newtonian Fluid with Thermal Radiation

**Submitted By:** Majid Razzaq

**Registration #:** 09 MS/MATH/S20

Master of Science in Mathematics (MS MATH)  
Title of the Degree

Mathematics  
Name of Discipline

Dr. Aisha Anjum  
Name of Research Supervisor

\_\_\_\_\_  
Signature of Research Supervisor

Dr. Sajid Shah  
Name of Research Co-Supervisor

\_\_\_\_\_  
Signature of Research Co-Supervisor

Dr. Sadia Riaz  
Name of HOD(MATH)

\_\_\_\_\_  
Signature of HOD (MATH)

Dr. Muhammad Noman Malik  
Name of Dean (FE&CS)

\_\_\_\_\_  
Signature of Dean (FE&CS)

July 17, 2023

## AUTHOR'S DECLARATION

I Majid Razzaq

Son of Muhammad Razzaq

Registration # 09 MS/MATH/S20

Discipline Mathematics

Candidate of **Master of Science in Mathematics (MS MATH)** at the National University of Modern Languages do hereby declare that the thesis **Numerical Investigation of Stagnation Point Flow of Non-Newtonian Fluid with Thermal Radiation** submitted by me in partial fulfillment of MS MATH degree, is my original work, and has not been submitted or published earlier. I also solemnly declare that it shall not, in future, be submitted by me for obtaining any other degree from this or any other university or institution. I also understand that if evidence of plagiarism is found in my thesis/dissertation at any stage, even after the award of a degree, the work may be cancelled and the degree revoked.

\_\_\_\_\_  
Signature of Candidate

Majid Razzaq  
Name of Candidate

July 17, 2023

Date

## ABSTRACT

### **Title: Numerical Investigation of Stagnation Point Flow of Non-Newtonian Fluid with Thermal Radiation**

The main objective of this dissertation is to focus on a numerical investigation of stagnation point flow of non-Newtonian fluid with thermal radiation. A mathematical model has been constructed for governs the physical flow condition. A similarity transformation set is used to transform the governing partial differential equations (PDEs) into non-linear ordinary differential equations (ODEs). With the help of the software MATLAB, the shooting technique was employed to produce numerical results. The influence of the governing parameters on the dimensionless velocity, temperature and concentration profile as well as the Biot numbers, Schmidt number and Prandtl number are analyzed. The influence of physical parameters such as Permeable parameter, Stagnation point, Magnetic parameter, Space dependent heat generation parameter, Eckert number, Prandtl number, Radiation parameter, Thermophoresis and Brownian motion parameter, Non-linear chemical reaction parameter, Grashof ratio parameter on the velocity profile, temperature distribution, concentration profile. Skin friction, Nusselt number and Sherwood number coefficient are presented in graphical and tabular forms.

# Contents

|          |  |           |
|----------|--|-----------|
| <b>1</b> | <b>INTRODUCTION</b>  | <b>11</b> |
| <b>2</b> | <b>LITERATURE REVIEW</b>                                   | <b>13</b> |
| <b>3</b> | <b>FUNDAMENTALS TERMS AND EQUATIONS</b>                    | <b>30</b> |
| 3.1      | Definitions . . . . .                                      | 30        |
| 3.1.1    | Fluid . . . . .  | 30        |
| 3.1.2    | Fluid Mechanics . . . . .                                  | 30        |
| 3.1.3    | Fluid Statics . . . . .                                    | 30        |
| 3.1.4    | Fluid Dynamics . . . . .                                   | 30        |
| 3.1.5    | Viscosity . . . . .  | 30        |
| 3.1.6    | Kinematic Viscosity . . . . .                              | 31        |
| 3.2      | Fluid Classifications . . . . .                            | 31        |
| 3.2.1    | Ideal Fluid . . . . .                                      | 31        |
| 3.2.2    | Real Fluid . . . . .                                       | 31        |
| 3.2.3    | Nano Fluid . . . . .                                       | 31        |
| 3.2.4    | Newtonian Fluid . . . . .                                  | 32        |
| 3.2.5    | Non-Newtonian Fluid . . . . .                              | 32        |
| 3.3      | <b>Mechanism and Properties of Heat Transfer</b> . . . . . | 32        |
| 3.3.1    | Heat Transfer . . . . .                                    | 32        |
| 3.3.2    | Conduction . . . . .                                       | 32        |
| 3.3.3    | Convection . . . . .                                       | 32        |
| 3.3.4    | Thermal Radiation . . . . .                                | 33        |
| 3.3.5    | Thermal Conductivity . . . . .                             | 33        |
| 3.3.6    | Thermal Diffusivity . . . . .                              | 33        |
| 3.4      | <b>Types of Flow</b> . . . . .                             | 33        |
| 3.4.1    | Incompressible Flow . . . . .                              | 33        |
| 3.4.2    | Compressible Flow . . . . .                                | 34        |
| 3.4.3    | Steady Flow . . . . .                                      | 34        |
| 3.4.4    | Unsteady Flow . . . . .                                    | 34        |

|          |  |           |
|----------|--|-----------|
| 3.4.5    | Uniform Flow   | 34        |
| 3.4.6    | Non-Uniform Flow   | 35        |
| 3.4.7    | Laminar Flow   | 35        |
| 3.4.8    | Three-dimensional Flow   | 35        |
| 3.4.9    | Rotational Flow  | 35        |
| 3.4.10   | Irrotational Flow  | 35        |
| 3.5      | Magnetohydrodynamics (MHD)   | 35        |
| 3.6      | Continuity Equation  | 36        |
| 3.7      | Momentum Equation  | 36        |
| 3.8      | Energy Equation  | 37        |
| 3.9      | Nondimensional Numbers   | 37        |
| 3.9.1    | Eckert Number  | 37        |
| 3.9.2    | Skin Friction Coefficient  | 37        |
| 3.9.3    | Reynolds Number (Re)   | 37        |
| 3.9.4    | Prandtl Number (Pr)  | 38        |
| 3.9.5    | Sherwood Number (Sh)   | 38        |
| <b>4</b> | <b>CASSON NANOFUID THREE-DIMENSIONAL HYDROMAGNETIC FLOW ANALYSIS USING EXPONENTIALLY STRETCHABLE SHEET</b> | <b>39</b> |
| 4.1      | Introduction   | 39        |
| 4.2      | Problem formulation  | 39        |
| 4.2.1    | Similarity Transformation  | 42        |
| 4.2.2    | Physical Quantities of Interest  | 43        |
| 4.3      | Methodology  | 44        |
| 4.4      | Graphical Discussions and Results  | 45        |
| <b>5</b> | <b>NUMERICAL ANALYSIS OF THERMAL RADIATION WITH STAGNATION POINT ON NON-NEWTONIAN FLUID</b>                | <b>56</b> |
| 5.1      | Introduction   | 56        |
| 5.2      | Problem Formulation  | 56        |
| 5.2.1    | Similarity Transformation  | 58        |
| 5.2.2    | Significant Physical Quantities  | 60        |
| 5.3      | Methodology  | 60        |
| 5.4      | Graphically Discussions and Results  | 61        |
| 5.4.1    | Influence of Casson Fluid Parameter $\beta$  | 61        |
| 5.4.2    | Influence of Parameter of Porosity $k_p$   | 63        |
| 5.4.3    | Influence of Brownian Motion $Nb$  | 65        |
| 5.4.4    | Influence of Thermophoresis Parameter $Nt$   | 66        |
| 5.4.5    | Influence of parameter of Mixed Convection $\lambda$   | 68        |
| 5.4.6    | Influence of Point of stagnation $A$   | 69        |

|          |  |           |
|----------|--|-----------|
| 5.4.7    | Influence of parameter of Suction/ Injection $Q$ . . . . .                   | 71        |
| 5.4.8    | Influence of Radiation Parameter $R$ . . . . .                               | 72        |
| 5.4.9    | Influence of Chemical Reaction $k_c$ . . . . .                               | 73        |
| 5.4.10   | Influence of Spaced Dependent Heat Generation Parameter $\delta^*$ . . . . . | 74        |
| <b>6</b> | <b>CONCLUSIONS AND FUTURE PROPOSE</b>  | <b>77</b> |
| 6.1      | Concluding Remarks . . . . .   | 77        |
| 6.2      | Future Work . . . . .  | 78        |
|          | <b>References</b>  | <b>79</b> |

# List of Figures

|      |  |    |
|------|--|----|
| 4.1  | Flow geometry. . . . .   | 40 |
| 4.2  | Depiction of $M$ on $\tilde{f}'(\tilde{\eta})$ . . . . .                 | 47 |
| 4.3  | Depiction of $M$ on $\tilde{g}'(\tilde{\eta})$ . . . . .                 | 47 |
| 4.4  | Depiction of $\delta$ on $\tilde{f}'(\tilde{\eta})$ . . . . .            | 48 |
| 4.5  | Depiction of $\delta$ on $\tilde{g}'(\tilde{\eta})$ . . . . .            | 48 |
| 4.6  | Depiction of $Pr$ on $\tilde{\theta}(\tilde{\eta})$ . . . . .            | 49 |
| 4.7  | Depiction of $R$ on $\tilde{\theta}(\tilde{\eta})$ . . . . .             | 49 |
| 4.8  | Depiction of $s$ on $\tilde{\theta}(\tilde{\eta})$ . . . . .             | 50 |
| 4.9  | Depiction of $Nb$ on $\tilde{\theta}(\tilde{\eta})$ . . . . .            | 50 |
| 4.10 | Depiction of $Nt$ on $\tilde{\theta}(\tilde{\eta})$ . . . . .            | 51 |
| 4.11 | Depiction of $Ec_x$ on $\tilde{\theta}(\tilde{\eta})$ . . . . .          | 51 |
| 4.12 | Depiction of $Ec_y$ on $\tilde{\theta}(\tilde{\eta})$ . . . . .          | 52 |
| 4.13 | Depiction of $Bi_c$ on $\tilde{\theta}(\tilde{\eta})$ . . . . .          | 52 |
| 4.14 | Depiction of $Bi_t$ on $\tilde{\theta}(\tilde{\eta})$ . . . . .          | 53 |
| 4.15 | Depiction of $S_c$ on $\tilde{\phi}(\tilde{\eta})$ . . . . .             | 53 |
| 4.16 | Depiction of $k_c$ on $\tilde{\phi}(\tilde{\eta})$ . . . . .             | 54 |
| 4.17 | Depiction of $Bi_c$ on $\tilde{\phi}(\tilde{\eta})$ . . . . .            | 54 |
| 4.18 | Depiction of $Nb$ on $\tilde{\phi}(\tilde{\eta})$ . . . . .              | 55 |
| 4.19 | Depiction of $Nt$ on $\tilde{\phi}(\tilde{\eta})$ . . . . .              | 55 |
| 5.1  | Physical model. . . . .  | 57 |
| 5.2  | Depiction of Casson fluid on $\tilde{f}'(\tilde{\eta})$ . . . . .        | 62 |
| 5.3  | Depiction of Casson fluid on $\tilde{g}'(\tilde{\eta})$ . . . . .        | 63 |
| 5.4  | Depiction of Porosity on $\tilde{f}'(\tilde{\eta})$ . . . . .            | 64 |
| 5.5  | Depiction of Porosity on $\tilde{g}'(\tilde{\eta})$ . . . . .            | 64 |
| 5.6  | Depiction of Brownian motion on $\tilde{\theta}(\tilde{\eta})$ . . . . . | 65 |
| 5.7  | Depiction of Brownian motion on $\tilde{\phi}(\tilde{\eta})$ . . . . .   | 66 |
| 5.8  | Depiction of Thermophoresis on $\tilde{\theta}(\tilde{\eta})$ . . . . .  | 67 |
| 5.9  | Depiction of Thermophoresis on $\tilde{\phi}(\tilde{\eta})$ . . . . .    | 67 |

|      |  |    |
|------|--|----|
| 5.10 | Depiction of mixed convection on $\tilde{f}'(\tilde{\eta})$ . . . . .                      | 68 |
| 5.11 | Depiction of mixed convection on $\tilde{g}'(\tilde{\eta})$ . . . . .                      | 69 |
| 5.12 | Depiction of Stagnation point on $\tilde{f}'(\tilde{\eta})$ . . . . .                      | 70 |
| 5.13 | Depiction of Stagnation point for different values on $\tilde{g}'(\tilde{\eta})$ . . . . . | 70 |
| 5.14 | Depiction of Suction/Injection on $\tilde{f}'(\tilde{\eta})$ . . . . .                     | 71 |
| 5.15 | Depiction of Suction/Injection on $\tilde{g}'(\tilde{\eta})$ . . . . .                     | 72 |
| 5.16 | Depiction of Radiation on $\tilde{\theta}(\tilde{\eta})$ . . . . .                         | 73 |
| 5.17 | Depiction of Chemical reaction on $\tilde{\phi}(\tilde{\eta})$ . . . . .                   | 74 |
| 5.18 | Depiction of Spaced dependent heat generation on $\tilde{\theta}(\tilde{\eta})$ . . . . .  | 75 |

# List of Tables

|     |  |    |
|-----|--|----|
| 4.1 | Numerical outcomes of $\tilde{g}''(0)$ , $\tilde{f}''(0)$ , $-\tilde{\phi}'(0)$ and $-\tilde{\theta}'(0)$ for differ values of $k_p = \beta = 0.5, Nt = Nb = 0.5, Pr = 5, Bi_c = Bi_t = 0.1, Sc = 0.6$ , . . . . .   | 46 |
| 5.1 | Numerically results of $-\tilde{\phi}'(0)$ and $-\tilde{\theta}'(0)$ , $\tilde{g}''(0)$ , $\tilde{f}''(0)$ , for differ values of $n = 2.0, \beta_1 = \beta_2 = 0.5, Nt = Nb = 0.5, \delta = 0.1, Q = 2.0, Bi_c = Bi_t = 0.1, \delta^* = 0.1$ , for newtonian fluid. . . . . | 76 |
| 5.2 | Numerically results of $-\tilde{\phi}'(0)$ and $-\tilde{\theta}'(0)$ , $\tilde{f}''(0)$ , $\tilde{g}''(0)$ , for differ values of $n = 2.0, Bi_c = \delta = Bi_t = 0.1, \beta_1 = \beta_2 = 0.5, \delta^* = 0.1, Nb = Nt = 0.5, Q = 2.0$ , for Casson Fluid. . . . .         | 76 |

# LIST OF ABBREVIATIONS

## Abbreviations

|      |                                 |
|------|---------------------------------|
| 3D   | Three Dimensional               |
| MHD  | Magnetohydrodynamics            |
| ODEs | Ordinary Differential Equations |
| PDEs | Partial Differential Equations  |
| IVP  | Initial Value Problem           |
| CFD  | Computational Fluid Dynamics    |
| RK   | Runge-Kutta                     |
| BC   | Boundary Condition              |

# LIST OF SYMBOLS

## Nomenclature

|                                   |   |
|-----------------------------------|---|
| $x, y, z$                         | Cartesian coordinates (m)                                       |
| $\tilde{u}, \tilde{v}, \tilde{w}$ | Velocity components in x, y and z directions respectively (m/s) |
| $B_0$                             | Magnetic field strength (N/mA)                                  |
| $\tilde{C}$                       | Concentration of the solute (kg/m <sup>3</sup> )                |
| $\tilde{T}_\infty$                | Ambient temperature (K)   |
| $\tilde{C}_\infty$                | Ambient concentration (kg/m <sup>3</sup> )                      |
| $\tilde{T}_f$                     | Reference temperature (K)                                       |
| $\tilde{C}_f$                     | Reference concentration (kg/m <sup>3</sup> )                    |
| $q_r$                             | Radiative heat flux (W/m)                                       |
| $S^*$                             | Heat source coefficient   |
| $Ec_x, Ec_y$                      | Eckert Number   |
| $K_c^*$                           | Reaction rate of the solute                                     |
| $K_c$                             | Chemical reaction parameter                                     |
| $M$                               | Magnetic parameter  |
| $R$                               | Radiation parameter   |
| $D_T$                             | Hermophoric diffusion coefficient (m <sup>2</sup> /s)           |
| $D_B$                             | Brownian motion coefficient (m <sup>2</sup> /s)                 |
| $S_c$                             | Schmidt number  |
| $A$                               | Stagnation Point  |
| $Bi_t$                            | Thermal Biot number   |
| $Bi_c$                            | Solute Biot number  |
| $Pr$                              | Prandtl number  |

## **Greek Symbols**

|                  |  |
|------------------|--|
| $\tilde{\eta}$   | Similarity variable                                  |
| $\psi$           | Stream function                                      |
| $\tilde{\theta}$ | Dimensionless temperature                            |
| $\tilde{\phi}$   | Dimensionless temperature                            |
| $\beta$          | Casson fluid parameter                               |
| $\delta$         | Velocity ratio parameter                             |
| $V_f$            | Kinematic viscosity of the fluid (m <sup>2</sup> /s) |
| $\mu_f$          | Dynamic viscosity of the fluid (kg/m s)              |
| $\rho_f$         | Density of the fluid (kg/m <sup>3</sup> )            |

# Acknowledgments

First of all I am thankful to **Allah** Almighty who blessed me with good health and give me the strength to complete this work.

Since my first step in life till now a lot of people guided me through my educational journey, my parents and my teachers in school, my lecturers in university and my supervisor in master degree. So many people have helped me along this journey. It is impossible to name everyone whose effort has allowed me to achieve my goals and dreams.

I am very grateful to my Supervisor **Dr. Aisha Anjum** and Co-supervisor **Dr. Sajid Shah** for their constant support and encouragement during my research work. I have learned a lot from them as a supervisor.

I am also very grateful to my Father **Muhammad Razzaq** and my Brothers **Muhammad Sajjad** and **Muhammad Sajid** for their financial support, because without it, it was not possible for me to continue my studies.

This acknowledgment would be incomplete without expressing my profound feelings to my parents, sisters and brothers who have been a constant source of inspiration and support all through my life.

Finally, I would like to acknowledge my friends and my colleagues in the department who have encouraged me to pursue higher studies.

**Majid Razzaq**

# *Dedication*

**To my Parents, Sisters**

**and**

**Brothers.**

# Chapter 1

## INTRODUCTION

A fluid deforms continuously in response to applied shear force. Fluid is characterized by its inability to withstand applied shear stress and it plays a critical role in many activities of daily life. Examples of fluids include liquids, gases and plasma. Researchers around the world are studying fluid movement in order to gain a deeper understanding of its properties and behavior. The sub-branch of science that investigates the characteristics of fluids is known as fluid dynamics. It provides insights into how forces affect the movement of liquids and it can be used to understand the rotation of blood, the movement of stars, oceans, currents and tectonic plates. Applications of fluid dynamics includes air conditioning systems, jet engines, wind turbines and pipeline lubrication.

Non-Newtonian liquids are a unique class of fluids that exhibit a non-linear relationship between strain rate and shear stress. The first mathematician to study fluid mechanics in depth was Archimedes. Non-Newtonian liquids are used in chemical and petroleum-based processes, including the synthesis of ethanol and gibberellic acid, the extraction of crude oil and the fermentation of syngas. These liquids include polymers, greases, blood, they have a huge range of applications in science, engineering and business. From the first fifteen years of the last century, the proper research of fluid mechanical details has been conducted. Depending on the interaction between the body quantities, such as the relationship between stress and strain, fluid can also be categorized as Newtonian or non-Newtonian fluid. Power-law fluid is the simplest fluid model in this context, however it has limits since it cannot precisely predict the flow parameters in lower and higher Newtonian areas. A single mathematical model cannot account for all the rheological fluid characteristics due to the diversity of flows. There are various liquid models exist which express non-Newtonian liquids. Casson fluid is one of them. The term "Casson

fluid" describes non-Newtonian fluid with yield strain. Human blood may also be regarded as a Casson fluid due to the blood cells' chain-like structure and the contents they contain, which include protein. Consequently, Casson fluid is crucial in both technological and medicinal sectors. Aside from these various applications, it is also employed in the creation of a solid matrix, warm geothermal energy generation, disposal of nuclear waste and reservoirs of petroleum. There are a number of models that have been developed to investigate non-Newtonian fluids, but none of them can fully describe all of the characteristics of the fluid.

The structure of the current dissertation is as follows:

Chapter 2 comprises the review of past published literature. In order to facilitate the readers, fundamental definitions and concepts has been discussed in Chapter 3 . The detailed assessment of Senapati et al. [106] work is covered in Chapter 4 . The numerical study of the Casson nano-liquid flow in three dimensions that is induced by an exponentially stretchy plate is presented in this chapter. A stagnation point motion characteristic are performed considering the non-linear mixed convective and injection/suction influences in this chapter. Casson nanomaterial is utilized to analyze Darcy flow characteristics through stretchable sheet. The heat and mass transportation phenomena are studied using a non-linear chemical process, space-dependent heat source and convective surface conditions. This study also takes into account MHD, radiative, viscous dissipation and joule heating. The similarity transformation was used to convert PDEs to ODEs. The converted ODEs are assessed using the RK-4 approach along with the shooting method [40- 43]. Graphical analysis of dimensionless profiles against involved parameters are provided. The Nusselt and Sherwood parameters as well as the skin friction coefficient are also investigated. Conclusions are contained in Chapter 6.

# Chapter 2

## LITERATURE REVIEW

Casson liquids are a category of non-Newtonian fluids. This type of fluid behaves like a rigid when shear stress is less than the applied tension, but it starts to movement when shear stress is greater than yield stress. Casson fluids are used in bio-medical and mechanical fields, as well as in the solid matrices design, heat geothermal energy production, petroleum reservoirs and disposal of nuclear waste. There are numerous models that are developed to study non-Newtonian materials, However, not only model can account for every characteristics of the fluid. Casson fluids have been studied by researchers such as Casson [1], Prameela *et al.* [2], Khan *et al.* [3], Reddy *et al.* [4], and Alzahrani *et al.* [5].The study of non-Newtonian fluid motion has been extensively researched and there are many notable studies in this field, as cited in references [6-15 ].

The concept of stagnation point refers to a specific surface in flow field where the fluid comes to a state of rest. At this point, the fluid can be described as being in a state of equilibrium and it can provide important information about the fluid's behavior and properties. Another important concept in fluid dynamics is the stagnation point, which refers to a specific surface in the flow field with zero local fluid velocity. There are several significant applications for the research of nanofluid flow beneath the stagnation point, such as the cooling of photoelectric devices by fans, emergency shutdown of atomic reactors, solar receivers and various hydro-dynamic processes. Because of these vital uses, the scientific world has devoted particular attention to stagnation point flow. Stagnation point deals to the flow field specific materia nearly this point the liquid come to at rest. From a functional standpoint, the stagnation point flow to stretched plate is highly beneficial and important. As a result, the stagnation point may be defined as the location in the movement field where the liquid's local velocity at point. The study of nanoliquid flow

that is almost to the point of stagnation has numerous practical applications. A few examples given by the ruling class include the abatement of photoelectric devices by fans, solar receivers, atomic reactors during emergency shutdowns, and various hydrodynamic processes. Because of these vital applications, the scientific world has devoted special attention to stagnation point flow. A liquid's resting place is referred to as a stagnation point. the area where stagnation pressure is currently being monitored. Intriguingly, at this moment, the fluid can only store pressure energy. Even once-flow-efficient objects still have stagnation spots. Similar to flat surfaces, rounded surfaces always have a point of stagnation while a fluid is moving over them. When attempting to achieve optimum efficiency, it is important to decrease the number of potential stagnation sites since they lead to inefficiencies in flow. Stalling points occur where the liquid is brought to rest by the body at the margins of objects in the flow field. Since it is greatest when the velocity is zero, the Bernoulli equation states that the pressure distribution is broadest at places of stagnation. This static pressure is known as the stagnation pressure. The liquid that is measured after an originally moving fluid is completely at rest is known as the stagnation pressure. Despite being stationary, the fluid continues to store mechanical energy via pressure. Numerous practical uses exist for stagnation pressure. Air travel is one of the most popular applications. The stagnation pressure, coupled with a few other measures taken with various instruments, is used to calculate plane velocity, and the Mach number. Similarly, the drag profile, downforce and aerodynamic behaviour in racing may be determined using the stagnation pressure. Measuring the pressure in an industrial context aids in analysing the flow of various fluids. We can see the pressures that rising fluids contain by using the stagnation pressure. The pressurisation profile of a fluid can be determined by measuring the stagnation pressure because measuring static pressure in pipes with fast-moving flows is difficult. As these finished goods have a propensity to shrink or stretch when exposed to their surrounding environment, it is useful in the development of polymer products that are tailored to meet the requirements of the end user, such as packaging, pipeline exterior coatings, and medical equipment. First to present the idea of a two-dimensional stagnation point flow was Hiemenz [16]. The energy equation was added by Eckert [17] to further the work of Hiemenz, and the role of the stagnation point in fluid flow analysis was covered by Sahoo [18]. Other researchers such as Wahid *et al.* [19], Abbasi *et al.* [20], Rehman *et al.* [21], Warke *et al.* [22], Yahaya *et al.* [23], Mehta *et al.* [24], and Akinbo *et al.* [25] have also conducted the studies in this field and reported on the influence of various factors such as dissipative characteristics, activation energy, stretching and Darcy effects in the flow of fluids near the stagnation point. References [26-29] include other

works in this area.

Significant industrial uses also include the extrusion of plastic sheets from dyes or the drawing of elastomers, both of which involve a viscous liquid flowing across a stretched sheet. In these processes, a viscous fluid is flowed over a stretched sheet, and the final product's properties are affected by factors such as the stretching rate, cooling time and approach of stretching. Other technical processes such as wire drawing, hot rolling, and melt-spinning, the manufacturing of optical fibres, the manufacture of plastic and rubber sheets, as well as the cooling in a bath of a huge metallic plate, entail the flow across a stretched surface. In the manufacturing process, sheets and filament made of polymer are continuously extruded dranging from a roller to a die that is a fixed interval away. Through a liquid film, the polymeric sheet creates a constantly having a non-uniform velocity flowing surface [30]. The flow caused by a stretched surface is also used in the continuous casting of metals, glass blowing, and spinning of fibers, and in each of these scenarios, the ultimate product's quality depends on how quickly heat moves over the stretching surface. According to measurements, the velocity of the stretching surface is generally inversely related to the separation from the opening [31]. On various technical processes, the movement of a viscous, elastic medium across a stretched sheet is crucial, extrudate produced by the die often drowns and concurrently stretches into a sheet that is subsequently solidified by quenching and slowly cooled by direct water exposure, particularly in the extrusion of a polymer in a melt-spinning process. Additionally, the flow caused by a stretched surface is utilised in the continuous casting of metals, glass blowing and spinning of fibres. In each of these scenarios, the ultimate product's quality depends on how quickly heat moves over the stretching surface. By stretched an elastomeric flat sheet that flows in it is own plane with velocity that varies linearly with distant from a set point as a result of the application of a uniform stress, Crane [32] addressed the steady 2D incompressible boundary layer movement of liquid. Assesment of the growth of the constant boundary layer movement, heat movement and tiny particle fraction across an exponentially stretchable sheet in a nanofluid is the goal of the current work. He computed the similarity solutions for this problem. A Prandtl number  $Pr$ , a Brownian motion number  $Nb$  and a thermophortic number  $Nt$  are required for this solution. A numeric study is carried out into the local Nusselt and local Sherwood numbers' dependence on these four variables. Other researchers have become interested in finding additional solutions to flow and heat-transportation problems involving stretching or shrinking material as a result of this factor and Crane's (1970) success in developing a closed-form analytical solution for the

movement induced by a stretching plate with a linearly varying velocity in a quiescent liquid. Ashraf and Kamal [33] explored the flow at the stagnation point of an electrically conducting fluid with heat transportation through a porosity surface and magnetic influence. Mohamed *et al.* [34] arrived the numerical analysis of stagnation point movement across stretched plate utilising boundary conditions for convection and Boundary layer for convection movement issues are significant in engineering and commercial activity. Such flows are used to control thermal effects in a variety of industrial outputs, including electronic devices, computer power supplies, and engine cooling systems like radiator heat sinks. A study by Rizwan *et al.* [35] examined how radiation and MHD affected the flow of a nanofluid's stagnation point over a flat sheet. Ibrahim [36] investigated the magnetic field, radiative heat movement, and convective heating impact together with the heat transmission of boundary layer nanofluid movement over a stretched material. Iqbal used heat radiation and fluid dissipation to construct the flow of a stagnation point such that an exponentially stretched surface dictates the flow direction.

The boundary layer is a useful notion in physics and fluid mechanics, where it is defined as the layer of fluid in a closed environment where viscosity has a strong influence. Therefore, the boundary layer can have a significant influence on the behavior of fluid originate in various engineering and industrial manufacturing processes. The boundary layer has been studied extensively in recent decades, due to its wide range of applications in fields such as aeronautics, missile launchers, naval structures, marine equipment, hydraulics, climatology, environmental science, chemical engineering, sanitary engineering, atomic reactors, astrophysics and the flow of gas and liquids in the human body are just a some of the fields where the the boundary layer is defined as the layer of fluid in a closed environment where viscosity has a strong influence. The quantity and variety of concerns posed regarding the behaviour of boundary layers have grown along with the diversity of interests in such layers. This article's goal is to provide for understanding of turbulent boundary layers within a correspondingly more inclusive analytical framework..The area where fluid is flowing, known as the boundary layer, is a critical area of study in fluid dynamics. It is impossible to prevent viscosity variations of 2nd or 3rd orders of magnitude for some fluids when lubrication issues and polymer development are taken into account. Therefore, the fundamental experimentally attained requirement of Newtonian law of viscosity is that fluid viscosity would be permitted to change with shear rate. The issues with boundary layer flow caused by an expanding surface became well-known among numerous scientists. In the course of extrusion, this kind of flow, such as crystal glass fibre and expanding.

The fluid under these circumstances relies on the cooling rate and the speed of stretching. The boundary layer concept was first proposed by Ludwig Prandtl in 1904. The area where the fluid is flowing is the layer known as the boundary layer, where fluid velocity are more prominent. Due to the numerous applications connected to this field that may be found in engineering and industrial manufacturing processes, boundary layer issues related to stretching surfaces have drawn a lot of study interest over the past few decades. The quantity and variety of concerns posed regarding the behaviour of boundry layers have grown along with the diversity of interests in such layers. The phrase boundary layer in computational fluid dynamics relates to a thin layer of moving liquid or gas in contact with a surface, such as the exterior of an aircraft wing or a boundary layer in turbulent flows. There is a variety of velocities around across border from maximum to zero, and the liquid contained in the boundary is susceptible to shearing forces. Only once the fluid makes touch with an object surface does this happen. An aircraft wing's boundary layer ideas are larger towards the trailing edge and thinner at the leading edge. The boundary region movement is typically laminar at the upper or stream and turbulent in the downstream or trailing region. According to the boundary-layer theory, a concrete boundary's velocity can only sustain zero when a genuine fluid is flowing across it. Consequently, the rate rises to the free stream speed if the item travels away from the boundary perpendicularly; this results in a velocity gradient. Since, outer boundary region velocity is the same as and consistent with the flow velocity, there is no velocity gradients beyond the boundary. Laminar, turbulent, and transitional areas make up the boundary region evolution. According to the boundaries layer theory of fluid mechanics, whenever a fluid moves in relation to a surface, the liquid particles nearest to it stick together. The "no-slip requirement" refers to this process of adhesion. This layer then acts as a barrier or opposes the following layer through viscous, slowing it down. This effects the layer above it, and so on. As a result, as an item moves closer to the surface, it passes through layers of fluid with increasing velocities until it reaches a layer where there is no velocity restriction or where the liquid advances into free stream velocity. As a result, the boundary layer is the only place where the true fluid phenomena may occur, which is why an item suffers resistance drag or vice versa. Additionally, the film will keep expanding along the display's length. Because it essentially alters the geometry of the airfoils, the boundary layer is important in aerodynamics. Laminar flow is created when the aerodynamic flow is connected to the aerofoil interface at lower angles of attack. Detached flow is created when the boundary layer flow is separated from the aerofoil surfaces at high angles of attack. When the forces operating on the boundary prevail over the drag force, the boundary becomes divorced

from the aerofoil and flows independently. Boundary layers are created by fluids moving over solid surfaces. The area of the flow that is closest to the surface and where friction slows the travel of air particles is known as the boundary layer. At some distance from the surface, the free-stream velocity takes control because molecules in direct contact with the surface stick to it and slow down their neighbours who are further away. Contrarily, the turbulent boundary layer continuously interchange air between the inside and outside layers; as a result, more air must be forced to reach aircraft speed or a speed near to it by rubbing against the skin. The turbulent boundary layer is a significantly better conductor of channel flow than a laminar one because to a phenomenon known as "momentum exchange." For the application of aerodynamics, boundary layer behaviour is of utmost significance. Free-stream flow that moves quickly is described as being "energetic," sweeping everything in its path. This article's goal is to provide our understanding of turbulent boundary layers within a correspondingly more inclusive analytical framework. In fact, the boundary layer is a useful motion in physics and fluid mechanics, where it is defined as the layer of fluid in a closed environment where viscosity has a strong influence. It is impossible to prevent viscosity variations of two (2) or three (3) orders of magnitude for some fluids when lubrication issues and polymer development are taken into account. Therefore, the fundamental experimentally attained requirement of Newton's law of viscosity is fluid viscosity be permitted to change with shear rate. The issues with boundary region flow caused by an expanding surface became well-known among numerous scientists. In the course of extrusion, this kind of flow, such as crystal glass fibre, etc., and expanding. The fluid under these circumstances relies on the cooling rate and the speed of stretching. The boundary region was first proposed by Ludwig Prandtl in 1904. The first researcher to explore the liquid flow issue with a boundary region over a stretchable sheet was Skiadis [37]. The study of boundary region movement has drawn the interest of numerous scholars. The first person to study boundary layer flow on a flat plate was Blasius [38]. References [39- 43] demonstrated the analysis in this direction.

A type of matter known as a fluid deforms or flows when an external force is applied. Liquids, gases and plasma are all types of fluid. It is a material that has vanishing shear modulus or, more accurately, a material that is unable to withstand applied shear stress. Fluid contain the basic demand for daily life use, due of its significance in many common procedures, researcher in different some world exist are trying to explore differing inside information regarding the flow of fluid. Depending on how two physical properties, especially the connection between

stress and strain, are related to one another, fluids can be further categorised as Newtonian or non-Newtonian fluids. Non-Newtonian liquids are ones in which shear stress and rate of deformation do not have a linear relationship. Fluids that defy Newton's viscosity rule are known as non-Newtonian liquids. Other liquids such as blood, ketchup, paint, shampoo and mud exhibit non-Newtonian behaviour. Numerous sectors, comprising petroleum generation, filters, polymer technology and porcelain making, utilise non-Newtonian fluid. The area of fluid mechanics called fluid dynamics is where we examine liquid flow, in addition to by resolve the causes flow how forces affect the movement of liquids. It offers ways to comprehend the movements of the stars, the ocean, the stream, the geological plate and the spinning of the blood. Heating and cooling systems, jet engines, windfarms and pipeline cleaning are a few significant uses of fluid flows. The very first scientist was Archimedes, the one who specifies systematically the Archimedes about the changeless of fluid and exist deliberate expected the basics of fluid mechanical details. The proper study of liquid mechanical details starts from early fifteenth of one hundred years. Fluid may be categorized further as a Newtonian or non-Newtonian liquid, with regard to the relationship middle from two points two concerning the body quantities that is, stress and strain. A unique class of heat movement liquids based on nanotechnology called nanofluids is produced by scattering and steadily suspending nanoparticles of ten nanometer-sized typical diameters. In 1995, Choi introduced the name nanofluids to designate this new family of heat transfer fluids based on nanotechnology with improved thermal properties, both superior to the characteristics of both typical particle liquid suspensions and their respective hosting liquids. The purpose of nanoliquids is to get the best thermal characteristics at the lowest concentrations (ideally 1 percent by volume) by uniform separation and providing secure of nanoparticles (preferably ten nm) in host fluids. Understanding how nanoparticles improve energy transmission in liquids is critical to achieving this aim. Many heterogeneity nanomaterials may be produced by combining nanoparticles with base liquids. Nanoparticle substances may comprise acetate, ceramic -  $\text{Al}_2\text{O}_3$ ,  $\text{CuO}$ ,  $\text{Cu}$ , metal carbides -  $\text{SiC}$ , nitrides -  $\text{AlN}$ , metals -  $\text{Al}$ . Additionally, magnetic fluids are specialized nanofluids that make use of the magnetic characteristics of the nanoparticles contained inside. For instance, magnetic liquid rotary seals may be used in a highly diverse variety of applications while requiring minimal maintenance and very little leakage. The nanomaterials in these nanoliquids may exhibit significant bio-medical features since some unique types of nanoparticles exhibit antibacterial or drug-delivery capabilities. The term "nanofluid" refers to a fluid that contains stable colloidal dispersion of extremely small or nanometric metals or ceramic particles. The use of nanofluids to increase heat transfer

and energy efficiency has enormous promise in a variety of industries, including power production, military, microelectronics and medicinal devices. It is common practise to stabilise the nanoparticles of nanofluids using additions like a surfactant or polymer. In order to increase the working liquids' thermal conductivity, nanofluids are ordinary fluids with tiny metal or metallic oxide particles added. The surfactant or polymer molecules attach to the nanoparticles' surfaces and give them good as a result. In many different applications, including paints, coatings, and medicinal formulations, nanofluids are crucial. Nanofluids are becoming more and more used as heat transfer fluids in a range of industrial applications due to their improved thermal conductivity and heat transfer qualities. The base fluids utilized to create heat transfer nanofluids are frequently oil, water and ethylene glycol. Typically, metals, oxides, or carbides are used to make the nanoparticles. The adeptness of separation of heat transfer exists dependent in contact the functioning of warm thermal conductivity of operating fluid, to a degree water, lubricate and ethyl glycol. If a little portion of nanoparticles in the way that (Cu, Ag, TiO<sub>2</sub> and Al<sub>2</sub>O<sub>3</sub>) happen deeply involved with a normal fluid a new category of fluids is obtained which is called nanofluids [44]. Nanofluids metal a new track to innovations in the refinement the characteristics of heat transfer. There happens wide type nanoparticles that happen categorized in accordance with their size, shape, warm and energetic generated power and heat transfer capability. They are containing metals, carbides and oxides. Some exist chosen as nanofibers, nanowires, nanotubes and nano sheets [45]. Nanofluid has various use in related to manufacturing devices, heat exchanger [46]. Drug delivery, medicines, vehicle driven on streets radiators, cooling of heat exchanging equipments, generator oil abate, electronic abate [47]. The diameter of the abstain nanoparticle differs between 1 to 100nm. Choi [48] used the term "nanofluid" to describe a brand-new kind of fluid. Small (nano size) particles suspended in a base fluid are known as nanofluids. The most common nanoparticles used in nanofluids are carbon nanotubes, carbides, metals, or oxides. These liquids are maked synthetically to have better thermal conductivity than any basic liquids. Utilizing tinyparticles of silver, copper, gold and other metals in the base fluid will boost the thermal conductivity of the nanofluid. Buongiorno [49] conducted research on the element that increases the heat conductivity of nanofluids. He observed that a change in the fluid's thermal conductivity is caused by both the thermophoresis effect and Brownian motion. Additionally, nanofluid can be employed as a coolant in the heavy vehicle and information technology industries. Overall, nanofluid is advantageous in various industrial, biomedical, and sectors that involve using material. Shahzad *et al.* [50] studied nanofluid flow along a horizontal plate in the appearance of an external magnetic field utilizing the Joule

heating effect. Buongiorno gave a thorough analysis of the convective transport mechanism in nanofluid in 2006. He discovered that Brownian diffusion and thermophoresis are the main mechanisms for improving heat transfer, and he came to the conclusion that the enormous temperature changes in the boundary layer zone cause a measurable loss in fluid viscosity, which in turn causes an increase in the coefficient of heat movement. Tiwari and Das [51] in 2007, further devised a model for the examination of nanofluid and heat transfer within a two-sided lid-driven square cavity and analyzed the role of nanoparticle volume fraction.

The discipline of mechanics known as magnetohydrodynamics deals with the elaborated of fluid movement in the presence of an external magnetic field. The relative movement of electrically charged and magnetized materials is reflected by the magnetic field, which is a vector field. Magnetic fields are frequently seen in action in permanent magnets, which pull on magnetic materials and either attract or repel other magnets. The study of magnetic characteristics of electrically conducting fluid is known as MHD. MHD is essential in the magnetic field. Salt water, body tissue, liquid metals and electrolytes comes the ordinary example of magneto fluid. Likewise, a number of functional variables that are uniform in magnetic composition and dependent on fluid confinement and stability. The term magnetohydrodynamics (or MHD) is shortened. The fundamental idea underlying MHD is that magnetic fields may cause a current to flow through a moving conducting field, polarizing the fluid and causing the magnetic field to vary. In 1791 to 1867, "Michael Faraday" made the first investigation of the usage of magnetohydrodynamic power sources while directing a fluid electrical material through a stationary magnetic field. Large-scale the production of electricity with minimal negative environmental effects is possible with MHD power generation. This article will provide an overview of magnetohydrodynamics as well as a discussion of some of its basic concepts. Many areas of physics, including celestial physics, where we shall explore the magnetohydrodynamics of the sun, astrophysics, plasma physics, etc., depend heavily on magnetohydrodynamics. The impact of the magnetic field on the dynamic liquid conducting fluid are the primary focus of MHD physics. Due to its relativistic research, MHD physics has a variety of applications. High electric pulses are generated using a cyclic MHD producer at faraway locations. Let's discuss a few significant Magnetohydrodynamics applications. Macroscopic force balance, equilibria, and dynamics are often addressed using MHD. On large - scale, ideal MHD characterises dynamics rather well. A reliable indicator of plasma stabilization is ideal MHD. The majority of catastrophic instability are unstable in perfect MHD, which is one of the noteworthy findings. It is discovered

that MHD physics is significant in laboratory plasmas, the solar atmosphere, etc. Systems like the solar wind and earth magnetosphere, as well as the inertial range of plasma turbulence and neutron star account by entering, are quite well characterized by MHD. In the vast majority of astronomical plasmas, MHD is a respectable approach. Extensions, nevertheless, are frequently required. Despite being poor at capturing the dynamics of research facility plasmas, MHD is nonetheless a strong predictor of stability. We shall see how the fluid responds at distinct viewpoints in the magnetic field's existence. Numerous authors [52-54] have made significant contributions to the vast research of electrically conducting nanofluids, including work on tube investigations, MHD pumps, MHD producers, and MHD behaviours. The characteristics of viscous dissipation, heat radiation, or thermal response to the boundary layer flow of the nanofluid, as well as the heat transfer coefficient imbedded in porous media, are additional noteworthy factors. This strategy is commonly utilized in oil supplies & geothermal engineering. Ahmad *et al.* [55] analyzed the behaviour of MHD viscous flow over an exponentially stretching plate with radiative effect in a permeable material under the affect of electric field. In the presence of thermal radiation through a permeable material over a linear stretchable plate, Williamson fluid film movement and heat movement was examined by Shah *et al.* [56]. In this study, they reported that an enhance in the permeable limit decreases movement of thin films and the Lorentz force influence the flow of liquid film. Mabood *et al.* [57] award the numerical solution of MHD stagnation point flow of nanofluid based water (Cuand Al<sub>2</sub>O<sub>3</sub>) over a porous surface under the influence of measure of capacity part of nanoparticles, radiations chemical reactions and viscous dissipation. Jang *et al.* [58] presented electrically conductive fluid movement liquids in electric and fields of magnetism is subject of MHD investigation. In MHD micropump, conductive, aqueous solutions are pumped using the Lorentz force. The Lorentz force push the conducting fluid in the MHD micropump's microchannel in a direction that is opposite to both the magnetic and electric fields. In order to find an exact similarity solution to this issue In the presence of a homogeneous magnetic transverse field. Pavlov [59] examined the boundary layer MHD flow of an electrically conducting fluid generated by stretching of a planar elastic surface. In their investigation, Chakrabarti and Gupta [60] looked at the temperature profiles in this boundary layer MHD over a stretched sheet in the absence of uniform suction.

Further classifications of the chemical reaction include homogeneous and heterogeneous processes. The reaction is heterogeneous in the strong compound system. As mentioned by Magyari and Chamkha *et al.* [61], the concentration rate is often dependent on the species itself

in chemical reaction processes. Chamkha and Rashad [62] revealed the impact of chemical reaction on MHD flow in the presence of heat production or absorption by uniform vertical permeable material. The consequences of chemical reaction and radiation on both mass and heat movement with the MHD flow were addressed by Das [63]. They applied the RK-4 procedure numerically. We looked at the Reynolds number, magnetic parameter, Schmidt number and thermophoretic parameter. Thin film flow analysis has gained significant support as a result of its extensive applications in engineering and technology over the past several years. Thin film flow issues are prevalent and wide-ranging, ranging from the unique circumstance of the movement in human lubricant problems to the lungs in industry. It's intriguing to see how structural mechanics, fluid mechanics, and religion combine when researching the applications of thin liquid film flow.

Several well-known applications for liquid films include the extrusion of polymer, metal, striating of food, continual shaping, drawing of elastic sheets, fluidization of devices, exchanges, and chemical treating apparatus. According to Kumar *et al.* [64], knowing the laminar and time-independent motions of a thin film flow over a stretched surface might be useful in a variety of technical, medical, and built-up processes. Jawad *et al.* [65] looked at the unstable horizontal stretched surface, the Darcy-Forchheimer laminar thin film flow with MHD and heat movement is examined. For thin film movement, the impact of heat radiation and velocistic dissipation are also taken into account. Due to its significance in various industrial processes, thin-film flow of diverse fluids has developed into an intriguing and significant topic. Qayyum *et al.* [66] award the processes include the spinning of fibres, the coling of metallic plates, and the extruded of polymers. A fractional assessment of the magneto- hydrodynamic fluid's thin-film steady movement over a permeable stretched material with changeable temperature conductivity and viscosity.

The viscosity of non-Newtonian liquid often depends on shear rate or the history of the shear rate, or else the viscosity is irrespective of shear rate but still displays typical stress differences or other non-Newtonian phenomena. In contrast to a Newtonian liquid, a non-Newtonian fluid has a distinct connection between shear rate and shear stress. A non-Newtonian liquid is homogeneous composition material that continuously deforms under tension or stress, independent of the intensity of the applied force; it is a matter that lacks its own shape and takes on the shape of the mould. Non-Newtonian liquid include a variety of solutes, molten, custard, toothpaste, starch

suspension, corn flour, paint, melted butter, and shampo. When under stress, non-Newtonian fluids alter their viscosity or flow characteristics. When these fluids are suddenly subjected to a force, such as when you strike or jump on them, they may suddenly thicken and behave more like solids, or, in other situations, they may behave differently and become quicker than they were before. The fluids will quickly revert to their original condition when the tension has been released. Non-Newtonian fluids have a huge assortment of engineering and business uses. A fluid having yield strain that is non-Newtonian is pertained to as Casson liquid. Human blood may also be regarded as a Casson fluid due to the blood cells' chain-like structure and the contents they contain, which include protein. Non-Newtonian liquid behaviour across a wide range of natural and technological applications. The concept of a non-Newtonian liquid is followed by a brief overview of various non-Newtonian features. Foams, suspensions, polymer solution, and melts are good illustrations of materials that, in the correct circumstances, display viscoelastic, time-dependent, and viscoplastic behaviour. The many types of non-Newtonian liquid behaviour have been demonstrated using measured findings on real materials. The Casson liquid is so crucial in both technological and medicinal domains. There are several uses for the exploration of non-Newtonian fluid motion in both the presence and exclusion of magnetic field. Examples include the flow of plasma, amalgams made of mercury, liquid elements and alloys, such as gallium at standard temperatures (30°C), and slurries made from nuclear fuel. Other applications include the construction of solid matrix, the production of geothermal heat, the disposal of nuclear waste, and petroleum extraction [67]. To investigate the non-Newtonian fluid, a number of models have been developed, however none of them can fully account for the fluid's characteristics. There is a category of non-Newtonian liquids called Casson liquid. This fluid behaves like when the stress (shear) is very very small than the employed forces because of its enlarge viscosity, which goes to infinity at zero rate of shear. On the other side, the liquid starts to movement if the stress (shear) is much larger than yield type stress. For the first time, Casson introduced the Casson model for various cylindrical particle suspensions. Soup, fruit juice, jelly, honey, and tomato sauce are a few examples of casson fluids. Animasaun *et al.* [68] studied the non-Newtonian Casson liquid flow in a laminar convective boundary layer thermally stabilised across a stretched sheet. Mustafa [69] used a revolving disc to numerically investigate the MHD flow of nanofluid. Heat transfer with MHD Casson liquid flow toward a nonlinear stretching sheet with temperature distribution was reported by Mustafa and Junaid [70]. Pramanik [71] presented heat transporting in the Casson nanofluid movement by taking heat radiation into account.

The Earth's water and air temperature stratified mass motion, which is typically investigated in geoscience, is the most striking example of mixed convection. Transition from laminar is present in many technical devices, which are systems with considerably smaller sizes. We'll use several instances involving channel flows, which are the most normal and frequent scenarios, to illustrate this point. Mixed convection nearly invariably occurs upon heating or cooling of channel walls and at the slow fluid flow rates typical of a flowing fluid. Only in capillaries can one attain complete forced laminar convection. When the buoyancy motion works in a direction opposite to the forced movement, this flow happens. A heated, vertical flat plate with a horizontal flow, such as the surface of a solar energy central receiver, is an illustration of this situation. The boundary layer at the plate rises when the free stream maintains its velocity in imposed direction. In very-high-power-output systems when forced convection is insufficient to disperse all of the required heat, combined forced and natural convection is frequently found. At this juncture, mixing forced and natural convection will frequently produce the desired output. Nuclear reactor technology and various elements of these processes include those of electronic cooling. In recent years, engineering (particularly aerospace and chemical engineering) has taken a particular interest in the concept of mixed convection movement, which is mixture of linked forced and free convection. Such a phenomena may have a variety of implications, including those related to different electrical devices, nuclear reactors, the food industry, energy storage, the age of astronomy, the lubricating phenomenon, fire control, chemical metallurgy, etc. The temperature differential between fluid particles coupled with isothermal stretching discs causes the phenomena of free convection. Forced convection is the phrase used to describe the use of magnetic force in processes of heat movement between stretched discs. The Archimedes number shows how much forced vs spontaneous convection contributes to a mixed convection flow. It is a well-established fact that when the Archimedes number is greater than unity, the phenomena of free convection becomes more dominant than forced convection. They are widely used in a variety of industrial operations, flows produced by heat provided in the presence of transportation processes that happened as a result of chemical reactions attracted the attention of researchers in the contemporary period of science. For simulating such acquiescence, when the movement is thermally fascinated by exothermic wall reaction, Arrhenius kinetics is used. Over a porous flat sheet, Maleque [72] investigated the influence of heat decomposition chemical processes when energy activation is present. This research revealed that the acquired observations might be applied to improve manufacturing and thermal extrusion

systems. Merkin and Mahmood [73] looked at the mixed convection movement on chemically re-active plate for outer movement in the presence of porosity material.

One of the transport processes that combines forced and natural convection flow is mixed convection process. Natural forces, such as buoyancy effects on temperature variations, are responsible for fluid motion in the system, whereas external forces are responsible for liquid motion in forced convection. If the movement of the fluid that is brought about by an external source is referred to as forced convection and the movement of the fluid that is not brought about by an external source is referred to as natural convection. In the recent years, a significant amount of research has been devoted to examining the effects of blockade on mixed convective flow in various cavity types with diverse borders. Many transportation systems, both naturally occurring and in technological applications are use in mixed convective flow. Industrial and technological procedures that use wind-exposed solar receivers as well as fans to cool electronic devices and nuclear reactors in the case of a sudden shutdown. With regard to mass exchange and Hall influence by Abo-Eldahab *et al.* [74] researched the megneto-hydrodynamic free temperature movement.  $\hat{A}$  flow across a semi-infinity verticaly strip. Hall current and Ohmic heating have a consequence on the boundary layer of mixed convection. The effects on the flow of a micropolar fluid from a circular cone with a power-law fluid at permeable stretched wall were examined by Abo-Eldahab *et al.* [75]. Salem and El-Aziz [76] talked about the affects of Hall a chemical reaction with current on the hydromagnetic movement of a vertical stretchable planes with inner temperature absorption. The mixture of free and forceful convection is knownas mixed (combined) convection. The earlier research shown that the combined convection flow at a stagnation point offers a variety of applications in various industrial issues. Regarding boundary layer flow with mixed convection and an insulated vertical plate in the presence of changeable physical features and continual free flowing, Santhi *et al.* [77] surveyed the situation. In each of the opposing and aiding drift portions, he also examined flow capacity. Subhashini *et al.* [78] proposed the description of the mixed flow of convection of a base fluid in conjunction with a flat channel. When investigating convective heat flow, it is typical to find in the literature that the issue is handled as either pure forced convection or pure free convection. In contrast, mixed convection, which combines forced and free convection, finds uses in both nature and engineering, including heating systems, electronic items, and atmospheric layer at surface fluxes. Vertical plates [79], inclined plates [80], and horizontal plates [81] have all been the subject of studies on mixed convection in laminar layer at surface flow. In the majority of

cases, the complete examination has been dominated by forced convection under the impact of comparatively weak to moderately strong buoyancy forces. Muhammad *et al.* [82] looked at in extremely high output devices when the forced convection is insufficient to disperse all of the necessary heat, mixed convection (forced + natural convection) is commonly observed. At this stage, combining forced and natural convection will generally produce the best results. The usage of nuclear reactor architecture and a few components of electronic cooling are two examples of these techniques. The difference in the concentration and temperature for mixed convective flow produces buoyant forces. These fluxes are significant in several industrial applications. For difficult engineering issues, the combined affects of mass and heat transmission in mixed convection flows are of remarkable significance. A porous stretched surface with transposal. of heat employing slip affects has been suggested by Mukhopadhyay [83] in time-dependent mixed convection fluid flow. The author of this work numerically addressed the modelled issue and found that increasing the unsteadiness parameter resulted in a commensurate decrease in both temperature and velocity. Convective boundary conditions were used by Hayat *et al.* [84] to study mixed convection flow across a stretched sheet. The authors of this study have examined numerical estimates for the Nusselt number and skin friction. They have also compared their findings to previously proposed solutions in the literature. Using Dufour and Soret effects, Turkyilmazoglu [85] has analytically investigated solutions for mixed convection heat movement of electrically conducting, viscous liquid flowpast a stretched wall.

Heat and mass movement have several industrial uses. Petrochemical refinement and fractional distillation, in which a portion of oil production is separated are examples of applications for mass transfer. Many development environments, including a variety of industrial drying applications, such as the manufacturing of construction materials such as concrete, bricks, and gypsum board, as well as food manufacturing, are interested in convective temperature and mass transportation from porous materials. The great bulk of these energy-intensive drying processes still take place via convection. In order to increase processing efficiency, the drying process must be optimised. In essence, mass transfer is a key component of any refinement process. Similar to how it is used in food processing, snack foods, and chemical manufacturing for batch reactors and continuous processes, heat transfer is also used in the cement and asphalt industry for concrete heated and hot mix paving, as well as in manufactral washer for flat team generators and work ironers. The concept of temperature and mass transmission over a stretched sheet is utilized in so many different sectors, including the manufacturing of fibreglas,

aerodynamic extrusion of plastic sheets, glass blowing, etc. In each of these applications, the rate of heat transportation at the stretchable surfaces has a major effect on the quality of final product. Many writers have written about heat and mass transfer as well as its uses, including Raju *et al.* [86]. Physically, micropolar fluids typically present fluids with stiff, randomly distributed (or spherical) dispersed in a viscous medium without consideration for the deform of the particles. Currently, micropolar fluids are the focus of most study because of their versatility in applications such as viscoelastic fluids, liquid crystals, and chemical droplets. Due to its numerous industrial uses, such as the fact that combustion devices must withstand extremely high temperatures, the transport of heat and mass susceptible to thermal radiation has emerged as the most well-liked field of study. Internal combustion engines, the burning of liquid propellants, and liquid rocket exhaust plumes are a few further uses. Mansour *et al.* [87] reviewed the applications of the transference of both heat and mass on MHD layer at surface movement. Using a micropolar liquid, the influence of MHD viscous dissipation free convection movement along a nonisothermal wall were addressed.

Any substance with atoms and molecules in it has the capacity to transport heat. At any one time, the atoms are moving in a variety of ways. Every substance possesses this thermal energy, which is created by the movement of molecules and atoms. The amount of temperature energy increases with the amount of molecular stirring. However, in terms of heat transfer, all that is meant is the action of moving temperature from a body that is warm to one that is Freezing. There are several methods for heat to go from one area to another. Conduction, convection, and radiation are some of the many types of heat transport. If there is a temperature difference between the two systems, heat will still find a way to pass from the higher to the lower system. A region with more kinetic energy is moved toward a region with less kinetic energy to transfer thermal energy. When high-speed and slow-moving particles collide, the slow-moving particles gain kinetic energy. This common type of heat transmission occurs when two objects physically touch. Conduction also goes by the terms thermal conduction and thermal conduction. Convection is the movement of liquid molecules from higher temperature regions to lower temperature regions. Boiling water is a good example of convection because the molecules move in a circular pattern, heating the water as the less dense ones go upward and the denser ones flow downward warm water near the equator travels away from it whereas cooler water in the poles does the reverse. Convection helps warm-blooded animals' bodies circulate blood, which regulates body temperature. Thermocouples are devices used to measure heat radiation

movement. A thermocouple is used to measure the temperature. Errors may arise when using radiant heat transfer to monitor temperature using this device. One doesn't have to look very far to find examples of heat transfer's practical uses in engineering systems and other spheres of daily life. For reactor engineers as well as all other engineers, understanding heat transport processes is crucial. A nuclear power plant is similar to a standard thermal power plant, with one exception. The building's heat source is a nuclear reactor. As is customary in all conventional thermal power plants, the heat is used to produce steam that powers a steam turbine connected to a generator that produces electricity. Reactors in nuclear power plants, however, generate a tremendous quantity of heat in a tiny space. Energy generation has a very high density, which places a strain on the heat transport system. As a result, we must begin with the production and evacuation of heat from the reactor. Hawart researched various solutions of the Blasius flat plate issue [88]. The enhance in radiation parameter causes a reduction in boundary region thickness. The figurative consequences of both Brownian motion and thermophoresis were explored by Sheikholeslami *et al.* [89]. The heat transportation and constant MHD movement in an electrically guarded rectangle pipe in the presence of the attractive field were statistically studied by Chutia and Deka [90]. Kelson *et al.* [91] looked into the implications of an angled magnetic field on liquid flow. Through their research, they revealed that the injection variable has a major influence on the plate's surface temperature when thermal slip or hydrodynamic suction are involved. Lee *et al.* [92] were investigated the creation and preservation of flow structures continue to be fundamental issues in fluid mechanics, as shown by experimental and computer investigations of wall-bounded flows. The topics of transition and turbulence in boundary layers have been extensively studied and reviewed. Guo *et al.* [93] discussed the planetary boundary layer, which is the stratosphere layer closest to the surface, regulates the vertically interchange of heat, moisture, momentum and pollutants in the air between the surface of the Earth and the free airspace. Sensible heat flux, frictional drag, evaporating and flow modulation are only a few of the elements that have a big impact on boundary film thickness and are crucial for weather, climate, and quality of air.

# Chapter 3

## FUNDAMENTALS TERMS AND EQUATIONS

### 3.1 Definitions

In order to continue the work for the following chapters, some few fundamental terms, terminologies, and basic laws are provided in this chapter.

#### 3.1.1 Fluid

A material that continuously deforms in response to applied shear stress called fluid.[94]

#### 3.1.2 Fluid Mechanics

A science field that is concerned with the characteristics of both static and flowing liquids.[95]

#### 3.1.3 Fluid Statics

The investigation of liquids that are at rest.[96]

#### 3.1.4 Fluid Dynamics

One branch of research that examines pressure distribution for moving fluids is liquid dynamics.[96]

#### 3.1.5 Viscosity

Fluid's viscosity is a characteristic that makes it challenging for one liquid to pass over an adjacent liquid. Viscosity is shows  $\tau$  . Mathematically form,

$$\tilde{\tau} \propto \frac{d\tilde{u}}{dy}, \quad (3.1)$$

or

$$\tilde{\tau} = \mu \frac{d\tilde{u}}{dy}, \quad (3.2)$$

The symbol  $\frac{d\tilde{u}}{dy}$  stands for the rate of shear strain. where the proportion constant  $\mu$ , commonly known as mu and sometimes referred to as the fluid viscosity co-efficient or simply viscosity, is present.[96]

### 3.1.6 Kinematic Viscosity

The link between dynamic viscosity and density is defined kinematic viscosity. The symbol for it is  $\nu$ .

Mathematically,

$$\nu = \frac{\text{viscosity}}{\text{density}} = \frac{\mu}{\rho}, \quad (3.3)$$

where  $\rho$  represents the density.[96]

## 3.2 Fluid Classifications

### 3.2.1 Ideal Fluid

The liquid is viscous-free. Ideal liquid is known as ( $\mu = 0$ ). Inviscid fluid is another name for it. Since the viscosity of a perfect fluid is diminishing, shear force does not exist.[97]

### 3.2.2 Real Fluid

A fluid with some viscosity influence is referred to as a genuine liquid or a viscous liquid if its  $\mu$  value is greater than 0.[97]

### 3.2.3 Nano Fluid

The nanofluid is the uniform mixture of the base fluid with nanomaterials. To attain high thermal characteristics at the lowest concentration is the goal of the nanofluid.[97]

### 3.2.4 Newtonian Fluid

A fluid is said to be Newtonian if the shear stress and gradients of velocity are directly relevant and linearly. Mathematically,

$$\tau_{yx} = \mu \frac{d\tilde{u}}{dy}, \quad (3.4)$$

where  $\mu$  is the dynamic viscosity and  $\tau_{yx}$  stands for shear stress. The typical examples of Liquids are silicon, oxygen gas, water and air.[97]

### 3.2.5 Non-Newtonian Fluid

Fluids with no inverse relationship between shear stress and deformation rate. Mathematically,

$$\tau_{yx} = \left(\frac{d\tilde{u}}{dy}\right)^m, m \neq 1, \quad (3.5)$$

$$\tau_{yx} = \mu \left(\frac{d\tilde{u}}{dy}\right)^m, \quad (3.6)$$

where  $m$  is an indicator of flowing performance and  $\mu$  stands for viscosity. Shampoo, grease, blood, and melt polymer are a few examples of these liquids.[97]

## 3.3 Mechanism and Properties of Heat Transfer

### 3.3.1 Heat Transfer

Heat transfer happens when a temperature difference allows thermal energy to flow from one point to another within a material or from one material to another.[98]

### 3.3.2 Conduction

Its a process by which thermal energy transport in direct physical contact of atoms and molecules. [98]

### 3.3.3 Convection

Convection need a medium, just like conduction does,unlike radiation. Convection, on the other hand, involves the heated fluid actually moving, whreas conduction involves the heat being transmitted from one molecule to another. Cold air in its path is either removed or displaced as its flows. Convection current is the term used to describe the flow of hot fluid in this scenario.[98]

### 3.3.4 Thermal Radiation

Electromagnetic waves are the carrier of thermal energy this process is called radiation.[98]

### 3.3.5 Thermal Conductivity

The Fourier thermal equation states that the relationship between heat flow and temperature difference is linear. Thermal conductivity is a characteristic of materials that determines the coefficient of proportionality. Mathematically,

$$K = -\frac{Q}{A} \cdot \frac{dx}{dT}, \quad (3.7)$$

here,  $A$ ,  $K$ ,  $Q$ ,  $\frac{dT}{dx}$ , signify rate of heated movement, Thermal conductivity, areas, and changeable temperature.[98]

### 3.3.6 Thermal Diffusivity

Thermal diffusivity is the connection between heat conduction and density times heat capacity. Mathematically,

$$\alpha = \frac{k}{\rho C_p}, \quad (3.8)$$

where,  $\alpha$  represents thermal diffusivity,  $k$  shows thermal conductivity,  $C_p$  elaborate specific heat, and  $\rho$  shows density.[99]

## 3.4 Types of Flow

### 3.4.1 Incompressible Flow

Incompressible movement defined as flow when the fluid does not vary during the flow. Mathematically it is expressed as;

$$\rho(x; y; z; t) = c.$$

where  $c$  is constant.[100]

### 3.4.2 Compressible Flow

A compressible flow is branch of fluid mechanics which varies significant changes during the fluid flow used in high-speed jet engines, aircrafts, rocket motors also in high-speed usage in a planetary atmosphere, gas pipelines and in commercial fields. Mathematically it is expressed as;

$$\rho(x; y; z; t) \neq c.$$

where 'c' is a constant.[100]

### 3.4.3 Steady Flow

A steady flow is characterised as one that remains constant throughout time. Mathematically can be written as:

$$\frac{d\tilde{\eta}^*}{dt} = 0, \quad (3.9)$$

here,  $\tilde{\eta}^*$  shows the liquid property.[100]

### 3.4.4 Unsteady Flow

The flow which continuously changes with respect to time is called unsteady flow. Mathematically, it can be written as

$$\frac{d\tilde{\eta}^*}{dt} \neq 0$$

Where  $\tilde{\eta}^*$  represents fluid property.[100]

### 3.4.5 Uniform Flow

Uniform flow is described as the flow when velocity and hydro-dynamic characteristics do not vary from one place to another place at any time, having same direction and megnitude during the liquid motion. Mathematically, it can be expressed as

$$\frac{\partial \tilde{v}}{\partial s} = 0$$

where  $\tilde{v}$  is the velocity and  $s$  is the displacement.[100]

### **3.4.6 Non-Uniform Flow**

When the velocity and hydrodynamic characteristics vary from one place to another and the velocity is not constant at all points of the fluid at once, the flow is said to be non-uniform. Mathematically, it can be expressed as

$$\frac{\partial \tilde{v}}{\partial s} \neq 0$$

where  $\tilde{v}$  is the velocity and  $s$  is the displacement.[100]

### **3.4.7 Laminar Flow**

When liquid particles move in definite or predictable routes without interruption from one another.[100]

### **3.4.8 Three-dimensional Flow**

Three-dimensional flow is referred to when the stream's lines of flow are shown as curves.[100]

### **3.4.9 Rotational Flow**

A form of flow called rotational flow involves the movement of fluid particles about their own axes as they travel along streamlines.[94]

### **3.4.10 Irrotational Flow**

The phrase "irrotational flow" refers to a flow along streamlines in which the fluid particles don't really rotate about their own axes.[94]

## **3.5 Magnetohydrodynamics (MHD)**

It deals with the interplay between magnetic fields and fluids that have electrically conductivity. The essential idea behind MHD is that a magnetic field may induce current in a flowing fluid, polarising the fluid as a result and changing the fluid's velocity.[101]

### 3.6 Continuity Equation

The entire mass of the system is conserved according to the mass conservation law, often known the continuity equation. Mathematically, it can be written as:

$$\frac{\partial \rho}{\partial t} + \nabla \cdot (\rho \tilde{V}) = 0. \quad (3.10)$$

Since time moves at a constant pace in a stable state, the continuity equation is:

$$\nabla \cdot (\rho \tilde{V}) = 0 \quad (3.11)$$

Since density does not change in the case of incompressible flow, mathematically:

$$\nabla \cdot \tilde{V} = 0, \quad (3.12)$$

here,  $\tilde{V}$  is a velocity region.[102]

### 3.7 Momentum Equation

For every fluid, following equation define as momentum conservation:

$$\nabla \cdot [(\tilde{V} \rho) \tilde{V}] + \frac{\partial}{\partial t} (\rho \tilde{V}) = \rho \tilde{g} + \nabla \cdot \tilde{T}^*, \quad (3.13)$$

for  $\tilde{T}^* = -pI + \tau$ , the previous equation becomes:

$$\nabla \cdot (-pI + \tau) + \rho \tilde{g} = \rho \left( \frac{\partial \tilde{V}}{\partial t} + \tilde{V} \cdot \nabla \tilde{V} \right). \quad (3.14)$$

By performing a dot product computation using basic vectors of an appropriate orthogonal cartesian system, three scalar components can be added to the vector equation to further simply it. If the gravity constant is set to  $\tilde{g} = \nabla_z$ , the above equation may be stated as; here z shows distance from a voluntary reference height in the direction of gravity.

$$\rho \left( \tilde{V} \cdot \nabla \tilde{V} + \frac{D\tilde{V}}{Dt} \right) = \rho \left( \frac{D\tilde{V}}{Dt} \right) = \rho (\tilde{g} \nabla_z) + \nabla \cdot (-pI + \tau), \quad (3.15)$$

here  $\frac{D}{Dt}$  denotes the substantial derivative. A particle enhance when it begins to travel cause to a net force indicated by the gradient of the pressure, viscosity and gravitational forces, according to the momentum equation.[102]

## 3.8 Energy Equation

The energy equation states that the system's overall energy is preserved, in line with the idea of energy conservation.

$$\nabla \cdot \rho \tilde{u} + \frac{\partial \rho}{\partial t} + \nabla \cdot q = Q + \varphi, \quad (3.16)$$

here,  $\varphi$  shows the dissipation impact.[98]

## 3.9 Nondimensional Numbers

### 3.9.1 Eckert Number

This number has no dimensions and is used in continuum mechanics. It describes the connection between movements and the enthalpy difference at layer border and is used to characterise heat dissipation. Mathematically,

$$E_c = \frac{\tilde{u}^2}{C_p \nabla \tilde{T}}, \quad (3.17)$$

where,  $C_p$  represent specific heat.[94]

### 3.9.2 Skin Friction Coefficient

Skin friction refers to the friction that develops between liquid particles and a plate. Mathematically, it is expressed by

$$C_f = \frac{2\tau_0}{\rho \tilde{u}_w^2}, \quad (3.18)$$

where,  $\rho$  expressed the density and  $\tau_0$  shows wall shear stress.[103]

### 3.9.3 Reynolds Number (Re)

Inertial and viscous forces are related. It provides information about how fluid moment behaves. Where,

$$Re = \frac{l\tilde{u}}{\nu} \quad (3.19)$$

here  $l$ ,  $\tilde{u}$ , and  $\nu$  elaborate the maximum velocity, kinematic viscosity and length.[104]

### 3.9.4 Prandtl Number (Pr)

Prandtl number refers to this proportion of momentum to heat flux. Mathematically,

$$Pr = \frac{\nu}{\alpha} = \frac{\mu c_p}{k}, \quad (3.20)$$

where,  $\alpha$ ,  $\nu$ , are shows the momentum diffusivity and thermal diffusivity.[104]

### 3.9.5 Sherwood Number (Sh)

The Sherwood number, often referred to as the mass transported Nusselt number, is a dimensionless number utilized in mass transport processes. It shows the ratio of diffusivity mass transportation rate to convective mass transport. Mathematically, it is defined as

$$S_h = \frac{h}{D} = \frac{(\text{Convective mass transfer rate})}{(\text{Diffusion rate})},$$

where  $L$  represent length characteristic,  $D$  shows mass diffusivity and  $h$  revealed convective mass transfer coefficient.[105]

# Chapter 4

## CASSON NANOFLUID THREE-DIMENSIONAL HYDROMAGNETIC FLOW ANALYSIS USING EXPONENTIALLY STRETCHABLE SHEET

### 4.1 Introduction

In this study, an exponentially stretchable plate used to investigate the three-dimensional hydromagnetic Casson nanofluid in a permeable media. The heat transpotation phenomenon is analyzed by considering heat-dependent generation and the joule heating, as well as the impacts ofthermally radiation and viscous dissipation. The analysis of heat and mass transport is further enriched by incorporating chemical reactions and convective boundary conditions for both thermal and solutal factors. By using appropriate variables,the shooting method is used to resolve the converted non-linear differential equations. The impact of different parameters on temperature, concentration and velocity is analyzed and illustrated graphically. Additionally, this chapter includes a review of a previous study by Senapati et al. [106].

### 4.2 Problem formulation

This study investigates the steady three-dimensional hydro-magnetic flow of Casson nanofluid affected by an exponentially stretchable wall in a porosity material. The plate is located on the cartesian plan and z-axis is normal to it. Sheet stretched exponentially in x and y directions. A magnetic region is applied in the normal direction as shown in (Figure 4.1) which creates resistance in the fluid's motion. The governing equation for the incompressible Casson fluid is given as:

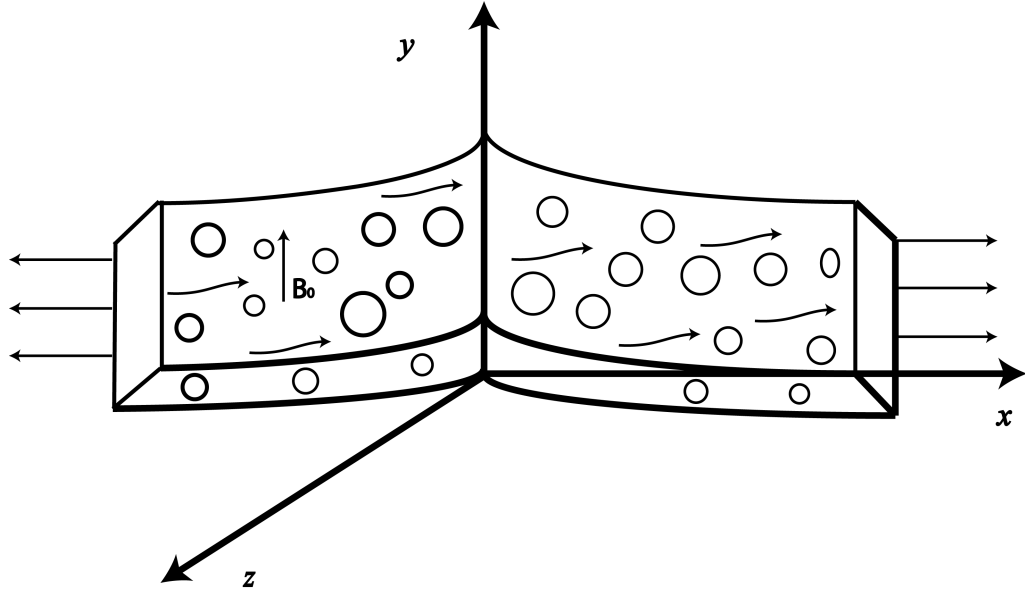


Figure 4.1: Flow geometry.

$$\tau_{ij} = \begin{cases} 2(\mu_\beta + \frac{p_y}{\sqrt{2\pi}})e_{ij}, \pi > \pi_c, \\ 2(\mu_\beta + \frac{p_y}{\sqrt{2\pi}})e_{ij}, \pi < \pi_c, \end{cases} \quad (4.1)$$

Here,  $\pi_c$  for the product's critical values based on the non-Newtonian fluid,  $e_{ij}$  shows for the (i,j)th components of the deformation rate,  $\pi$  for the product of the deformation rate component with itself,  $\mu_\beta$  for the plastic absolute solution,  $p_y$  for fluid yield stress. Now

$$\tau_{xz} = \frac{\partial \tilde{w}}{\partial x} \text{ and } \mu_\beta \left( \frac{\partial \tilde{w}}{\partial x} + \frac{\partial \tilde{u}}{\partial \tilde{v}} \right) \left( 1 + \frac{1}{\beta} \right) = 0, \quad (4.2)$$

where the Casson fluid parameter  $\beta = \mu_\beta \sqrt{\frac{2\pi_c}{p_y}}$  is shown.

The above assumptions, governing equations are expressed as follows:

$$\frac{\partial}{\partial x}(\tilde{u}) + \frac{\partial}{\partial y}(\tilde{v}) = -\frac{\partial}{\partial z}(\tilde{w}), \quad (4.3)$$

$$\tilde{u}\frac{\partial}{\partial x}(\tilde{u}) + \tilde{v}\frac{\partial}{\partial y}(\tilde{u}) + \tilde{w}\frac{\partial}{\partial z}(\tilde{u}) = \nu_f(1 + \frac{1}{\beta})\frac{\partial^2\tilde{u}}{\partial z^2} - \frac{\nu_f\tilde{u}}{k_p^*} - \frac{\sigma B_0^2\tilde{u}}{\rho_f}, \quad (4.4)$$

$$\tilde{u}\frac{\partial}{\partial x}(\tilde{v}) + \tilde{v}\frac{\partial}{\partial y}(\tilde{v}) + \tilde{w}\frac{\partial}{\partial z}(\tilde{v}) = \nu_f(1 + \frac{1}{\beta})\frac{\partial^2\tilde{v}}{\partial z^2} - \frac{\nu_f\tilde{v}}{k_p^*} - \frac{\sigma B_0^2\tilde{v}}{\rho_f}, \quad (4.5)$$

$$\begin{aligned} \tilde{u}\frac{\partial}{\partial x}(\tilde{T}) + \tilde{v}\frac{\partial}{\partial y}(\tilde{T}) + \tilde{w}\frac{\partial}{\partial z}(\tilde{T}) &= \alpha_f\frac{\partial^2\tilde{T}}{\partial z^2} + \frac{(\rho c)_p}{(\rho c)_f}\left[\frac{D_T}{\tilde{T}_\infty}\left(\frac{\partial\tilde{T}}{\partial z}\right)^2 + D_B\frac{\partial\tilde{C}}{\partial z}\frac{\partial\tilde{T}}{\partial z}\right] \\ &+ \frac{\sigma B_0^2}{(\rho c)_f}(\tilde{u}^2 + \tilde{v}^2) - \frac{1}{(\rho c)_f}\left(\frac{\partial q_r}{\partial z}\right) + \frac{\mu_f}{(\rho c)_f}\left(1 + \frac{1}{\beta}\right)\left[\left(\frac{\partial\tilde{u}}{\partial z}\right)^2 + \left(\frac{\partial\tilde{v}}{\partial z}\right)^2\right] + \\ &\frac{s^*}{(\rho c)_f}(\tilde{T} - \tilde{T}_\infty), \end{aligned} \quad (4.6)$$

$$\tilde{u}\frac{\partial}{\partial x}(\tilde{C}) + \tilde{v}\frac{\partial}{\partial y}(\tilde{C}) + \tilde{w}\frac{\partial}{\partial z}(\tilde{C}) = D_B\frac{\partial^2\tilde{C}}{\partial z^2} - k_c^*(\tilde{C} - \tilde{C}_\infty) + \frac{D_T}{\tilde{T}_\infty}\frac{\partial^2\tilde{T}}{\partial z^2}. \quad (4.7)$$

The corresponding boundary conditions are as follows:

$$\left. \begin{aligned} -D_m\left(\frac{\partial\tilde{C}}{\partial z}\right) &= h_m(\tilde{C}_f - \tilde{C}), \tilde{u} = \tilde{U}_w = \tilde{U}_0 e^{\frac{x+y}{L}}, \\ \tilde{v} = \tilde{V}_0 e^{\frac{x+y}{L}}, -k_s\left(\frac{\partial\tilde{T}}{\partial z}\right) &= h_f(\tilde{T}_f - T), \tilde{w} = 0, \text{ at } z=0, \\ \tilde{v} \rightarrow 0, \tilde{u} \rightarrow 0, \tilde{C} \rightarrow \tilde{C}_\infty, \tilde{T} \rightarrow \tilde{T}_\infty, &\quad \text{at } z \rightarrow \infty. \end{aligned} \right\} \quad (4.8)$$

Here,  $\tilde{u}$ ,  $\tilde{v}$  and  $\tilde{w}$  stands for the components of velocity.  $s^*$  denotes the heat source coefficient,  $D_T$  represent the thermophoretic diffusion coefficient, The porosity parameter is  $K_{p^*}$ , radiational heat flow, Electric conductivity is represented by  $q_r$  and  $\sigma$ , applied magnetic strength is represented by  $B_0$ , density is represented by  $\rho_f$ , and thermal conductivity is represented by  $k_f$ . The Brownian diffusion coefficient is represented by  $D_B$ . The ambient temperature is represented by  $\tilde{T}_\infty$ . Heat and mass transport coefficients are  $h_s$  and  $h_m$ . Temperature and concentration of a suspended fluid are represented by  $\tilde{T}$  and  $\tilde{C}$ , respectively.

## 4.2.1 Similarity Transformation

Making use of:

$$\left. \begin{aligned} \tilde{v} &= \tilde{V}_0 e^{\frac{x+y}{L}} \tilde{g}'(\tilde{\eta}), \tilde{u} = \tilde{U}_0 e^{\frac{x+y}{L}} \tilde{f}'(\tilde{\eta}), \\ \tilde{w} &= -\sqrt{\frac{\nu_f \tilde{U}_0}{2L}} e^{\frac{x+y}{2L}} [\tilde{g}(\tilde{\eta}) + \tilde{\eta} \tilde{g}'(\tilde{\eta}) + \tilde{f}(\tilde{\eta}) + \tilde{\eta} \tilde{f}'(\tilde{\eta})], \\ \tilde{\eta} &= z \sqrt{\frac{\tilde{U}_0}{2\nu_f L}} e^{\frac{x+y}{2L}}, \tilde{\theta} = \frac{\tilde{T} - \tilde{T}_\infty}{\tilde{T}_f - \tilde{T}_\infty}, \tilde{\phi} = \frac{\tilde{C} - \tilde{C}_\infty}{\tilde{C}_f - \tilde{C}_\infty} \end{aligned} \right\} \quad (4.9)$$

Following were the governing equations:

$$(\tilde{f} + \tilde{g})\tilde{f}'' - (k_p \tilde{f}' + M \tilde{f}') - 2(\tilde{f}'\tilde{f}' + \tilde{g}'\tilde{f}') = -(1 + \frac{1}{\beta})\tilde{f}''', \quad (4.10)$$

$$(\tilde{f} + \tilde{g})\tilde{g}'' - (k_p \tilde{g}' + M \tilde{g}') - 2(\tilde{f}'\tilde{g}' + \tilde{g}'\tilde{g}') = -(1 + \frac{1}{\beta})\tilde{g}''', \quad (4.11)$$

$$\begin{aligned} Pr[Ec_y \tilde{g}''^2 + Nt \tilde{\theta}'^2 + Nb \tilde{\phi}' \tilde{\theta}' + Ec_x \tilde{f}''^2 + MEc_x \tilde{f}'^2 + MEc_y \tilde{g}'^2 + S\tilde{\theta}] = \\ - [1 + \frac{4}{3}R]\tilde{\theta}'' + pr(\tilde{f} + \tilde{g})\tilde{\theta}', \end{aligned} \quad (4.12)$$

$$\tilde{\phi}'' + \frac{Nt}{Nb} \tilde{\theta}'' - k_c Sc \tilde{\phi} + Sc(\tilde{f} + \tilde{g})\tilde{\phi}' = 0. \quad (4.13)$$

Associated boundary conditions are:

$$\left. \begin{aligned} \tilde{f}'(0) = 1, \tilde{f}(0) = 0, \tilde{\phi}'(0) = -Bi_c[1 - \tilde{\phi}(0)], \\ \tilde{g}'(0) = \delta, \tilde{\theta}'(0) = -Bi_t[1 - \tilde{\theta}(0)], \tilde{g}(0) = 0, \\ \tilde{g}'(\infty) \rightarrow 0, \tilde{f}'(\infty) \rightarrow 0, \tilde{\phi}(\infty) \rightarrow 0, \tilde{\theta}(\infty) \rightarrow 0. \end{aligned} \right\} \quad (4.14)$$

here,  $M$  shows magnetic parameter,  $\beta$  depicts the Casson fluid parameter,  $K_p$  is the porosity parameter,  $R$  shows radiation parameter,  $K_c$  shows chemical reaction,  $Sc$  is Schmidt number,  $Pr$  shows Prandtl number,  $Ec_x$  follows Eckert number,  $\delta$  is the velocity ratio behavior,  $Bi_t, Bi_c$  expressed the Biot number with respect to temperature and concentration  $Nb$  revealed the Brownian motion,  $s$  denote heat generation,  $Nt$  is the thermophoresis.

The parameters involved take the following mathematical form:

$$\begin{aligned}
Pr &= \frac{\nu_f}{\alpha_f}, Ec_x = \frac{\tilde{U}_w^2}{\rho_f(\tilde{T}_f - \tilde{T}_\infty)}, M = \frac{2\sigma B_0^2 L}{\rho_f \tilde{U}_w}, Ec_y = \frac{\tilde{V}_w^2}{\rho_f(\tilde{T}_f - \tilde{T}_\infty)}, \\
k_p &= \frac{2\nu L}{\tilde{U}_w K_p^*}, s = \frac{2s^* L}{\tilde{U}_w e^{\frac{x+y}{L}} (\rho c)_f}, Nb = \frac{(\rho c)_p D_B (\tilde{C}_f - \tilde{C}_\infty)}{(\rho c)_p (\nu)_f}, \delta = \frac{\tilde{v}_0}{\tilde{u}_0}, \\
Sc &= \frac{\nu_f}{D_B}, Nt = \frac{(\rho c)_p D_T (\tilde{T}_f - \tilde{T}_\infty)}{(\rho c)_f \tilde{T}_\infty (\nu)_f}, Bi_t = \frac{h_f}{K_s} \sqrt{\frac{2\nu L}{\tilde{U}_w}}, Bi_c = \frac{h_m}{D_m} \sqrt{\frac{2\nu L}{\tilde{U}_w}}, R = \frac{4\sigma^* \tilde{T}_\infty^3}{kk^*} \quad (4.15)
\end{aligned}$$

## 4.2.2 Physical Quantities of Interest

The physical quantities of importance in this case are skin friction, Nusselt number, and Sherwood number, which are expressed as:

$$\tilde{C}_{fy} = \frac{2\tilde{\tau}_{wy}}{\rho_f \tilde{U}_w^2}, Nu = \frac{\tilde{x} \tilde{q}_w}{k_f (\tilde{T}_f - \tilde{T}_\infty)}, \tilde{C}_{fx} = \frac{2\tilde{\tau}_{wx}}{\rho_f \tilde{U}_w^2}, Sh = \frac{\tilde{x} \tilde{q}_m}{D_B (\tilde{C}_f - \tilde{C}_\infty)}, \quad (4.16)$$

where  $\tilde{\tau}_{wx}, \tilde{q}_w, \tilde{\tau}_{wy}$ , and  $\tilde{q}_m$  represent shear stresses, heat and mass fluxes respectively. Mathematically,

$$\tau_{wy} = \left( \frac{\partial \tilde{v}}{\partial z} + \frac{\partial \tilde{w}}{\partial y} \right)_{z=0} \left( 1 + \frac{1}{\beta} \right) \mu_f, \quad (4.17)$$

$$\tau_{wx} = \mu_f \left( 1 + \frac{1}{\beta} \right) \left( \frac{\partial \tilde{w}}{\partial x} + \frac{\partial \tilde{u}}{\partial z} \right)_{z=0}, \quad (4.18)$$

$$-k_f \left( \frac{\partial \tilde{T}}{\partial Z} \right)_{z=0} = (q_r)_{z=0} + q_w, q_m = -D_B \left( \frac{\partial \tilde{C}}{\partial Z} \right)_{z=0}, \quad (4.19)$$

Without dimensions form:

$$\left( \frac{Re_x}{2} \right)^{\frac{1}{2}} \tilde{C}_{fx} = \left( \frac{\beta}{\beta + 1} \right) \tilde{f}''(0), \quad (4.20)$$

$$\left( \frac{Re_x}{2} \right)^{\frac{1}{2}} \tilde{C}_{fy} = \left( \frac{\beta}{\beta + 1} \right) \tilde{g}''(0), \quad (4.21)$$

$$Nu_x = - \left( 1 + \frac{4}{3} R \right) \left( \frac{Re_x}{2} \right)^{\frac{1}{2}} \tilde{\theta}'(0) \frac{x}{L} \quad (4.22)$$

$$- \sqrt{\frac{Re_x L}{2}} \frac{Sh_x}{x} = \tilde{\phi}'(0) \quad (4.23)$$

### 4.3 Methodology

Here, The computation of the coupled and non-linear governing differential equations (4.10)–(4.13) uses the Runge-Kutta technique of order 4 in conjunction with a shooting system up to  $10^{-5}$  accuracy. With this method, the governing differential equations of the flow are reduced to a set of first-order differential equations.

$$\tilde{f} = y_1; \quad (4.24)$$

$$y_2 = y'_1 = \tilde{f}';$$

$$y_3 = y'_2 = \tilde{f}'';$$

$$\tilde{f}''' = y'_3 = \frac{\beta}{\beta + 1} (2(y_2 y_2 + y_5 y_2) + M y_2 + k_p y_2 - (y_1 y_3 + y_4 y_3)), \quad (4.25)$$

$$\tilde{g} = y_4; \quad (4.26)$$

$$y_5 = y'_4 = \tilde{g}';$$

$$\tilde{g}'' = y'_5 = y_6,$$

$$\tilde{g}''' = y'_6 = \frac{\beta}{\beta + 1} (2(y_2 y_5 + y_5 y_5) - (y_1 y_6 + y_4 y_6) + (M y_5 + k_p y_5)), \quad (4.27)$$

$$\tilde{\theta} = y_7; \quad (4.28)$$

$$y_8 = y'_7 = \tilde{\theta}';$$

$$\begin{aligned} \tilde{\theta}'' = y'_8 = & \frac{-Pr}{(1 + \frac{4}{3}R)} [(y_1 y_8 + y_8 y_4) + N b y_{10} y_8 + N t (y_8^2) + E c_x (y_3^2) + E c_y (y_6^2) \\ & + M E c_x (y_2^2) + M E c_y (y_5^2) + S y_7], \end{aligned} \quad (4.29)$$

$$\tilde{\phi} = y_9; \quad (4.30)$$

$$y_{10} = y'_9 = \tilde{\phi}';$$

$$\begin{aligned} \tilde{\phi}'' = y_{10}' = & -S c (y_1 + y_4) y_{10} + \left( \frac{N t}{N b} \right) \left( \frac{Pr}{(1 + \frac{4}{3}R)} \right) [(y_1 y_8 + y_8 y_4) + N b y_8 y_{10} \\ & + N t (y_8^2) + E c_x (y_3^2) + E c_y (y_6^2) + M E c_x (y_2^2) + M E c_y (y_5^2) + S y_7] + K c S c y_9, \end{aligned} \quad (4.31)$$

Associated initial approximations

$$\left. \begin{aligned} y_1(0) = 0; y_4(0) = 0; y_2(0) = 1; y_5(0) = \delta, \\ y_7(0) = \frac{y_8(0) + B i_t}{B i_t}; y_9(0) = \frac{y_{10}(0) + B i_c}{B i_c} \\ y_2(\infty) \rightarrow 0; y_5(\infty) \rightarrow 0, y_7(\infty) \rightarrow 0, y_9(\infty) \rightarrow 0. \end{aligned} \right\} \quad (4.32)$$

## 4.4 Graphical Discussions and Results

The graphical representation and explanation of rheological features, including velocity, temperature and concentration profiles for involved dimensionless parameters are covered in this section. The engineering parameters are numerically estimated in Table (4.1) against certain predefined values for  $s$ ,  $Ec_y$  and  $\delta$ . Skin friction is seen to rise as Nusselt and Sherwood numbers decline. In Figures (4.2) and (4.3), the influence of the magnetic parameter  $M$  on the velocity field is further explained. Here, we observed a decline in velocity that was dependent on  $M$ . When a magnetic parameter is physically increased, more resistive electromagnetic forces results which eventually cause the velocity field to decay. Additionally, it is observed that Newtonian fluid's velocity is always accelerated by Casson nanofluid. The effects of the velocity ratio parameter  $\delta$  on primary  $f'(\eta)$  and secondary  $g'(\eta)$  velocity changes are shown in Figs. (4.4) and (4.5). In this case, the primary velocity field shows a decrease while the secondary velocity field is intensified by a greater velocity ratio value. Further observation reveals that the momentum diffusivity process in both velocity fields is accelerated by the Casson fluid contribution. In Figures (4.6–4.14), fluid temperature depicts a dominant tendency against greater  $s$ ,  $N_b$ ,  $N_t$ ,  $Ec_y$ ,  $Bi_c$ ,  $R Bi_t$  and  $Ec_x$ , whereas intensification in  $Pr$  resulting in a decrease in temperature because of reduced thermal conductivity. We thus draw the conclusion that other relevant factors possess stronger thermal conductivity properties than  $Pr$ . Additionally, in these figures, Casson fluid reduces the thermal diffusivity process. Schmidt number ( $Sc$ ) characteristics vs concentration field are shown in Fig. (4.15). Because of the low diffusion coefficient, concentration decreases as  $Sc$  increases. In this instance, Casson fluid has a little lower concentration than in the Newtonian example. Due to the fluid molecules' fast velocity, Fig. (4.16) showed that an increasing exothermic reaction decreases the concentration field, whereas an endothermic reaction exhibits the opposite tendency. From Figs. (4.17) to (4.19), it can be seen that higher concentration levels are produced by bigger values of  $N_b$  and  $Bi_c$  (solutal Biot number), but concentration levels are decreased by larger values of  $N_t$ .

| $M$ | $\delta$ | $R$ | $EC_x$ | $EC_y$ | $s$  | $k_c$ | $f''(0)$ | $g''(0)$ | $-\theta(0)$ | $-\phi(0)$ |
|-----|----------|-----|--------|--------|------|-------|----------|----------|--------------|------------|
| 0   | 0.1      | 0   | 0.1    | 0.1    | 0    | 0     | 2.6357   | 0.2636   | 0.0854       | 0.1505     |
| 0.5 |          |     |        |        |      |       | 2.9082   | 0.2909   | 0.0783       | 0.0766     |
| 1.0 |          |     |        |        |      |       | 3.1568   | 0.3157   | 0.0718       | 0.0789     |
|     | 0.5      |     |        |        |      |       | 3.4561   | 1.7281   | 0.0723       | 0.0835     |
|     | 1.0      |     |        |        |      |       | 3.7968   | 3.7968   | 0.0640       | 0.0912     |
|     |          | 0.1 |        |        |      |       | 3.7968   | 3.7968   | 0.0747       | 0.0903     |
|     |          | 0.5 |        |        |      |       | 3.7968   | 3.7968   | 0.1139       | 0.0878     |
|     |          |     | 0.3    |        |      |       | 3.7968   | 3.7968   | -0.0701      | 0.1002     |
|     |          |     | 0.5    |        |      |       | 3.7968   | 3.7968   | -0.0254      | 0.1126     |
|     |          |     |        | 0.3    |      |       | 3.7968   | 3.7968   | -0.0206      | 0.1251     |
|     |          |     |        | 0.5    |      |       | 3.7968   | 3.7968   | -0.0677      | 0.1378     |
|     |          |     |        |        | -0.4 |       | 3.7968   | 3.7968   | -0.0060      | 0.1223     |
|     |          |     |        |        | -0.2 |       | 3.7968   | 3.7968   | -0.0310      | 0.1288     |
|     |          |     |        |        | 0.2  |       | 3.7968   | 3.7968   | -0.1244      | 0.1517     |
|     |          |     |        |        | 0.4  |       | 3.7968   | 3.7968   | -0.2434      | 0.1794     |
|     |          |     |        |        |      | 0.1   | 3.7968   | 3.7968   | -0.2501      | 0.1862     |
|     |          |     |        |        |      | 0.2   | 3.7968   | 3.7968   | -0.2585      | 0.1916     |
|     |          |     |        |        |      | -0.1  | 3.7968   | 3.7968   | -0.2389      | 0.1702     |
|     |          |     |        |        |      | -0.2  | 3.7968   | 3.7968   | -0.2378      | 0.1566     |

Table 4.1: Numerical outcomes of  $\tilde{g}''(0)$ ,  $\tilde{f}''(0)$ ,  $-\tilde{\phi}'(0)$  and  $-\tilde{\theta}'(0)$  for differ values of  $k_p = \beta = 0.5, Nt = Nb = 0.5, Pr = 5, Bi_c = Bi_t = 0.1, Sc = 0.6$ ,

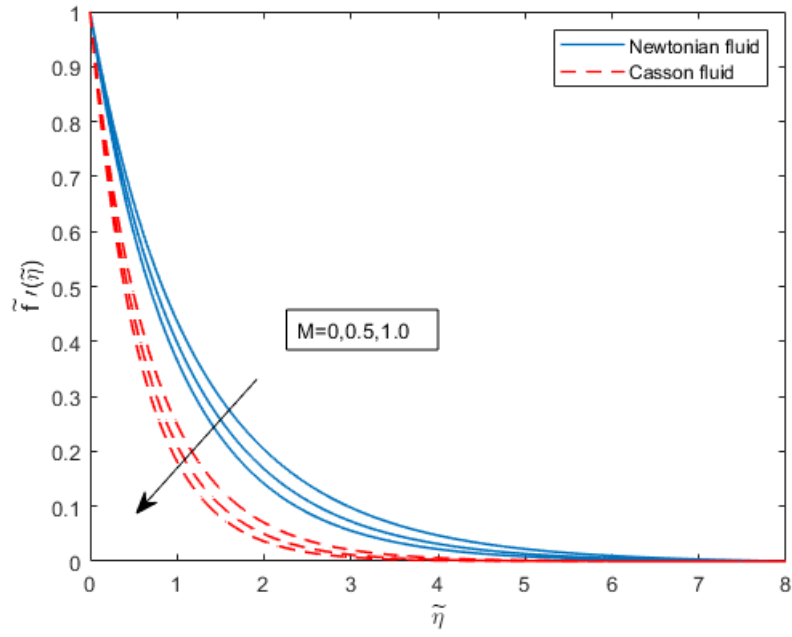


Figure 4.2: Depiction of  $M$  on  $\tilde{f}'(\tilde{\eta})$

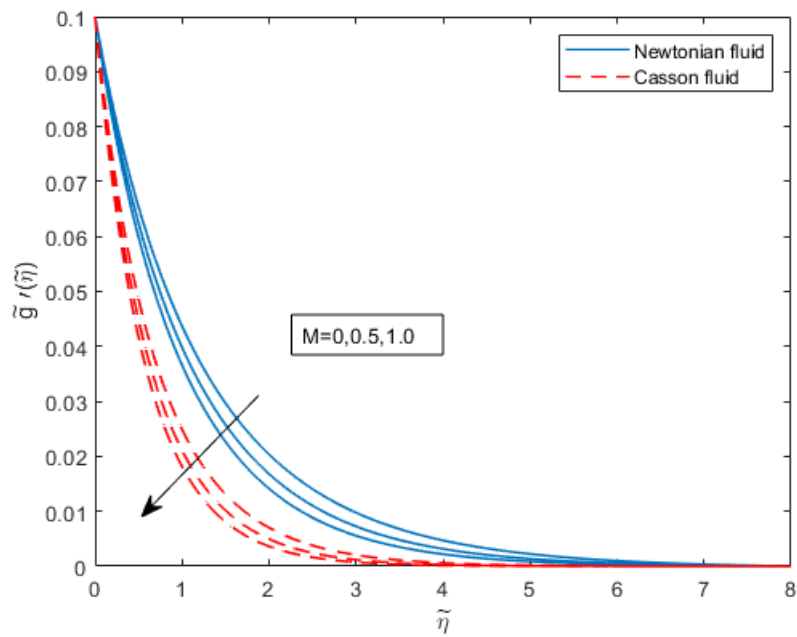


Figure 4.3: Depiction of  $M$  on  $\tilde{g}'(\tilde{\eta})$

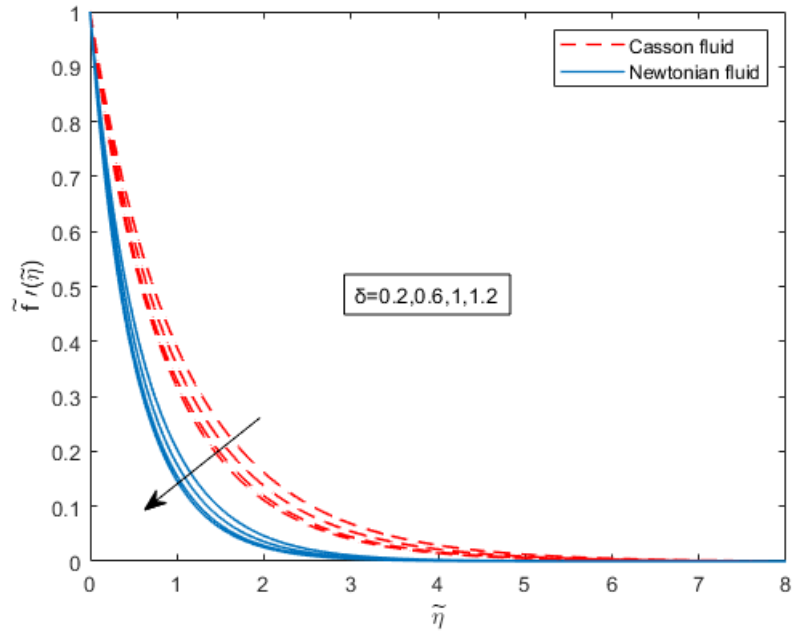


Figure 4.4: Depiction of  $\delta$  on  $\tilde{f}''(\tilde{\eta})$

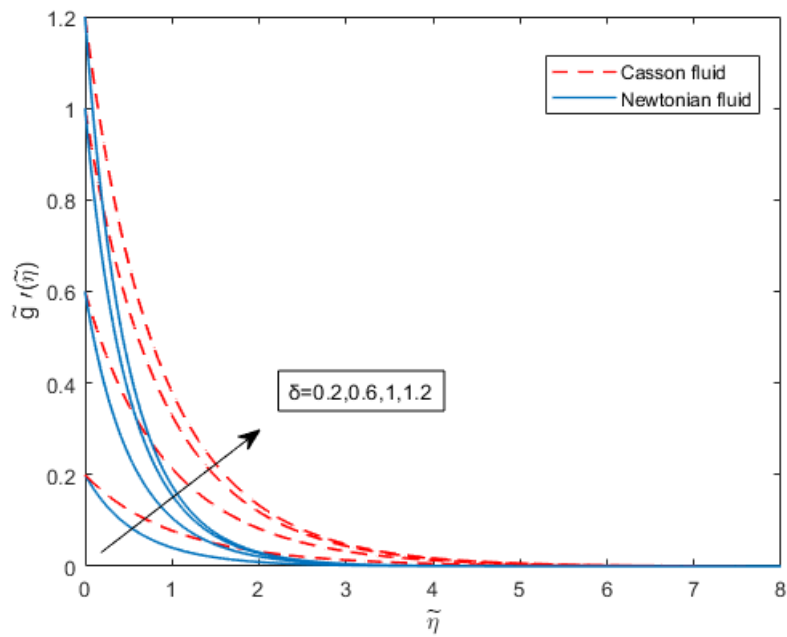


Figure 4.5: Depiction of  $\delta$  on  $\tilde{g}''(\tilde{\eta})$

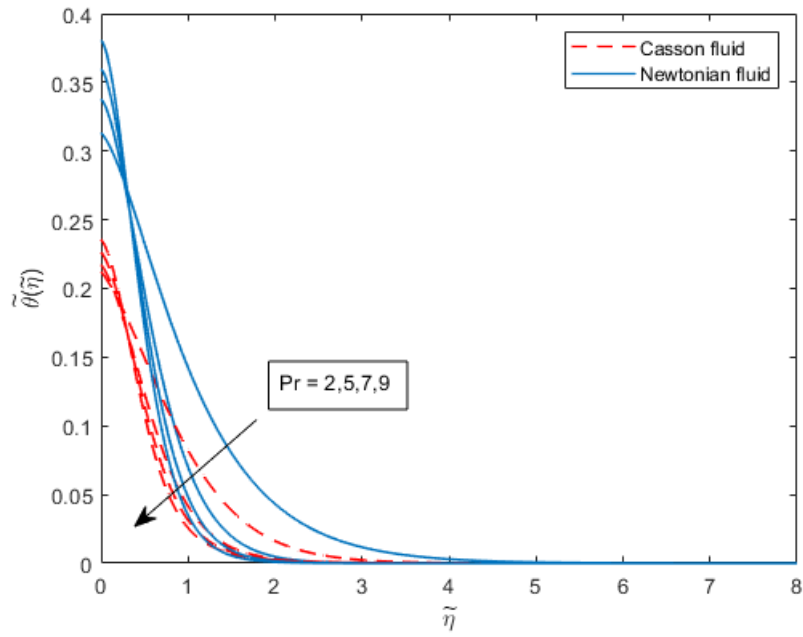


Figure 4.6: Depiction of  $Pr$  on  $\tilde{\theta}(\tilde{\eta})$

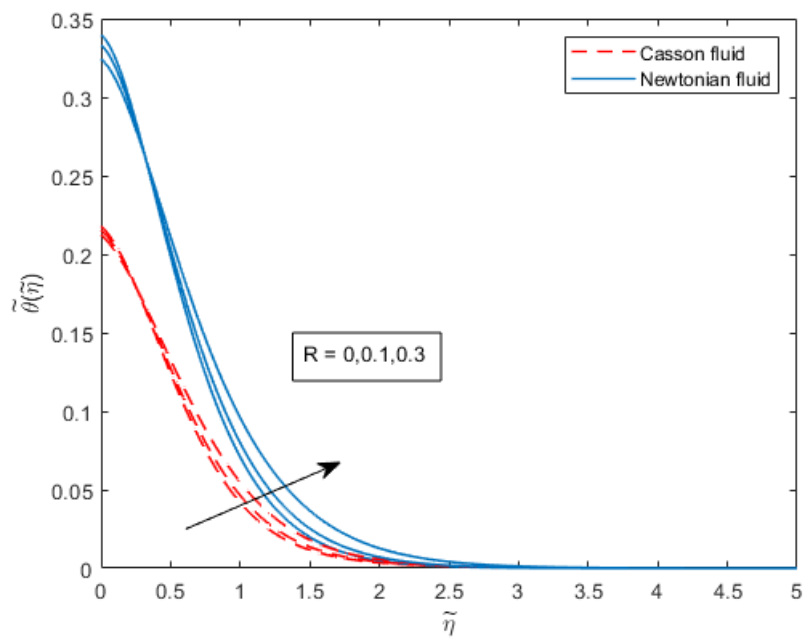


Figure 4.7: Depiction of  $R$  on  $\tilde{\theta}(\tilde{\eta})$

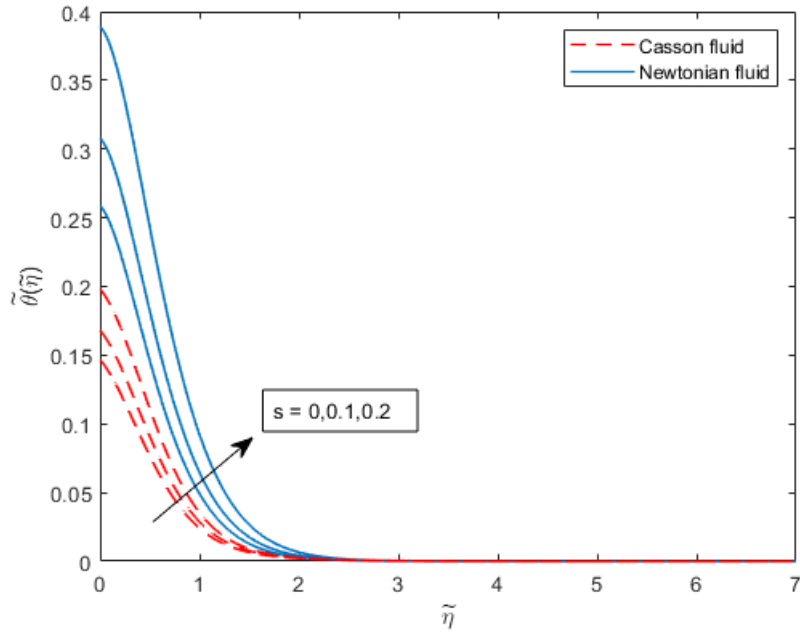


Figure 4.8: Depiction of  $s$  on  $\tilde{\theta}(\eta)$

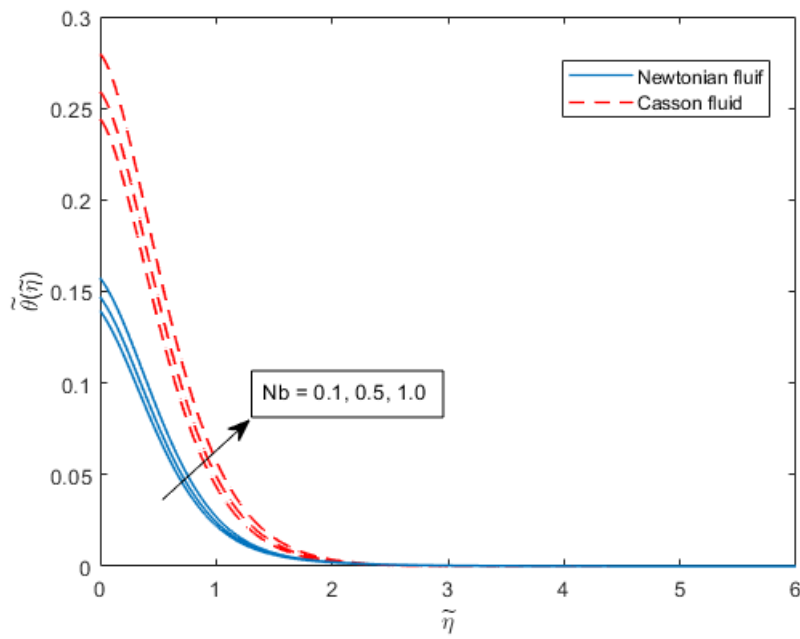


Figure 4.9: Depiction of  $Nb$  on  $\tilde{\theta}(\tilde{\eta})$

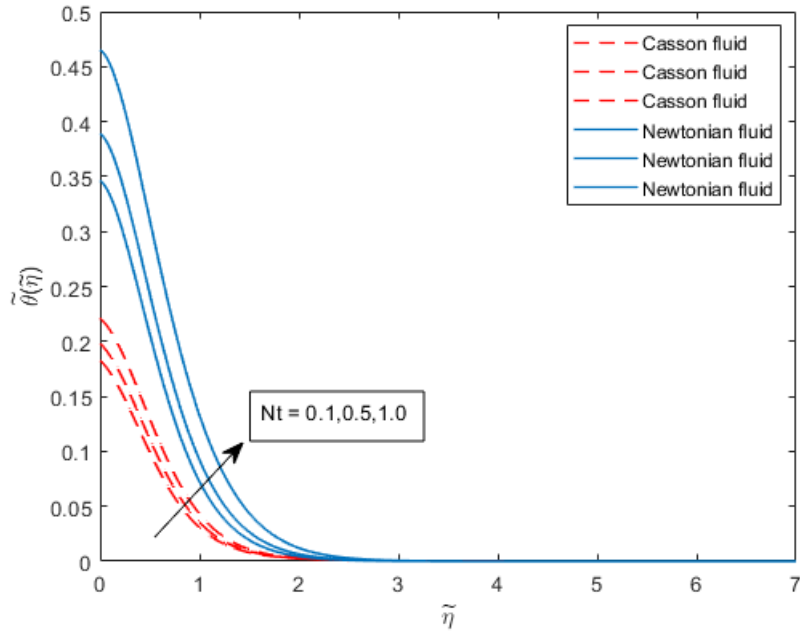


Figure 4.10: Depiction of  $Nt$  on  $\tilde{\theta}(\tilde{\eta})$

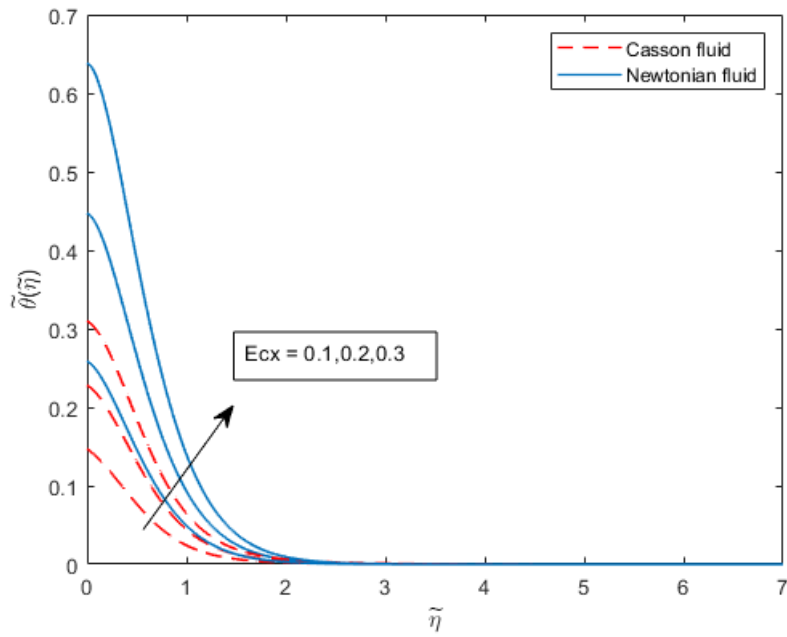


Figure 4.11: Depiction of  $Ec_x$  on  $\tilde{\theta}(\tilde{\eta})$

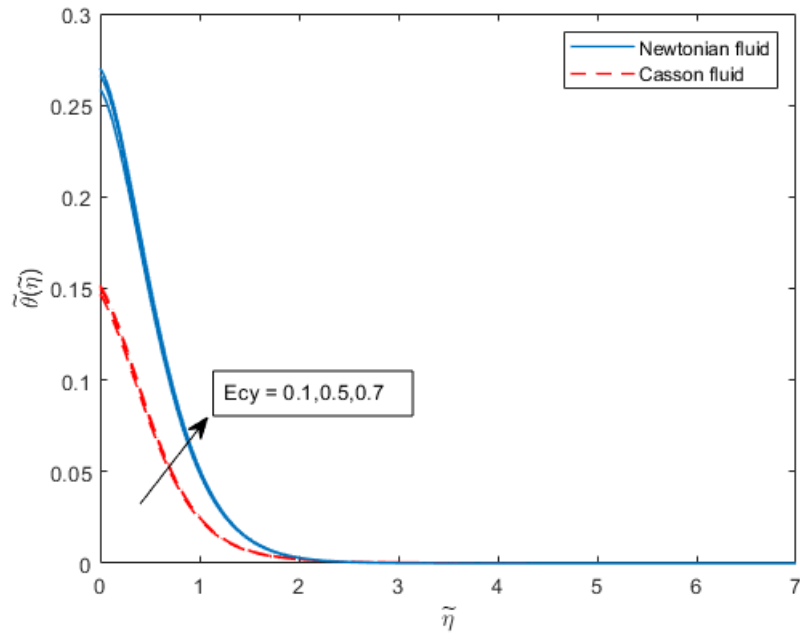


Figure 4.12: Depiction of  $E_{cy}$  on  $\tilde{\theta}(\tilde{\eta})$

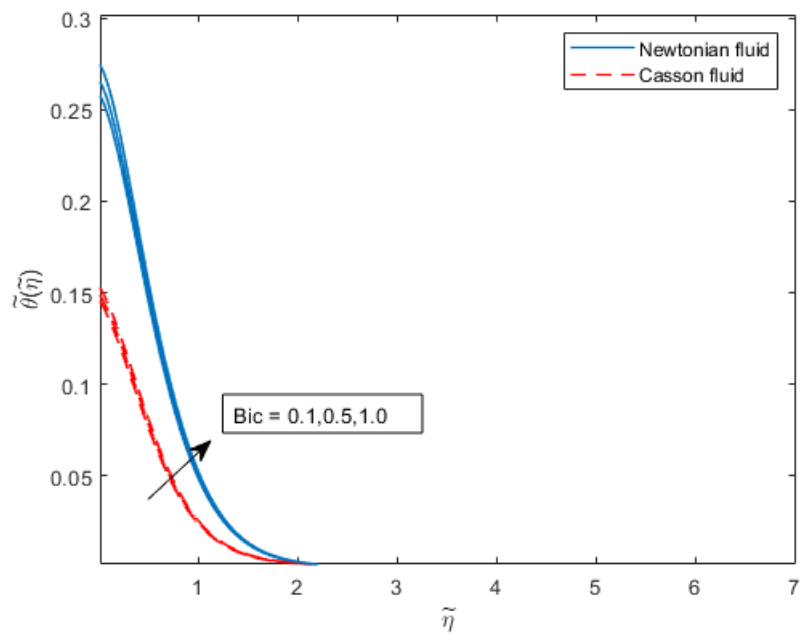


Figure 4.13: Depiction of  $Bi_c$  on  $\tilde{\theta}(\tilde{\eta})$

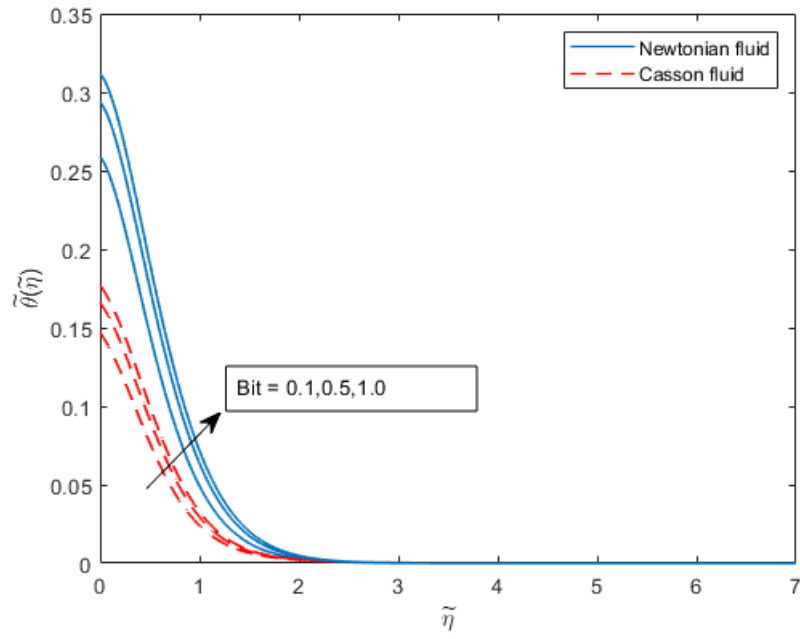


Figure 4.14: Depiction of  $Bi_t$  on  $\tilde{\theta}(\tilde{\eta})$

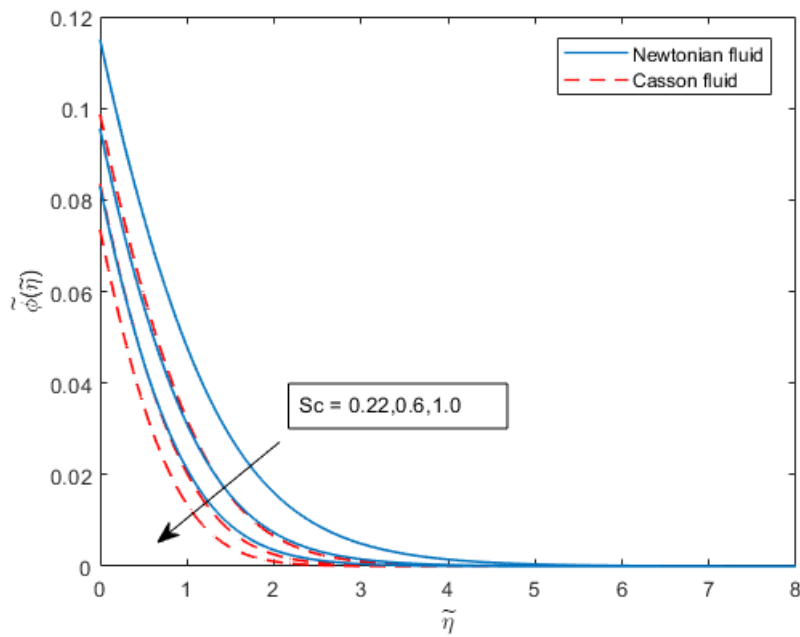


Figure 4.15: Depiction of  $Sc$  on  $\tilde{\phi}(\tilde{\eta})$

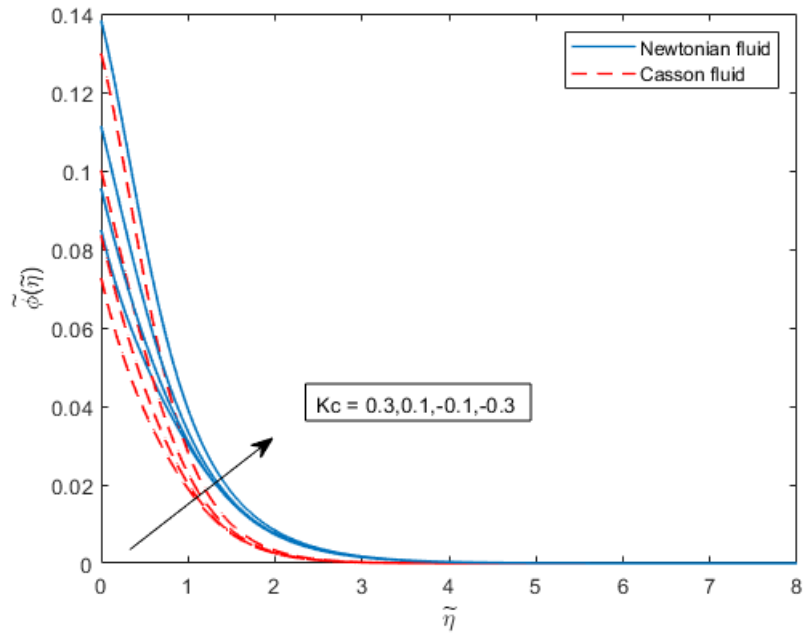


Figure 4.16: Depiction of  $k_c$  on  $\tilde{\phi}(\tilde{\eta})$

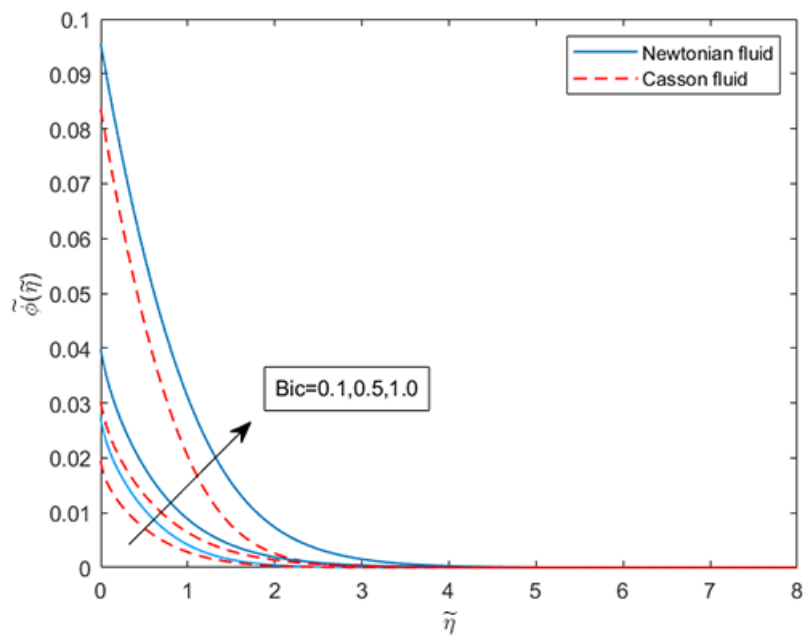


Figure 4.17: Depiction of  $Bi_c$  on  $\tilde{\phi}(\tilde{\eta})$

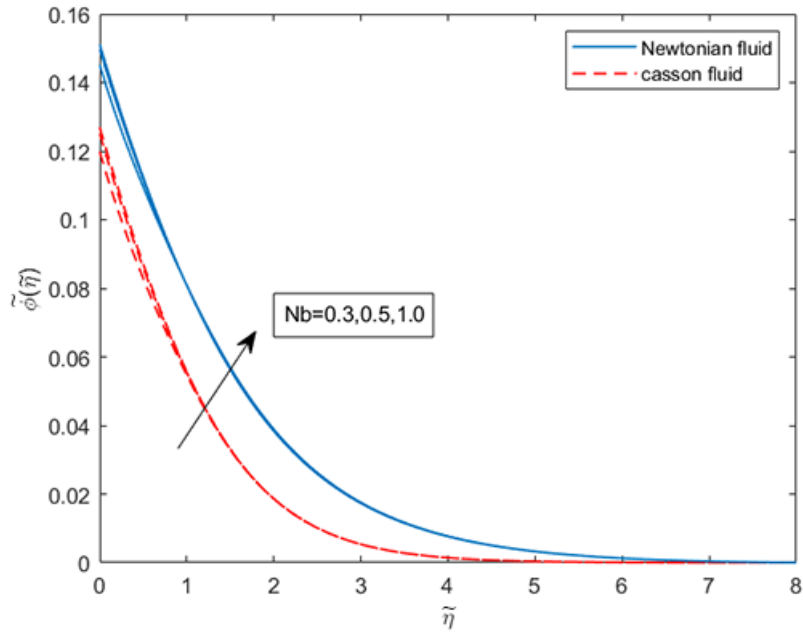


Figure 4.18: Depiction of  $Nb$  on  $\tilde{\phi}(\tilde{\eta})$

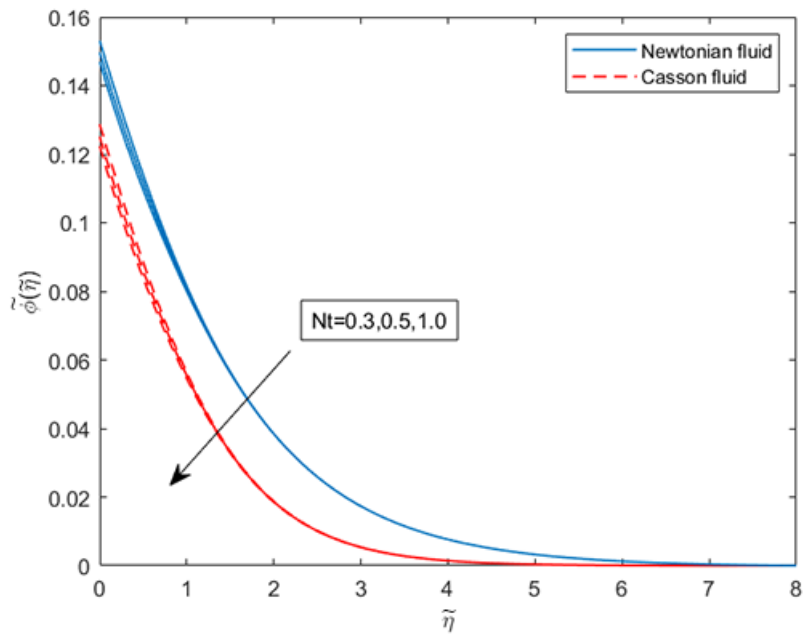


Figure 4.19: Depiction of  $Nt$  on  $\tilde{\phi}(\tilde{\eta})$

# Chapter 5

## NUMERICAL ANALYSIS OF THERMAL RADIATION WITH STAGNATION POINT ON NON-NEWTONIAN FLUID

### 5.1 Introduction

A stagnation point motion characteristic are performed considering the non-linear mixed convective and injection/suction influences in this chapter. Casson nanomaterial heat and mass transportation phenomena are studied using a non-linear chemical process, space-dependent heat source and convective surface conditions. This study also take similarity transformation was used to convert PDEs to ODEs. The converted ODEs are assessed using the RK-4 approach along with the shooting method [40-43]. Graphical Nusselt and Sherwood parameters as well as the skin friction coefficient are also investigated.

### 5.2 Problem Formulation

It is taken into account how a Casson incompressible nanofluid moves in three dimensions steadily and laminarly inside a porous substance. An exponentially stretchable plate compresses the fluid under consideration with a velocity of  $\tilde{U}_w$  close to the stagnation point. The z-axis is normal to the convectively heated sheet when it is situated on the xy plane. In Fig. (5.1), a magnetic liquid with a low Reynolds number is utilised the vertical direction.

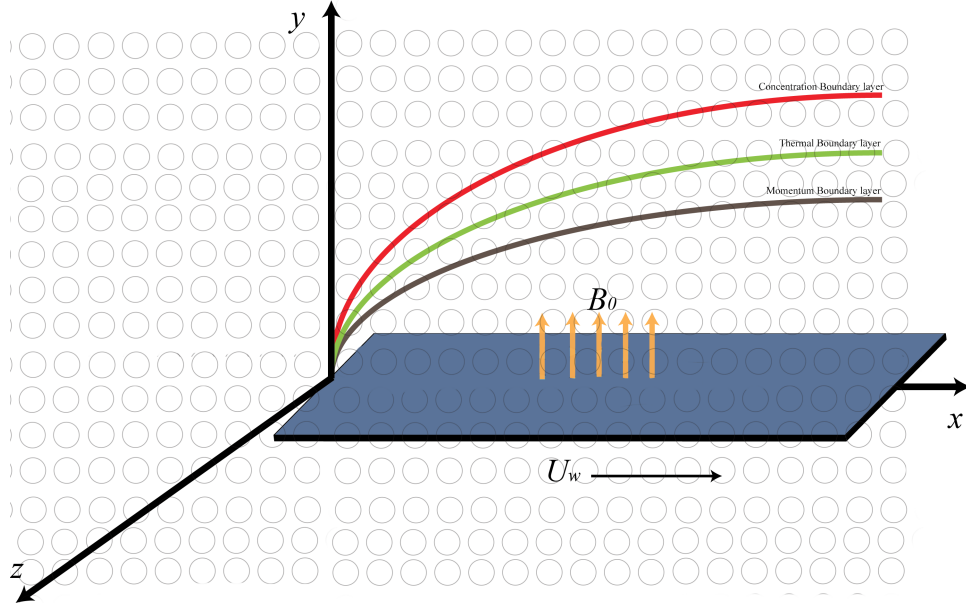


Figure 5.1: Physical model.

The relevant governing equations using boundary layer approximation are expressed as:

$$\frac{\partial}{\partial y}(\tilde{v}) + \frac{\partial}{\partial z}(\tilde{w}) + \frac{\partial}{\partial x}(\tilde{u}) = 0, \quad (5.1)$$

$$\begin{aligned} \tilde{U}_s \frac{\partial \tilde{u}_s}{\partial x} + \tilde{g}[\lambda_1(\tilde{T} - \tilde{T}_\infty) + \lambda_2(\tilde{T} - \tilde{T}_\infty)^2] - \frac{\nu_f}{k_p^*}(\tilde{U} - \tilde{U}_s) - \frac{\sigma B_0^2}{\rho_f}(\tilde{U} - \tilde{U}_s) + \nu_f(1 + \frac{1}{\beta}) \frac{\partial^2 \tilde{u}}{\partial z^2} \\ + \tilde{g}[\lambda_3(\tilde{C} - \tilde{C}_\infty) + \lambda_4(\tilde{C} - \tilde{C}_\infty)^2] = \tilde{u} \frac{\partial}{\partial x}(\tilde{u}) + \tilde{v} \frac{\partial}{\partial y}(\tilde{u}) + \tilde{w} \frac{\partial}{\partial z}(\tilde{u}), \end{aligned} \quad (5.2)$$

$$\begin{aligned} \tilde{V}_s \frac{\partial \tilde{v}_s}{\partial x} + \tilde{g}[\lambda_1(\tilde{T} - \tilde{T}_\infty) + \lambda_2(\tilde{T} - \tilde{T}_\infty)^2] - \frac{\nu_f}{k_p^*}(\tilde{V} - \tilde{V}_s) - \frac{\sigma B_0^2}{\rho_f}(\tilde{V} - \tilde{V}_s) + \nu_f(1 + \frac{1}{\beta}) \frac{\partial^2 \tilde{v}}{\partial z^2} \\ + \tilde{g}[\lambda_3(\tilde{C} - \tilde{C}_\infty) + \lambda_4(\tilde{C} - \tilde{C}_\infty)^2] = \tilde{u} \frac{\partial}{\partial x}(\tilde{v}) + \tilde{v} \frac{\partial}{\partial y}(\tilde{v}) + \tilde{w} \frac{\partial}{\partial z}(\tilde{v}), \end{aligned} \quad (5.3)$$

$$\begin{aligned} \tilde{u} \frac{\partial}{\partial x}(\tilde{T}) + \tilde{v} \frac{\partial}{\partial y}(\tilde{T}) + \tilde{w} \frac{\partial}{\partial z}(\tilde{T}) = -\frac{1}{(\rho c)_f} \left( \frac{\partial q_r}{\partial z} \right) + \alpha_f \frac{\partial^2 \tilde{T}}{\partial z^2} + \frac{Q_0(\tilde{T} - \tilde{T}_\infty)}{\rho C_p} \exp\left(-\sqrt{\frac{\tilde{u}_0}{2\nu L}} e^{\frac{x+y}{L}} \cdot z\right) \end{aligned} \quad (5.4)$$

$$\begin{aligned} + \frac{(\rho c)_p}{(\rho c)_f} [D_B \frac{\partial \tilde{C}}{\partial z} \frac{\partial \tilde{T}}{\partial z}] + \frac{\sigma B_0^2}{(\rho c)_f} [(\tilde{U} - \tilde{U}_s)^2 + (\tilde{V} - \tilde{V}_s)^2] + \frac{(\rho c)_p}{(\rho c)_f} \left[ \frac{D_T}{\tilde{T}_\infty} \left( \frac{\partial \tilde{T}}{\partial z} \right)^2 \right] \\ + \frac{\mu_f}{(\rho c)_f} \left( 1 + \frac{1}{\beta} \right) \left[ \left( \frac{\partial \tilde{u}}{\partial z} \right)^2 + \left( \frac{\partial \tilde{v}}{\partial z} \right)^2 \right] + \frac{s^*}{(\rho c)_f} (\tilde{T} - \tilde{T}_\infty), \end{aligned}$$

$$\tilde{u} \frac{\partial}{\partial x}(\tilde{C}) + \tilde{v} \frac{\partial}{\partial y}(\tilde{C}) + \tilde{w} \frac{\partial}{\partial z}(\tilde{C}) = D_B \frac{\partial^2 \tilde{C}}{\partial z^2} - k_c^*(\tilde{C} - \tilde{C}_\infty)^n + \frac{D_T}{T_\infty} \frac{\partial^2 \tilde{T}}{\partial z^2}. \quad (5.5)$$

Here, ambient velocity is represented by  $\tilde{U}_s$ ,  $\tilde{V}_s$ , and thermal conductivity is represented by  $k_f$ . The fluid coefficient is represented by  $\beta$ , density is defined by  $\rho$ , Brownian motion coefficient is represented by  $D_B$ , kinematic viscosity is defined by  $\nu_f$ , and The heat production coefficient is  $Q_0$ . The term " $\sigma$ " refers to electrical conductivity,  $g$  stands for the gravitational constant,  $\mu_f$  for absolute viscosity, and  $k_p^*$  for permeability. The terms  $s^*$ ,  $\tilde{T}$ ,  $\tilde{C}$ , and  $k_c^*$  stand for the heat source coefficient, temperature, concentration and chemical reaction parameter, respectively.

Following are the adjusted boundary conditions :

$$\left. \begin{aligned} \tilde{u} = \tilde{U}_w = a\tilde{U}_0 e^{\frac{x+y}{L}}, \tilde{w} = -\tilde{W}(x)\tilde{v} = \tilde{V}_w = a\tilde{V}_0 e^{\frac{x+y}{L}}, \\ -D_m \left( \frac{\partial \tilde{C}}{\partial z} \right) = h_m(\tilde{C}_f - \tilde{C}), -k_s \left( \frac{\partial \tilde{T}}{\partial z} \right) = h_f(\tilde{T}_f - \tilde{T}), \text{ at } z=0, \\ \tilde{u} \rightarrow \tilde{U}_s = b\tilde{U}_0 e^{\frac{x+y}{L}}, v \rightarrow \tilde{V}_s = b\tilde{V}_0 e^{\frac{x+y}{L}}, \tilde{C} \rightarrow \tilde{C}_\infty, \tilde{T} \rightarrow \tilde{T}_\infty, \text{ at } z \rightarrow \infty. \end{aligned} \right\} \quad (5.6)$$

The variables  $\tilde{U}_w$  and  $\tilde{V}_w$  define stretching velocities in the  $x - y$ -direction,  $h_m$ ,  $h_f$  stand for heat and mass transfer coefficients,  $c_f$  stands for the temperature and concentration of suspended fluid,  $\tilde{T}_\infty$  for ambient temperature,  $\tilde{U}_0$ ,  $\tilde{V}_0$  for reference velocities and  $D_m$  for diffusion coefficient.

### 5.2.1 Similarity Transformation

Following are the adjusted boundary conditions :

$$\left. \begin{aligned} \tilde{v} = a\tilde{V}_0 e^{\frac{x+y}{L}} \tilde{g}'(\tilde{\eta}), \tilde{u} = a\tilde{U}_0 e^{\frac{x+y}{L}} f'(\tilde{\eta}), \\ \tilde{w} = -\sqrt{\frac{a\nu_f \tilde{U}_0}{2L}} e^{\frac{x+y}{2L}} [\tilde{g}(\tilde{\eta}) + \tilde{\eta} \tilde{g}'(\tilde{\eta}) + \tilde{f}(\tilde{\eta}) + \tilde{\eta} \tilde{f}'(\tilde{\eta})], \\ \tilde{\eta} = z \sqrt{\frac{a\tilde{U}_0}{2\nu_f L}} e^{\frac{x+y}{2L}}, \tilde{\theta} = \frac{\tilde{T} - \tilde{T}_\infty}{\tilde{T}_f - \tilde{T}_\infty}, \tilde{\phi} = \frac{\tilde{C} - \tilde{C}_\infty}{\tilde{C}_f - \tilde{C}_\infty} \end{aligned} \right\} \quad (5.7)$$

The above equations have the following forms:

$$\begin{aligned} -2(\tilde{f}'\tilde{f}'' + \tilde{g}'\tilde{g}'') - M(\tilde{f}' - A) + (1 + \frac{1}{\beta})\tilde{f}''' + \lambda\tilde{\theta}(1 + \beta_1\tilde{\theta}) + \lambda N^*\tilde{\phi}(1 + \beta_2\tilde{\phi}) - K_p(\tilde{f}' - A) \\ + (\tilde{f}\tilde{f}'' + \tilde{g}\tilde{g}'') + 2A^2 = 0, \end{aligned} \quad (5.8)$$

$$\begin{aligned} (\tilde{f}\tilde{g}'' + \tilde{g}\tilde{f}'') + 2A^2 + (1 + \frac{1}{\beta})\tilde{g}''' - M(\tilde{g}' - A) + \lambda\tilde{\theta}(1 + \beta_1\tilde{\theta}) + \lambda N^*\tilde{\phi}(1 + \beta_2\tilde{\phi}) - K_p(\tilde{g}' - A) \\ - 2(\tilde{f}'\tilde{g}' + \tilde{g}'\tilde{f}') = 0, \end{aligned} \quad (5.9)$$

$$Pr[Nb\tilde{\theta}'\tilde{\phi}' + (1 + \frac{1}{\beta})(Ec_x\tilde{f}''^2 + Ec_y\tilde{g}''^2) + (\tilde{f} + \tilde{g})\theta' + MEc_y(\tilde{g}' - A)^2 + \delta^*exp(-\tilde{\eta})] + MEc_x(\tilde{f}' - A)^2 + s\tilde{\theta} + Nt\tilde{\theta}'^2 + [1 + \frac{4}{3}.R]\theta'' = 0, \quad (5.10)$$

$$-k_cSc\tilde{\phi}^n + \phi'' + \frac{Nt}{Nb}\tilde{\theta}'' + Sc(f + g)\tilde{\phi}' = 0, \quad (5.11)$$

The modified boundary conditions are shown below:

$$\left. \begin{aligned} \tilde{f}(0) + \tilde{g}(0) &= Q, \tilde{g}'(0) = \delta, \tilde{f}'(0) = 1, \\ \tilde{\phi}'(0) &= -Bi_c[1 - \tilde{\phi}(0)], \tilde{\theta}'(0) = -Bi_t[1 - \tilde{\theta}(0)], \\ \tilde{f}'(\infty) &\rightarrow A, \tilde{g}'(\infty) \rightarrow A, \tilde{\phi}(\infty) \rightarrow 0, \tilde{\theta}(\infty) \rightarrow 0. \end{aligned} \right\} \quad (5.12)$$

Here, the Casson fluid parameter is represented by  $\beta$ , while the radiation parameter is represented by  $R$  and the magnetic parameter by  $M$ . Schmidt number is represented by  $Sc$ . Prandtl number, porosity parameter, Eckert number, velocity ratio parameter, Brownian motion parameter and reaction parameter are all represented by the symbols  $Pr$ ,  $K_p$ ,  $Ec_x$ ,  $\delta$ , and  $K_c$ , respectively. The heat production parameter is  $s$ . A thermophoresis parameter is represented by  $Nt$ . The Biot number is represented by  $Bi_t$  and  $Bi_c$  in terms of temperature and concentration.

The parameters involved take the following mathematical form:

$$\begin{aligned} M &= \frac{2\sigma B_0^2 L}{\rho_f \tilde{U}_w}, Ec_y = \frac{\tilde{V}_w^2}{\rho_f(\tilde{T}_f - \tilde{T}_\infty)}, R = \frac{4\sigma^* \tilde{T}_\infty^3}{kk^*}, Ec_x = \frac{\tilde{U}_w^2}{\rho_f(\tilde{T}_f - \tilde{T}_\infty)} \\ \beta_2 &= \frac{\lambda_4}{\lambda_3}(\tilde{C}_s\tilde{\phi} - \tilde{C}_\infty), \beta_1 = \frac{\lambda_2}{\lambda_1}(\tilde{T}_s - \tilde{T}_\infty)\theta, \lambda = \frac{Gr}{Re_x^2}, A = \frac{b}{a}, N^* = \frac{\lambda_3(C_s - C_\infty)}{\lambda_1(\tilde{T}_s - \tilde{T}_\infty)} \\ s &= \frac{2s^*L}{\tilde{U}_w e^{\frac{x+y}{L}}(\rho c)_f}, Nb = \frac{(\rho c)_p D_B(\tilde{C}_f - \tilde{C}_\infty)}{(\rho c)_p(v)_f}, k_p = \frac{2\nu L}{\tilde{U}_w K_p^*}, \delta = \frac{\tilde{v}_0}{\tilde{u}_0}, Sc = \frac{\nu_f}{D_B}, \\ Nt &= \frac{(\rho c)_p D_T(\tilde{T}_f - \tilde{T}_\infty)}{(\rho c)_f T_\infty(v)_f}, Bi_t = \frac{h_f}{K_s} \sqrt{\frac{2\nu L}{U_w}}, Pr = \frac{\nu_f}{\alpha_f}, Bi_c = \frac{h_m}{D_m} \sqrt{\frac{2\nu L}{U_w}}. \end{aligned} \quad (5.13)$$

## 5.2.2 Significant Physical Quantities

Nusselt number, skin friction and Sherwood numbers are expressed as following:

$$\tilde{C}_{fx} = \frac{2\tilde{\tau}_{wx}}{\rho_f \tilde{U}_w^2}, \quad (5.14)$$

$$Nu = \frac{x\tilde{q}_w}{k_f(\tilde{T}_f - T_\infty)}, \quad (5.15)$$

$$Sh = \frac{xq_m}{D_B(\tilde{C}_f - \tilde{C}_\infty)}, \quad (5.16)$$

$$\tilde{C}_{fy} = \frac{2\tilde{\tau}_{wy}}{\rho_f \tilde{U}_w^2}. \quad (5.17)$$

where  $\tau_{wx}$ ,  $\tau_{wy}$ ,  $q_w$  and  $q_m$  are: Mathematically,

$$\begin{aligned} \tau_{wy} = \left( \frac{\partial \tilde{w}}{\partial y} + \frac{\partial \tilde{v}}{\partial z} \right)_{z=0} \left( \frac{\beta}{\beta+1} \right) \mu_f, \quad \tau_{wx} = \mu_f \left( \frac{\beta}{\beta+1} \right) \left( \frac{\partial \tilde{w}}{\partial x} + \frac{\partial \tilde{u}}{\partial z} \right)_{z=0}, \\ -k_f \left( \frac{\partial \tilde{T}}{\partial Z} \right)_{z=0} = (q_r)_{z=0} + q_w, \quad q_m = -D_B \left( \frac{\partial \tilde{C}}{\partial Z} \right)_{z=0}. \end{aligned} \quad (5.18)$$

These quantities are written as follows in non dimensional form:

$$\left( \frac{Re_x}{2} \right)^{\frac{1}{2}} \tilde{C}_{fx} = \frac{\beta}{\beta+1} \tilde{f}''(0), \quad (5.19)$$

$$\left( \frac{Re_x}{2} \right)^{\frac{1}{2}} \tilde{C}_{fy} = \frac{\beta}{\beta+1} \tilde{g}''(0), \quad (5.20)$$

$$\left( \frac{Re_x}{2} \right)^{-\frac{1}{2}} Sh_x \frac{L}{x} = -\tilde{\phi}'(0). \quad (5.21)$$

$$\left( \frac{Re_x}{2} \right)^{-\frac{1}{2}} Nu_x = -\left( 1 + \frac{4}{3}R \right) \tilde{\theta}'(0) \frac{x}{L}, \quad (5.22)$$

$$(5.23)$$

where

Reynolds number represents as;

$$Re_x = \frac{\tilde{U}_w L}{\nu_f}.$$

## 5.3 Methodology

The solution of connected non-dimensional flow equations is estimated using the numerical methodology of the fourth order Range- Kutta method and a shooting approach with  $10^{-5}$

precision. This method converts the system of controlling ODEs into a set of first order ODEs. Graphs are used to display numerical data for velocity, temperature, and concentration for the different associated parameters.

$$\tilde{f} = y_1; \quad (5.24)$$

$$y_2 = y_1 = \tilde{f}';$$

$$y_3 = y_2' = \tilde{f}'';$$

$$\tilde{f}''' = y_3' = \frac{\beta}{\beta+1} (2(y_2 y_2 + y_5 y_2) + M(y_2 - A) + k_p(y_2 - A) - (y_1 y_3 + y_4 y_3) - 2A^2 - \lambda y_7 (1 + \beta_1 y_7) - \lambda N^* y_9 (1 + \beta_2 y_9), \quad (5.25)$$

$$\tilde{g} = y_4; \quad (5.26)$$

$$\tilde{g}' = y_5 = y_4';$$

$$\tilde{g}'' = y_5' = y_6,$$

$$\tilde{g}''' = y_6' = \frac{\beta}{\beta+1} (2(y_2 y_5 + y_5 y_5) + M(y_5 - A) + k_p(y_5 - A) - (y_1 y_6 + y_4 y_6) - 2A^2 - \lambda y_7 (1 + \beta_1 y_7) - \lambda N^* y_9 (1 + \beta_2 y_9), \quad (5.27)$$

$$\tilde{\theta} = y_7; \quad (5.28)$$

$$\tilde{\theta}' = y_7' = y_8,$$

$$\tilde{\theta}'' = y_8' = \frac{-Pr}{(1 + \frac{4}{3}R)} [(y_1 y_8 + y_4 y_8) + N b y_{10} y_8 + N t (y_8^2) + \delta^* \exp(-\tilde{\eta} + (1 + \frac{1}{\beta})) (E c_x y_3^2 + E c_y (y_6^2) + M E c_x (y_2 - A)^2 + M E c_y (y_5 - A)^2 + S y_7], \quad (5.29)$$

$$\tilde{\phi} = y_9; \quad (5.30)$$

$$\tilde{\phi}' = y_9' = y_{10}$$

$$\tilde{\phi}'' = y_{10}' = -S c (y_1 y_{10} + y_4 y_{10}) - (\frac{N t}{N b}) y_8' + K c S c y_9^n, \quad (5.31)$$

## 5.4 Graphically Discussions and Results

### 5.4.1 Influence of Casson Fluid Parameter $\beta$

Fig. (5.2) illustrates the relationship between the Casson parameter and the velocity field  $\tilde{f}'(\tilde{\theta})$ . When values of Casson parameter ( $\beta$ ) are arise, the fluid behaves like a Newtonian liquid. Fluid

velocity steadily decay as the Casson parameter ( $\beta$ ) is enhanced. The viscosity of the fluid increases as the Casson parameter ( $\beta$ ) is increased because there is less fluid velocity and greater resistance between the two fluid layers. While the secondary velocity,  $\tilde{g}'(\tilde{\eta})$ , increases for the dominating Casson fluid parameter, the primary velocity,  $\tilde{f}'(\tilde{\eta})$ , decreases. The relationship between velocity  $\tilde{g}'(\tilde{\eta})$  and the Casson parameter ( $\beta$ ) is seen in Fig.(5.3). When the Casson parameter ( $\beta$ ) is set to greater values, the fluid velocity increases. Physically, fluid viscosity decreases as  $\beta$  increases. As a result, velocity  $\tilde{g}'(\tilde{\eta})$  increases.

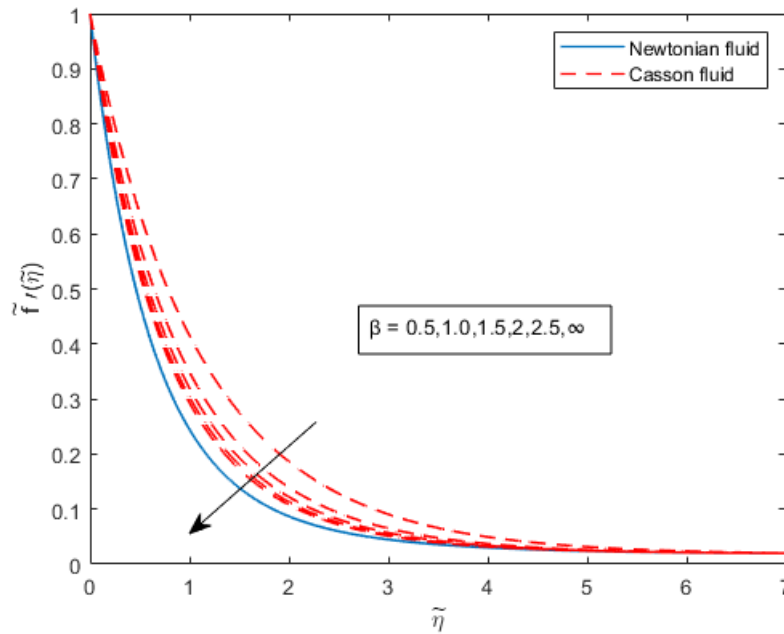


Figure 5.2: Depiction of Casson fluid on  $\tilde{f}'(\tilde{\eta})$

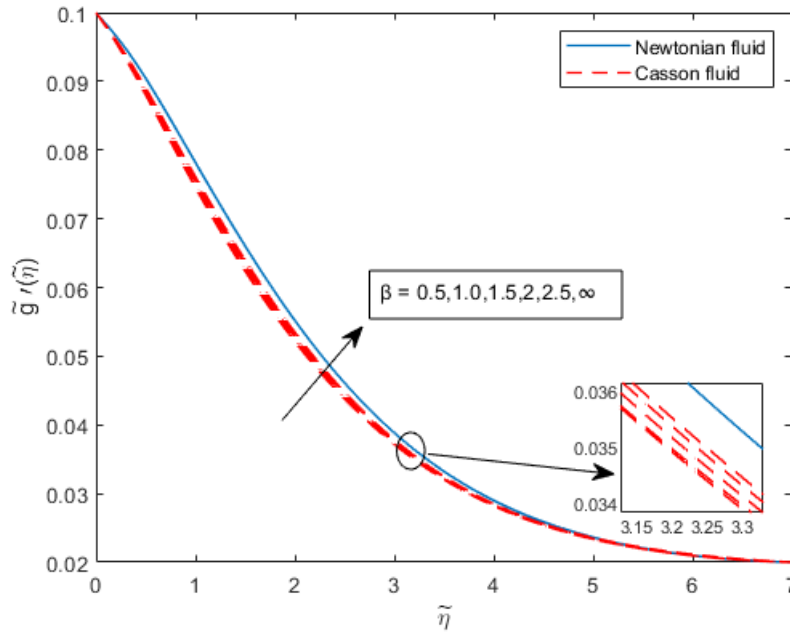


Figure 5.3: Depiction of Casson fluid on  $\tilde{g}'(\tilde{\eta})$

#### 5.4.2 Influence of Parameter of Porosity $k_p$

The effects of the porous parameter  $K_p$  on velocity profiles  $\tilde{f}'(\tilde{\eta})$  and  $\tilde{g}'(\tilde{\eta})$  are shown in Figs. (5.4) and (5.5). These phenomena occur for  $\tilde{g}'(\tilde{\eta})$  and  $\tilde{f}'(\tilde{\eta})$  when the value of  $K_p$  velocity profile is increased, and eventually the porosity parameter  $K_p$  depends on viscosity. For dominant  $k_p$ , there is a decrease in both the velocity fields. Physically, less fluid deformation occurs as  $k_p$  rises cause to the resistance provided by the porous material. So velocity profiles deteriorate.

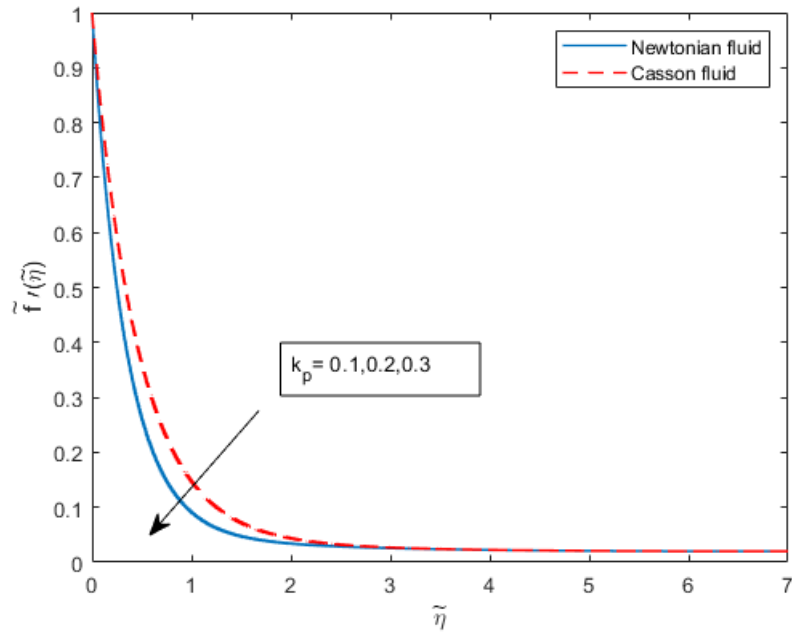


Figure 5.4: Depiction of Porosity on  $\tilde{f}'(\tilde{\eta})$

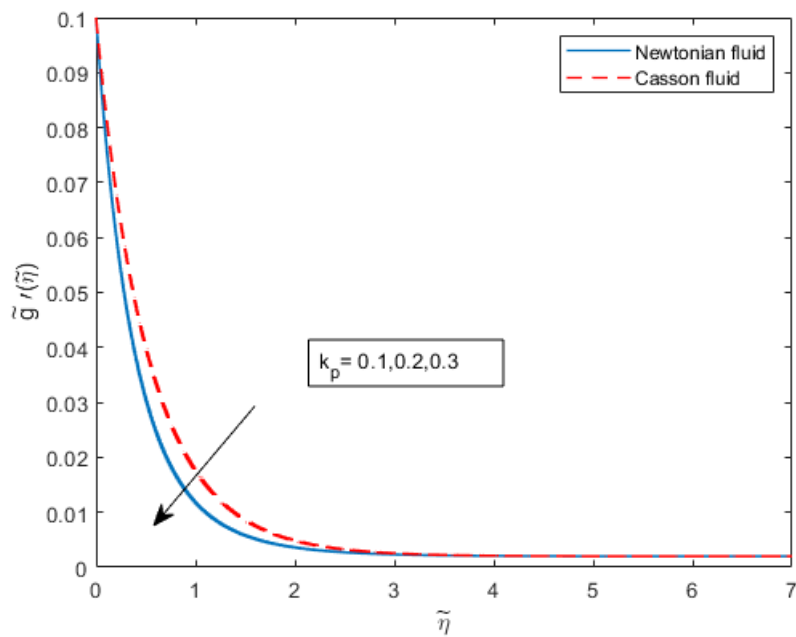


Figure 5.5: Depiction of Porosity on  $\tilde{g}'(\tilde{\eta})$

### 5.4.3 Influence of Brownian Motion $Nb$

The effects of Brownian motion on temperature, concentration, heat transportation rate, and mass transportation rate will now be examined. Figures (5.6) shows that when the Brownian motion parameter rises, the temperature and rate of heat transfer boundary layer thickness increase. Figures (5.7) shows that raising the temperature induces heating, yet the rate of heat transmission rises fast and then falls down. Figures (5.7) demonstrate increasing concentration as Brownian motion parameter rise, although increasing the Brownian motion parameter also arise the rate of mass transfer. Higher  $Nb$  is associated with dominant temperature and concentration behaviour. Greater molecular collisions caused by higher  $Nb$  raise temperature.

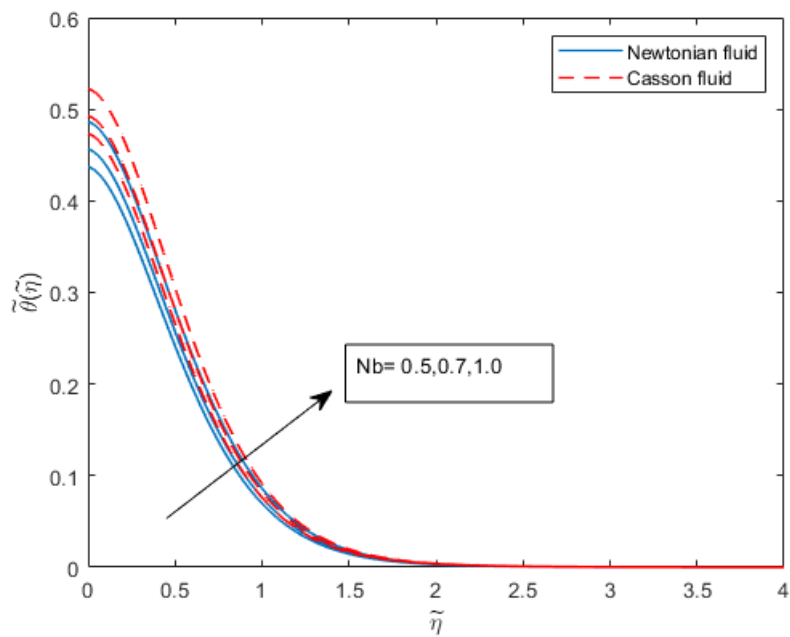


Figure 5.6: Depiction of Brownian motion on  $\tilde{\theta}(\tilde{\eta})$

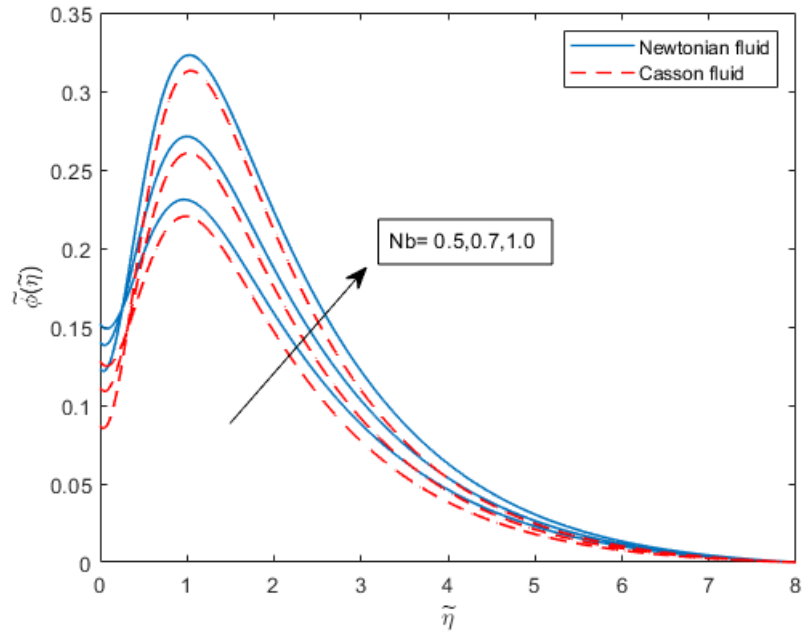


Figure 5.7: Depiction of Brownian motion on  $\tilde{\phi}(\tilde{\eta})$

#### 5.4.4 Influence of Thermophoresis Parameter $Nt$

Fig. (5.8) illustrates the behaviour of temperature as it relates to changes in incremental values of thermophoresis parameter ( $Nt$ ). This enhance in temperature occurs throughout the flow's route in the surface as a result of the thermophoresis phenomenon, which due hot fluid molecules to transfer from warm to cold locations. The influence of the thermophoresis parameter ( $Nt$ ) on the concentration field is seen in Fig. (5.9). As  $Nt$  values rise, the concentration level diminishes. In contrast to concentration fields, which show a falling tendency in line with  $Nt$ , temperature fields are shown to exhibit dominating behaviour. Physically, the thermophoresis mechanism causes temperature to rise by pulling molecules from a hotter to a colder surface.

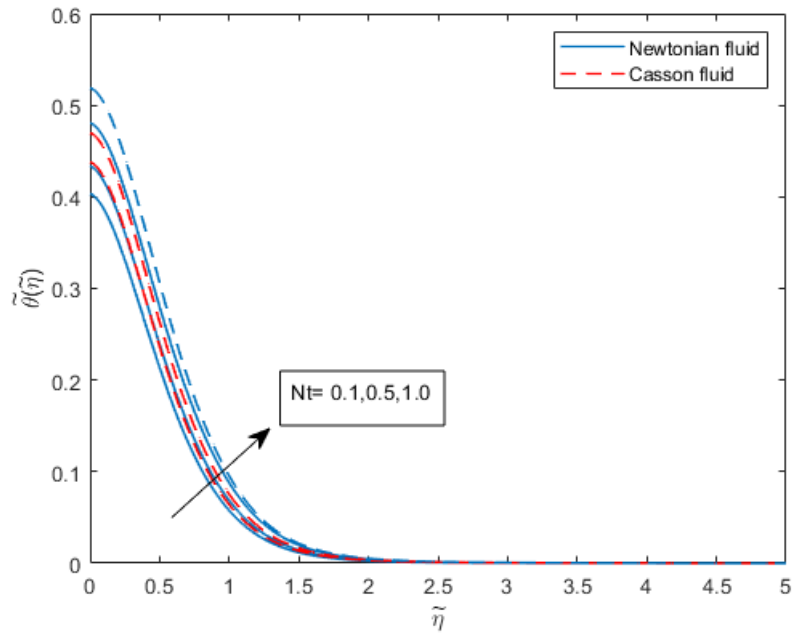


Figure 5.8: Depiction of Thermophoresis on  $\tilde{\theta}(\tilde{\eta})$

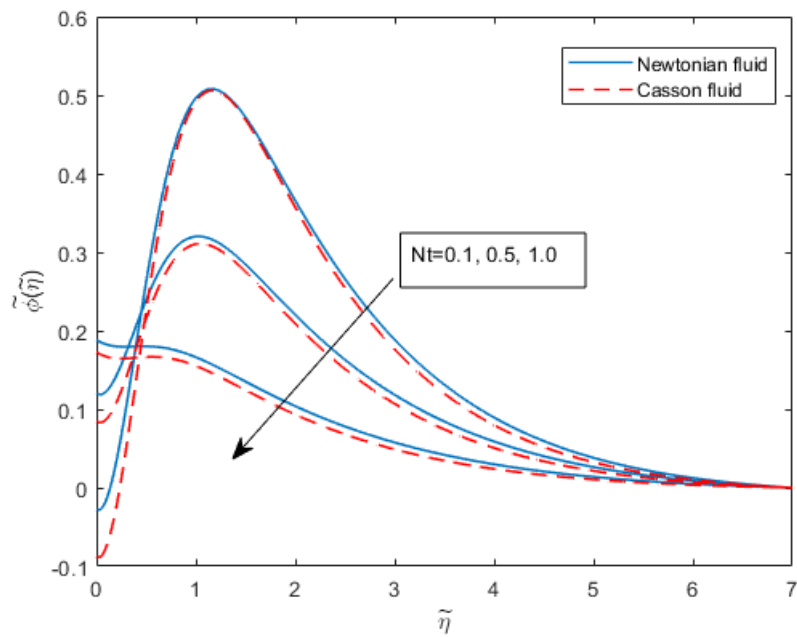


Figure 5.9: Depiction of Thermophoresis on  $\tilde{\phi}(\tilde{\eta})$

### 5.4.5 Influence of parameter of Mixed Convection $\lambda$

The variations in the  $\tilde{f}'(\tilde{\eta})$  and  $\tilde{g}'(\tilde{\eta})$  velocity profiles are expressed in Figures (5.10) and (5.11). Both velocities reportedly exhibit dominating behaviour consistent with ( $\lambda$ ). Physically speaking, larger ( $\lambda$ ) causes increased buoyancy effects, which in turn boost velocity fields. Additionally, it was shown that the mixed convection parameter affects  $\tilde{f}'(\tilde{\eta})$  differently than  $\tilde{g}'(\tilde{\eta})$ , when the slope of  $\tilde{f}'(\tilde{\eta})$  increases.

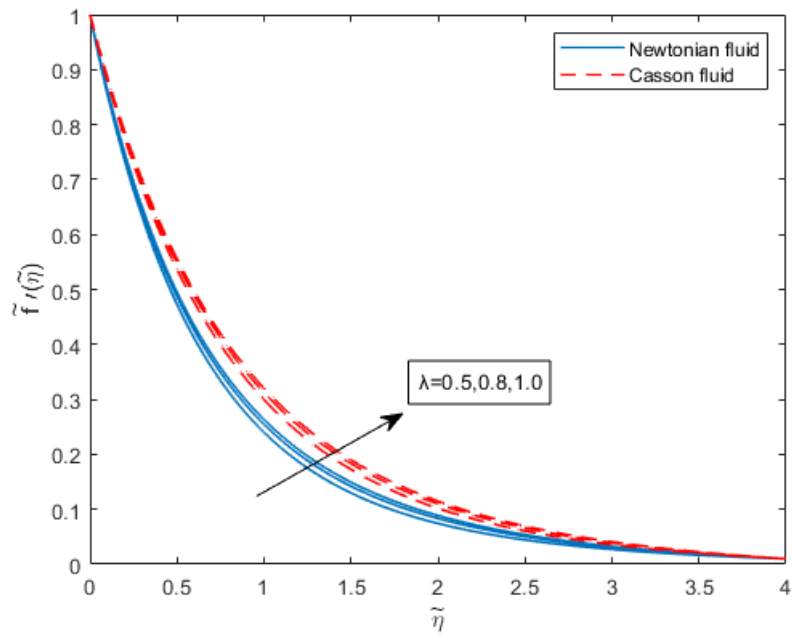


Figure 5.10: Depiction of mixed convection on  $\tilde{f}'(\tilde{\eta})$

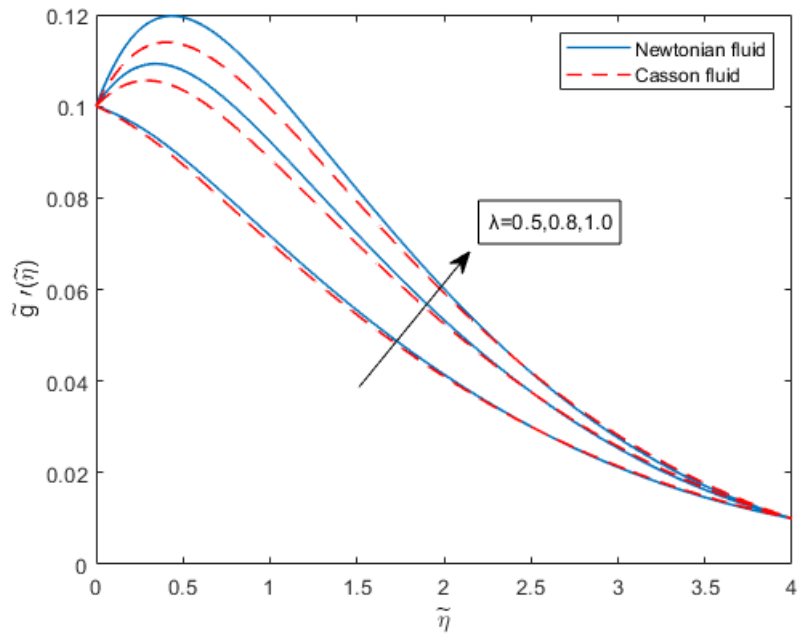


Figure 5.11: Depiction of mixed convection on  $\tilde{g}'(\tilde{\eta})$

#### 5.4.6 Influence of Point of stagnation $A$

The effect of the stretching parameter  $A$  on the velocity distribution of  $\tilde{g}'(\tilde{\eta})$  and  $\tilde{f}'(\tilde{\eta})$  is shown in Figures (5.12–5.13). The velocity and boundary layer thickness rise with an increase in  $A$  for small values of  $(0 \leq A < 1)$ . A progressive rise in  $A$  results in an increase in the free stream velocity, which causes an rise in the velocity, which follows. An improvement in velocities results from the fact that the free stream velocity is raised by gradual rise in  $A$ , which causes an increase in velocities. Increased  $A$  improves velocity dispersion as a result.

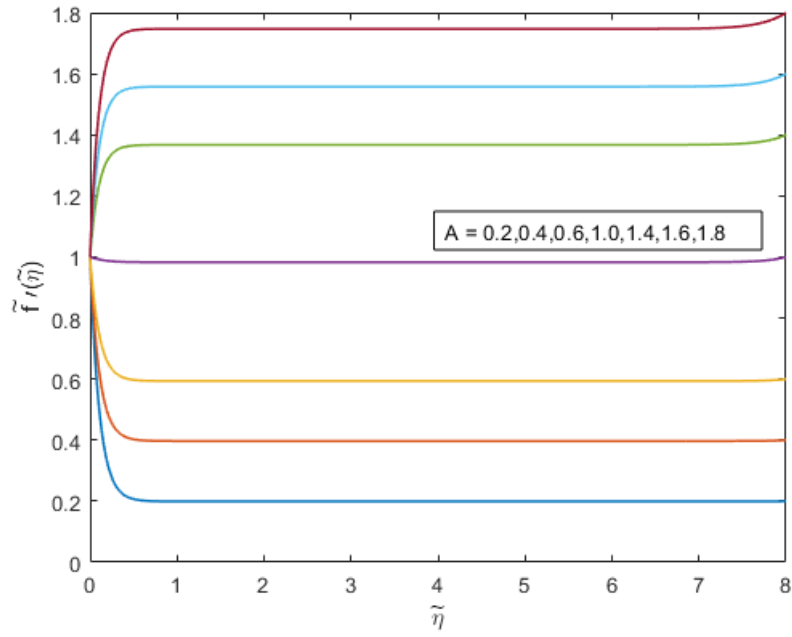


Figure 5.12: Depiction of Stagnation point on  $\tilde{f}'(\tilde{\eta})$

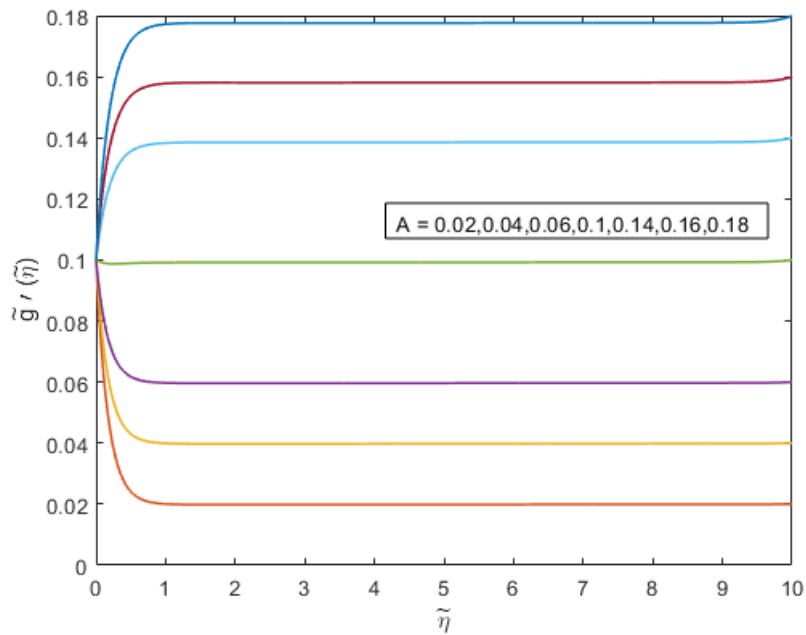


Figure 5.13: Depiction of Stagnation point for different values on  $\tilde{g}'(\tilde{\eta})$

### 5.4.7 Influence of parameter of Suction/ Injection $Q$

The suction/injection parameter  $Q$  behaviour with respect to the fluid velocities  $\tilde{f}'(\tilde{\eta})$  and  $\tilde{g}'(\tilde{\eta})$  is depicted in Figures (5.14) and (5.15). For the dominating  $Q$ , decrement behaviour is seen. In contrast to closer to the porous stretchy sheet, velocity decreases more quickly when moving away from it. As a result, velocity fields are reduced.

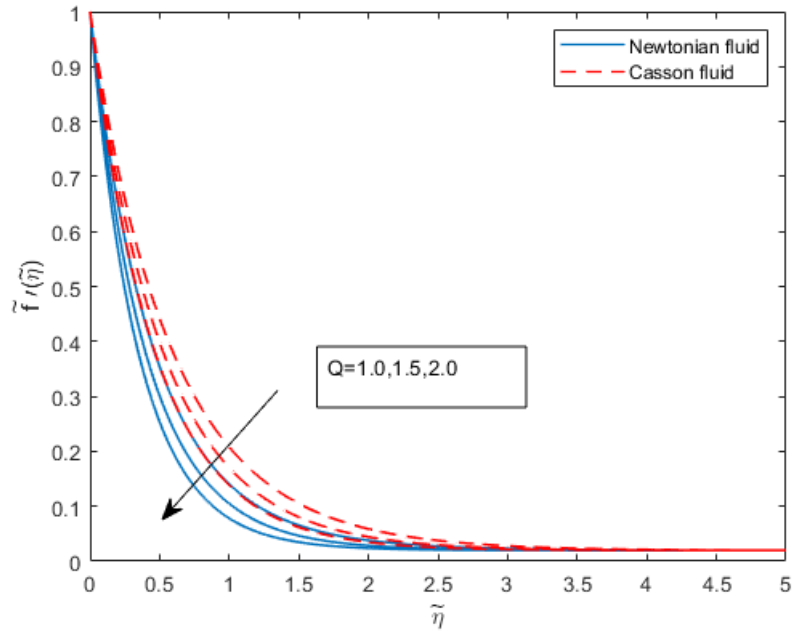


Figure 5.14: Depiction of Suction/Injection on  $\tilde{f}'(\tilde{\eta})$

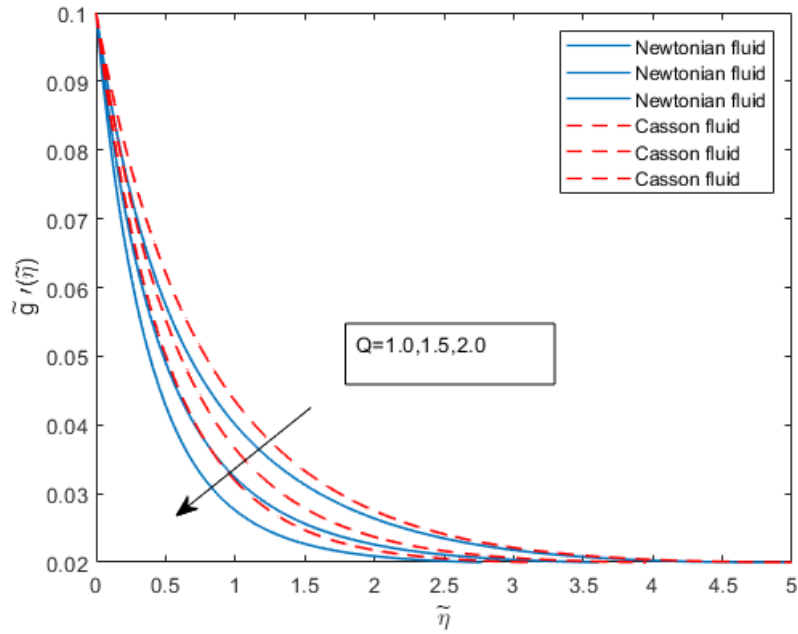


Figure 5.15: Depiction of Suction/Injection on  $\tilde{g}'(\tilde{\eta})$

#### 5.4.8 Influence of Radiation Parameter $R$

The affect of the radiation parameter ( $R$ ) on temperature velocity is seen in Figure (5.16). The temperature profile may be seen to be improving. The impact of boosting the radiation parameter on the thermal boundary layer may be the reason why the radiation parameter ( $R$ ) grows. Additionally, it has been discovered that the Casson fluid exerts a higher effect than the Newtonian fluid as the radiation parameter increases. Larger ( $R$ ) actually causes the temperature field to rise as more heat is movement from the heated plate to the fluid.

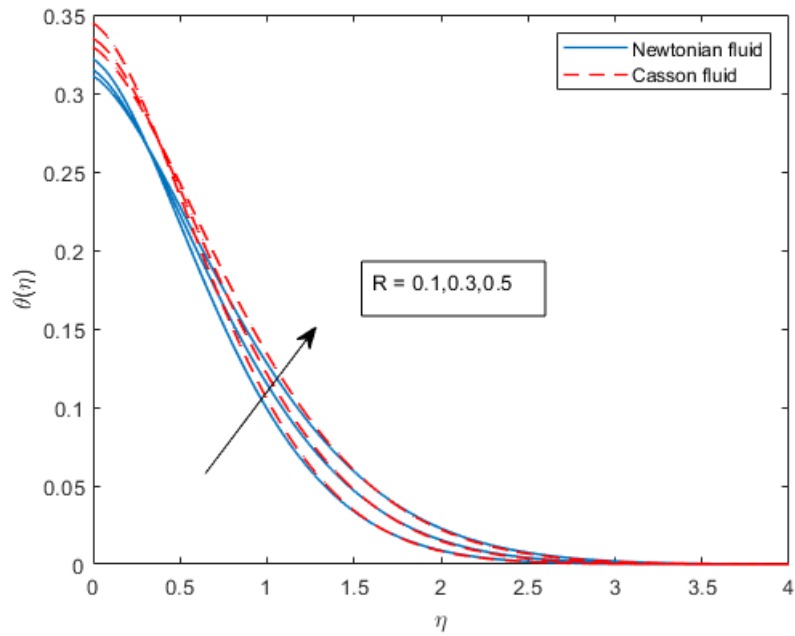


Figure 5.16: Depiction of Radiation on  $\tilde{\theta}(\tilde{\eta})$

#### 5.4.9 Influence of Chemical Reaction $k_c$

The effect of the chemical reaction ( $K_c$ ) on the concentration field is shown in Figure (5.17). As seen in fig. (5.17), the concentration profile decrease as the value of a chemical reaction parameter rises. According to Fig. 5.17, an increasing exothermic reaction decay the concentration field due to the fluid molecules' fast mobility, whereas an increasing endothermic reaction exhibits the opposite tendency.

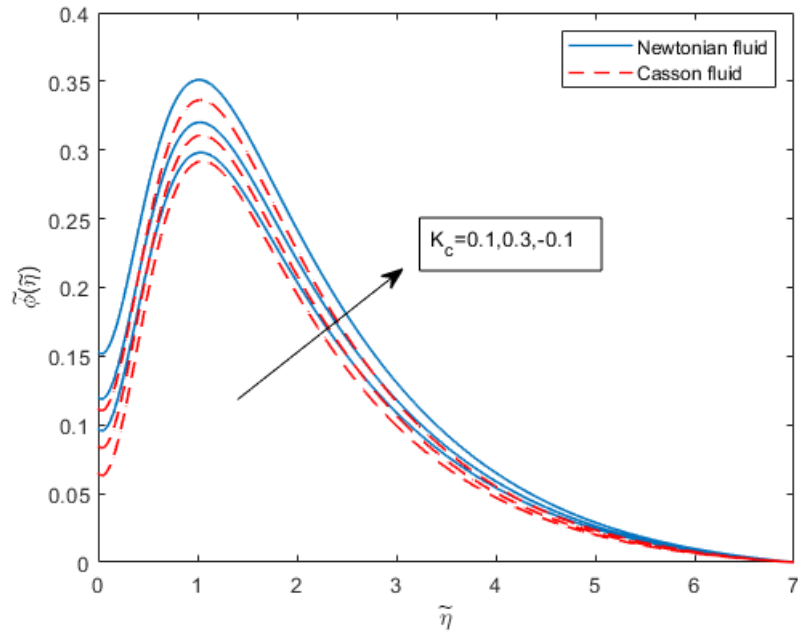


Figure 5.17: Depiction of Chemical reaction on  $\tilde{\phi}(\tilde{\eta})$

#### 5.4.10 Influence of Spaced Dependent Heat Generation Parameter $\delta^*$

We discuss how the temperature distribution is impacted by the exponential spaced dependent heat generation parameter (ESDHG). Various temperature curves for degrees of exponentially spaced dependent heat generation are shown in Figure (5.18). With the exponentially spaced dependent parameter, the temperature field grew. Additionally, it has been found that the thermal field is significantly influenced by the (ESDHG) aspect. The sluggish system receives heat at varying intensities depending on the value of the (ESDHG) parameter, producing a separate temperature curve.

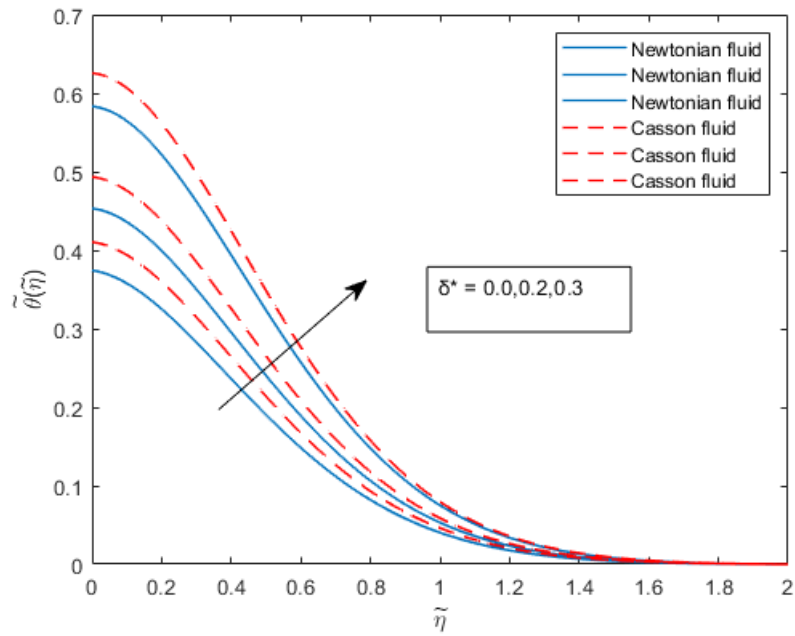


Figure 5.18: Depiction of Spaced dependent heat generation on  $\tilde{\theta}(\tilde{\eta})$

Skin friction, the Nusselt and Sherwoos number and relevant factors are numerically estimated and described in Tables 5.1 and 5.2. The amount of interest is growing as can be observed.

Table 5.1: Numerically results of  $-\tilde{\phi}'(0)$  and  $-\tilde{\theta}'(0)$ ,  $\tilde{g}''(0)$ ,  $\tilde{f}''(0)$ , for differ values of  $n=2.0$ ,  $\beta_1=\beta_2=0.5$ ,  $Nt=Nb=0.5$ ,  $\delta=0.1$ ,  $Q=2.0$ ,  $Bi_c=Bi_t=0.1$ ,  $\delta^*=0.1$ , for newtonian fluid.

| $A$ | $M$ | $K$ | $Pr$ | $R$ | $S$  | $Kc$ | $\lambda$ | $N^*$ | $Sc$ | $Ec_x$ | $Ec_y$ | $\sqrt{\frac{Re_x}{2}} C_{fx}$ | $\sqrt{\frac{Re_x}{2}} C_{fy}$ | $(\frac{Re_x}{2})^{-\frac{1}{2}} Nu_x \frac{L}{x}$ | $\sqrt{\frac{2}{Re_x} \frac{L}{x}} Sh_x$ |
|-----|-----|-----|------|-----|------|------|-----------|-------|------|--------|--------|--------------------------------|--------------------------------|--|--|
| 0   | 1.0 | 0.1 | 7    | 0.1 | 0.1  | 0.1  | 0.5       | 0.5   | 0.6  | 0.1    | 0.1    | 2.924091                       | 0.261121                       | 0.103465   | 0.087470                                 |
| 0.2 |     |     |      |     |      |      |           |       |      |        |        | 2.576362                       | -0.172057                      | 0.105941   | 0.088118                                 |
| 0.3 |     |     |      |     |      |      |           |       |      |        |        | 2.385390                       | -0.401638                      | 0.106764   | 0.088321                                 |
| 0.2 | 1.0 |     |      |     |      |      |           |       |      |        |        | 2.576362                       | -0.172057                      | 0.105941   | 0.088118                                 |
|     | 2.0 |     |      |     |      |      |           |       |      |        |        | 2.738660                       | -0.221170                      | 0.105105   | 0.088258                                 |
|     | 3.0 |     |      |     |      |      |           |       |      |        |        | 2.891591                       | -0.258089                      | 0.104325   | 0.088380                                 |
|     | 1.0 | 0.1 |      |     |      |      |           |       |      |        |        | 2.576362                       | -0.172057                      | 0.105941   | 0.088118                                 |
|     |     | 0.2 |      |     |      |      |           |       |      |        |        | 2.593038                       | -0.177744                      | 0.105913   | 0.088124                                 |
|     |     | 0.3 |      |     |      |      |           |       |      |        |        | 2.609640                       | -0.183195                      | 0.105885   | 0.088130                                 |
|     |     | 0.1 | 5.0  |     |      |      |           |       |      |        |        | 2.575611                       | -0.172917                      | 0.105658   | 0.088146                                 |
|     |     |     | 7.0  |     |      |      |           |       |      |        |        | 2.576362                       | -0.172057                      | 0.105941   | 0.088118                                 |
|     |     |     | 9.0  |     |      |      |           |       |      |        |        | 2.576777                       | -0.171583                      | 0.106099   | 0.088102                                 |
|     |     |     | 7.0  | 0.1 |      |      |           |       |      |        |        | 2.576362                       | -0.172057                      | 0.105941   | 0.088118                                 |
|     |     |     |      | 0.3 |      |      |           |       |      |        |        | 2.575921                       | -0.172561                      | 0.130663   | 0.088134                                 |
|     |     |     |      | 0.5 |      |      |           |       |      |        |        | 2.575477                       | -0.173070                      | 0.155307   | 0.088151                                 |
|     |     |     |      | 0.1 | 0.0  |      |           |       |      |        |        | 2.576747                       | -0.171925                      | 0.106021   | 0.088105                                 |
|     |     |     |      | 0.1 | 0.1  |      |           |       |      |        |        | 2.576362                       | -0.172057                      | 0.105941   | 0.088118                                 |
|     |     |     |      | 0.2 | 0.2  |      |           |       |      |        |        | 2.576241                       | -0.172105                      | 0.105858   | 0.088130                                 |
|     |     |     |      | 0.1 | 0.1  | 0.1  |           |       |      |        |        | 2.576362                       | -0.172057                      | 0.105941   | 0.088118                                 |
|     |     |     |      |     | 0.3  | 0.3  |           |       |      |        |        | 2.576455                       | -0.171949                      | 0.105941   | 0.088184                                 |
|     |     |     |      |     | -0.1 | -0.1 |           |       |      |        |        | 2.576267                       | -0.172167                      | 0.105941   | 0.088049                                 |
|     |     |     |      |     | 0.1  | 0.1  | 0.5       |       |      |        |        | 2.576362                       | -0.172057                      | 0.105941   | 0.088118                                 |
|     |     |     |      |     |      |      | 0.8       |       |      |        |        | 2.563779                       | -0.186318                      | 0.105975   | 0.088123                                 |
|     |     |     |      |     |      |      | 1.0       |       |      |        |        | 2.555436                       | -0.195772                      | 0.105997   | 0.088126                                 |
|     |     |     |      |     |      |      | 0.5       | 0.1   |      |        |        | 2.588718                       | -0.157799                      | 0.105902   | 0.088111                                 |
|     |     |     |      |     |      |      |           | 0.3   |      |        |        | 2.582529                       | -0.164942                      | 0.105922   | 0.088114                                 |
|     |     |     |      |     |      |      |           | 0.5   |      |        |        | 2.576362                       | -0.172057                      | 0.105941   | 0.0881180                                |
|     |     |     |      |     |      |      |           | 0.5   | 0.22 |        |        | 2.544774                       | -0.209608                      | 0.106084   | 0.073613                                 |
|     |     |     |      |     |      |      |           |       | 0.6  |        |        | 2.576362                       | -0.172057                      | 0.105941   | 0.088118                                 |
|     |     |     |      |     |      |      |           |       | 1.0  |        |        | 2.583444                       | -0.163763                      | 0.105916   | 0.092421                                 |
|     |     |     |      |     |      |      |           |       | 0.6  | 0.1    |        | 2.576362                       | -0.172057                      | 0.105941   | 0.0881180                                |
|     |     |     |      |     |      |      |           |       |      | 0.2    |        | 2.567876                       | -0.181615                      | 0.0995162  | 0.089146                                 |
|     |     |     |      |     |      |      |           |       |      | 0.3    |        | 2.559073                       | -0.191521                      | 0.093060   | 0.090184                                 |
|     |     |     |      |     |      |      |           |       |      | 0.1    | 0.1    | 2.576362                       | -0.172057                      | 0.105941   | 0.088118                                 |
|     |     |     |      |     |      |      |           |       |      | 0.5    |        | 2.575720                       | -0.172807                      | 0.105639   | 0.088160                                 |
|     |     |     |      |     |      |      |           |       |      | 0.7    |        | 2.575400                       | -0.173181                      | 0.105487   | 0.088811                                 |

Table 5.2: Numerically results of  $-\tilde{\phi}'(0)$  and  $-\tilde{\theta}'(0)$ ,  $\tilde{g}''(0)$ ,  $\tilde{f}''(0)$ , for differ values of  $n=2.0$ ,  $Bi_c=\delta=Bi_t=0.1$ ,  $\beta_1=\beta_2=0.5$ ,  $\delta^*=0.1$ ,  $Nb=Nt=0.5$ ,  $Q=2.0$ , for Casson Fluid.

| $A$ | $M$ | $K$ | $Pr$ | $R$ | $S$  | $Kc$ | $\lambda$ | $N^*$ | $Sc$ | $Ec_x$ | $Ec_y$ | $\sqrt{\frac{Re_x}{2}} C_{fx}$ | $(\frac{Re_x}{2})^{\frac{1}{2}} C_{fy}$ | $-\sqrt{\frac{Re_x}{2}} Nu_x \frac{L}{x}$ | $\sqrt{\frac{2}{Re_x} \frac{L}{x}} Sh_x$ |
|-----|-----|-----|------|-----|------|------|-----------|-------|------|--------|--------|--------------------------------|---|---|--|
| 0   | 1.0 | 0.1 | 7    | 0.1 | 0.1  | 0.1  | 0.5       | 0.5   | 0.6  | 0.1    | 0.1    | 3.258214                       | 0.292201                                | 0.102404                                  | 0.087973                                 |
| 0.2 |     |     |      |     |      |      |           |       |      |        |        | 2.888593                       | -0.181813                               | 0.105172                                  | 0.088406                                 |
| 0.3 |     |     |      |     |      |      |           |       |      |        |        | 2.679581                       | -0.438398                               | 0.106108                                  | 0.088546                                 |
| 0.2 | 1.0 |     |      |     |      |      |           |       |      |        |        | 2.888593                       | -0.181813                               | 0.105172                                  | 0.088406                                 |
|     | 2.0 |     |      |     |      |      |           |       |      |        |        | 3.097960                       | -0.241437                               | 0.104084                                  | 0.088579                                 |
|     | 3.0 |     |      |     |      |      |           |       |      |        |        | 3.292524                       | -0.286860                               | 0.103083                                  | 0.088731                                 |
|     | 1.0 | 0.1 |      |     |      |      |           |       |      |        |        | 2.888593                       | -0.181813                               | 0.105172                                  | 0.088406                                 |
|     |     | 0.2 |      |     |      |      |           |       |      |        |        | 2.910341                       | -0.188637                               | 0.105134                                  | 0.088412                                 |
|     |     | 0.3 |      |     |      |      |           |       |      |        |        | 2.931930                       | -0.195194                               | 0.105096                                  | 0.088419                                 |
|     |     | 0.1 | 5.0  |     |      |      |           |       |      |        |        | 2.887807                       | -0.182718                               | 0.104900                                  | 0.088433                                 |
|     |     |     | 7.0  |     |      |      |           |       |      |        |        | 2.888593                       | -0.181813                               | 0.105172                                  | 0.088406                                 |
|     |     |     | 9.0  |     |      |      |           |       |      |        |        | 2.889029                       | -0.181314                               | 0.105324                                  | 0.088391                                 |
|     |     |     | 7.0  | 0.1 |      |      |           |       |      |        |        | 2.888593                       | -0.181813                               | 0.105172                                  | 0.088406                                 |
|     |     |     |      | 0.3 |      |      |           |       |      |        |        | 2.888131                       | -0.182344                               | 0.129721                                  | 0.088422                                 |
|     |     |     |      | 0.5 |      |      |           |       |      |        |        | 2.887668                       | -0.182879                               | 0.154195                                  | 0.088437                                 |
|     |     |     |      | 0.1 | 0.0  |      |           |       |      |        |        | 2.888751                       | -0.181634                               | 0.105275                                  | 0.088389                                 |
|     |     |     |      | 0.1 | 0.1  |      |           |       |      |        |        | 2.888593                       | -0.181813                               | 0.105172                                  | 0.088406                                 |
|     |     |     |      | 0.2 | 0.2  |      |           |       |      |        |        | 2.888429                       | -0.182000                               | 0.105066                                  | 0.088423                                 |
|     |     |     |      | 0.1 | 0.1  | 0.1  |           |       |      |        |        | 2.888593                       | -0.181813                               | 0.105172                                  | 0.088406                                 |
|     |     |     |      |     | 0.3  | 0.3  |           |       |      |        |        | 2.88868                        | -0.181705                               | 0.105172                                  | 0.088470                                 |
|     |     |     |      |     | -0.1 | -0.1 |           |       |      |        |        | 2.888498                       | -0.181924                               | 0.105172                                  | 0.088341                                 |
|     |     |     |      |     | 0.1  | 0.1  | 0.5       |       |      |        |        | 2.888593                       | -0.181813                               | 0.105172                                  | 0.088406                                 |
|     |     |     |      |     |      |      | 0.8       |       |      |        |        | 2.874770                       | -0.197506                               | 0.105205                                  | 0.088409                                 |
|     |     |     |      |     |      |      | 1.0       |       |      |        |        | 2.865597                       | -0.207917                               | 0.105226                                  | 0.088412                                 |
|     |     |     |      |     |      |      | 0.5       | 0.1   |      |        |        | 2.901244                       | -0.167145                               | 0.105136                                  | 0.088402                                 |
|     |     |     |      |     |      |      |           | 0.3   |      |        |        | 2.894909                       | -0.174491                               | 0.105154                                  | 0.088404                                 |
|     |     |     |      |     |      |      |           | 0.5   |      |        |        | 2.888593                       | -0.181813                               | 0.105172                                  | 0.088406                                 |
|     |     |     |      |     |      |      |           | 0.5   | 0.22 |        |        | 2.855973                       | -0.221105                               | 0.105306                                  | 0.074206                                 |
|     |     |     |      |     |      |      |           |       | 0.6  |        |        | 2.888593                       | -0.181813                               | 0.105172                                  | 0.0884062                                |
|     |     |     |      |     |      |      |           |       | 1.0  |        |        | 2.895826                       | -0.173281                               | 0.105152                                  | 0.092599                                 |
|     |     |     |      |     |      |      |           |       | 0.6  | 0.1    |        | 2.888593                       | -0.181813                               | 0.105172                                  | 0.0884062                                |
|     |     |     |      |     |      |      |           |       |      | 0.2    |        | 2.878099                       | -0.193670                               | 0.0979721                                 | 0.0895763                                |
|     |     |     |      |     |      |      |           |       |      | 0.3    |        | 2.867154                       | -0.206020                               | 0.090731                                  | 0.090758                                 |
|     |     |     |      |     |      |      |           |       |      | 0.1    | 0.1    | 2.88593                        | -0.181813                               | 0.105172                                  | 0.088406                                 |
|     |     |     |      |     |      |      |           |       |      | 0.5    |        | 2.887860                       | -0.182678                               | 0.104848                                  | 0.088451                                 |
|     |     |     |      |     |      |      |           |       |      | 0.7    |        | 2.887494                       | -0.183110                               | 0.104686                                  | 0.088474                                 |

# Chapter 6

## CONCLUSIONS AND FUTURE PROPOSE

### 6.1 Concluding Remarks

This thesis presents the, flow non-linear fluid under the impact of lorentz force and thermal radiation. Flow is also assumed to be stagnation at a point in flow field. The outcomes for skin friction, Nusselt number and sherwood obtained in tabular form by using shooting method to solve the linear ODEs whose iterations are being executed by MATLAB. The behaviour of velocity, temperature, concentration fields for different physical parameters is investigated. The results are also elaborated in graphical and tabular form.

The Nusselt and Sherwoos numbers, as well as the numerical calculation of skin friction, are described in Tables 5.1 and 5.2 in relation to the relevant parameters. The amount of interest is increasing as is evident.

Momentum boundary layer thickens as  $A$  grows and becomes thinner as  $\lambda$ ,  $\beta$  and  $\delta^*$  increase. For the major porosity parameter, the velocity field shrank. Nanoparticle friction rises in the presence of,  $Nt_i$  and falls in the presence of  $A$ ,  $Nb$ , and nonlinear chemical reaction. The velocity field increased due to the greater mixed convection parameter. The Prandtl number ( $Pr$ ) can be utilised to quicken the cooling process in conducting flows. The velocity field grew as the stagnation point parameter rose. As the Casson parameter rises, the surface shear stress rises as well. Suction/injection parameter used to deaccelerate the velocity field. The fluid temperature increased as the heat source changed. Enhancement of the temperature field for a greater space-dependent heat production parameter. For a dominating value of a chemical reaction parameter, the concentration field expands.

## **6.2 Future Work**

The current study may be extended in the following directions:

Three dimensional nonlinear mixed convective flow of Jeffrey fluid with linear stratification.

Three dimensional squeezing nanofluid flow with variable thermal conductivity. Characteristics of thermal stratification in Jeffrey nanofluid flow over a sheet with variable thickness.

Three-dimensional Casson nanofluid flow with Cattaneo-Christov heat flux model. Three-dimensional Maxwell fluid flow through porous medium with nonlinear thermal and solutal stratifications. The stretching can also be assumed as non linear.

# References

- [1] Casson, N. (1995). A flow equation for pigment-oil suspensions of the printing ink type. *Rheology of disperse systems*. Pergamon Press: Oxford, UK, 84-104.
- [2] Prameela, M., Gangadhar, K., & Reddy, G. J. (2022). MHD free convective non-Newtonian Casson fluid flow over an oscillating vertical plate. *Partial Differential Equations in Applied Mathematics*, 5, 100366.
- [3] Khan, M. N., Ahmed, A., Ahammad, N.A., Alqahtani, T., & Algarni, S. (2022). Insights into 3D flow of Casson fluid on exponential stretchable surface in rotating frame through porous medium. *A in Shams Engineering Journal*, 14, 101849.
- [4] Reddy, S. S., Raju, K. V., Mopuri, O., Ganteda, C., Khan, S. U., Boujelbene, M., ... & Elbadawi, I. (2022). Applications of variable plastic viscosity and thermal conductivity for Casson fluid with slip effects and space dependent internal heat generation. *Journal of the Indian Chemical Society*, 99, 100712.
- [5] Alzahrani, A. K., Abbas, Z., & Ullah, M.Z. (2022). Chemically reactive two-phase flow of viscous-Casson fluids in a rotating channel. *Alexandria Engineering Journal*, 62, 403-413.
- [6] Raju, Reddy, S. S., K. V., Mopuri, O., Ganteda, C., Khan, S. U., Boujelbene, M., ... & Elbadawi, I. (2022). Applications of variable plastic viscosity and thermal conductivity for

Casson fluid with slip effects and space dependent internal heat generation. *Journal of the Indian Chemical Society*, 99(10), 100712.

[7] Hussain, S., & Zeeshan, M. (2022). Irreversibility analysis for the natural convection of Casson fluid in an inclined porous cavity under the effects of magnetic field and viscous dissipation. *International Journal of Thermal Sciences*, 179, 107699.

[8] Ali, G., Ali, F., Khan, A., Ganie, A. H., & Khan, I. (2022). A generalized magnetohydrodynamic two-phase free convection flow of dusty Casson fluid between parallel plates. *Case Studies in Thermal Engineering*, 29, 101657.

[9] Swarnalathamma, B. V., Babu, D. P., & Krishna, M. V. (2022). Combined impacts of Radiation absorption and Chemically reacting on MHD Free Convective Casson fluid flow past an infinite vertical inclined porous plate. *Journal of Computational Mathematics and Data Science*, 5, 100069.

[10] Chu, Y. M., Khan, M. I., Khan, N. B., Kadry, S., Khan, S. U., Tlili, I., & Nayak, M. K. (2020). Significance of activation energy, bio-convection and magnetohydrodynamic in flow of third grade fluid (non-Newtonian) towards stretched surface: A Buongiorno model analysis. *International Communications in Heat and Mass Transfer*, 118, 104893.

[11] Raza, J., Mebarek-Oudina, F., Ram, P., & Sharma, S. (2020). MHD flow of non-Newtonian molybdenum disulfide nanofluid in a converging/diverging channel with Rosseland radiation. In *Defect and Diffusion Forum* 401, 92-106).

[12] El-Dabe, N., Abou-Zeid, M. Y., Mohamed, M. A., & Abd-Elmoneim, M. M. (2021). MHD peristaltic flow of non-Newtonian power-law nanofluid through a non-Darcy porous medium in-

side a non-uniform inclined channel. *Archive of Applied Mechanics*, 91(3), 1067-1077.

[13] Siva, T., Jangili, S., & Kumbhakar, B. (2021). Heat transfer analysis of MHD and electroosmotic flow of non-Newtonian fluid in a rotating microfluidic channel: an exact solution. *Applied Mathematics and Mechanics*, 42(7), 1047-1062.

[14] Anwar, M. I., Firdous, H., Zubaidi, A. A., Abbas, N., & Nadeem, S. (2022). Computational analysis of induced magnetohydrodynamic non-Newtonian nanofluid flow over nonlinear stretching sheet. *Progress in Reaction Kinetics and Mechanism*, 47, 14686783211072712.

[15] Ishtiaq, F., Ellahi, R., Bhatti, M. M., & Alamri, S. Z. (2022). Insight in thermally radiative cilia-driven flow of electrically conducting non-Newtonian Jeffrey fluid under the influence of induced magnetic field. *Mathematics*, 10(12), 2007.

[16] Hiemenz, K. (1911). The boundary layer on a straight circular cylinder immersed in the uniform liquid flow. *J. Dinglers polytech*, 326, 321-324.

[17] Eckert, E. (1942). The calculation of the heat transfer in the laminar boundary layer around the body. *VDI research issue*, 416, 1-24.

[18] Sahoo, S. (2022). Stagnation point flow of a viscous incompressible fluid. *Metrials Today: Proceeding*, 67, 1069-1072.

[19] Wahid, N. S., Arifin, N. M., Pop, I., Bachok, N., & Hafidzuddin, M. E. H. (2022). MHD stagnation-point flow of nanofluid due to a shrinking sheet with melting, viscous dissipation

and Joule heating effects,. Alexandria Engineering Journal, 61, 12661-12672.

[20] Abbasi, A., Khan, S. U., Al-Khaled, K., Khan, M. I., Farooq, W., Galal, A. M., ... & Malik, M. Y. (2022). Thermal prospective of Casson nano-materials in radiative binary reactive flow near pblique stagnation point flow with activation energy applications. Chemical Physics Letters, 786. 139172.

[21] Rehman, M. I. U., Chen, H., Jamshed, W., Eid, M.R., Guedri, K., & El Din, S. M. (2022). Thermal radiative flux and energy of Arrhenius evaluation on stagnation point flowing of Carreau nanofluid: Athermal case study. Case Studies in Thermal Engineering, 40, 102583.

[22] Warke, A. S., Ramesh, K., Mebarek-Oudina, F., & Abidi, A. (2022). Numerical investigation of the stagnation point flow of radiative magnetomicropolar liquid past a heated porous stretching sheet. Journal of Thermal Analysis and Calorimetry, 147(12), 6901-6912.

[23] Yahaya, R. I., Arifin, N. M., Pop, I., Ali, F. M., & Isa, S. S. P. M. (2022). Dual solutions for MHD hybrid nanofluid stagnation point flow due to a radially shrinking disk with convective boundary condition. International Journal of Numerical Methods for Heat & Fluid Flow, (ahead-of-print).

[24] Mehta, R., Kumar, R., Rathore, H., & Singh, J. (2022). Joule heating effect on radiating MHD mixed convection stagnation point flow along vertical stretching sheet embedded in a permeable medium and heat generation/absorption. Heat Transfer, 51(8), 7369-7386.

[25] B J, A., & B I, O. (2022). Stagnation-point flow of a Walters' B fluid towards a vertical stretching surface embedded in a porous medium with elastic-deformation and chemical reaction. Journal of Heat and Mass Transfer Research, 9(1), 27-38.

- [26] Mabood, F., Abbasi, A., Farooq, W., Hussain, Z., & Badruddin, I.A. (2022). Effect of non-linear radiation and chemical reaction on Oldroyd-B nanofluid near oblique stagnation point flow. *Chinese Journal of Physics*, 77, 1197-1208.
- [27] Bai, Y., Wang, X., & Zhang, Y. (2022). Unsteady oblique stagnation-point flow and heat transfer of fractional Maxwell fluid with convective derivative under modified pressure field. *Computers & Mathematics with Applications*, 123, 13-25.
- [28] Sahu, S. K., Rout, S., Shaw, S., Dash, N., Thatoi, D. N., & Nayak, M. K. (2022). Hydrothermal stagnation point flow of Carreau nanofluid over a moving thin needle with non-linear Navier's slip and cubic autocatalytic chemical reactions in Darcy-Forchheimer medium. *Journal of the Indian Chemical Society*, 99(11), 100741.
- [29] Ramana, R. M., Raju, K. V., & Kumar, J. G. (2022). Multiple slips and heat source effects on MHD stagnation point flow of casson fluid over a stretching sheet in the presence of chemical reaction. *Materials Today: Proceedings*, 49, 2306-2315.
- [30] H.S. Takhar, A.J. Chamkha, G. Nath, (2001). Unsteady three dimensional MHD boundary layer flow due to the impulsive motion of a stretching surface, *Acta Mech.* 146 59-71.
- [31] J. Vlegaar, (1977). Laminar boundary layer behaviour on continuous accelerating surface, *Chem. Eng. Sci.* 32, 1517-1525.
- [32] L.J. Crane,(1970). Flow past a stretching plate, *J. Appl. Math. Phys. (ZAMP)* 21 645-647.

- [33] M. Ashraf and M. A. Kamal,(2011). "Numerical simulation of MHD stagnation point flow towards a heated axisymmetric surface," *The anziam journal*, 52, 301- 308.
- [34] M. K. A. Mohamed, M. Z. Salleh, R. Nazar, and A. Ishak, (2013). "Numerical investigation of stagnation point flow over a stretching sheet with convective boundary conditions," *Boundary value problem.*, 2013, 1- 4.
- [35] M. K. A. Mohamed, M. Z. Salleh, R. Nazar, and A. Ishak,(2013). "Numerical investigation of stagnation point flow over a stretching sheet with convective boundary conditions," *Boundary value problems*. 2013, 1- 4.
- [36] W. Ibrahim, (2015). "Nonlinear radiative heat transfer in magnetohydrodynamic (MHD) stagnation point flow of nanofluid past a stretching sheet with convective boundary condition," *Propulsion and power research*, 4, 230-239.
- [37] B. C. Sakiadis,(1961). "Boundary-layer behavior on continuous solid surfaces: I. boundary-layer equations for two-dimensional and axisymmetric flow," *AICHE Journal*, 7, 26-28.
- [38] H. Blasius, (1907). *Grenzschichten in Flüssigkeiten mit kleiner Reibung*. Druck von BG Teubner.
- [39] M. Sheikholeslami, D. D. Ganji, M. Y. Javed, and R. Ellahi, (2015). "Effect of thermal radiation on magnetohydrodynamics nanofluid flow and heat transfer by means of two phase model," *Journal of Magnetism and Magnetic Materials*, 374, 36-43.

- [40] Khan, M. I., Shah, F., Khan, S. U., Ghaffari, A., & Chu, Y. M. (2022). Heat and mass transfer analysis for bioconvective flow of Eyring Powell nanofluid over a Riga surface with nonlinear thermal features. *Numerical Methods for Partial Differential Equations*, 38(4), 777-793.
- [41] Varun Kumar, R. S., Gunderi Dhananjaya, P., Naveen Kumar, R., Punith Gowda, R. J., & Prasannakumara, B. C. (2022). Modeling and theoretical investigation on Casson nanofluid flow over a curved stretching surface with the influence of magnetic field and chemical reaction. *International Journal for Computational Methods in Engineering Science and Mechanics*, 23(1), 12-19.
- [42] Tawade, J. V., Guled, C. N., Noeiaghdam, S., Fernandez-Gamiz, U., Govindan, V., & Balamuralitharan, S. (2022). Effects of thermophoresis and Brownian motion for thermal and chemically reacting Casson nanofluid flow over a linearly stretching sheet. *Results in Engineering*, 15, 100448.
- [43] Singh, J. (2022). Shooting method for solving two-point boundary value problems in ODEs numerically. arXiv preprint arXiv 2208.13221.
- [44] S. Choi, D. Singer, H. Wang, (1995). "Developments and applications of nonNewtonian flows," *ASME FED*, 66, 99-105.
- [45] R. Pal,(2014). "A novel method to determine the thermal conductivity of interfacial layers surrounding the nanoparticles of a nanofluid," *Nanomaterials*, 4, 844- 855.

[46] M. H. Bahmani, G. Sheikhzadeh, M. Zarringhalam, O. A. Akbari, A. A. Alrashed, G. A. S. Shabani, and M. Goodarzi (2018). "Investigation of turbulent heat transfer and nanofluid flow in a double pipe heat exchanger" *Advanced Powder Technology*, 29, 273-282.

[47] M. Bahiraei, M. Jamshidmofid, and M. Goodarzi,(2019). "Efficacy of a hybrid nanofluid in a new microchannel heat sink equipped with both secondary channels and ribs," *Journal of Molecular Liquids*, 273, 88-98.

[48] S. U. S. Choi, (1998). "Nanofluid technology: current status and future research," Argonne national lab. (ANL), Argonne, IL (United States), Tech. Rep.

[49] J. Buongiorno, (2006). "Convective transport in nanofluids," *Journal of heat transfer*, 128, 240-250.

[50] F. Shahzad, M. Sagheer, and S. Hussain,(2019). "MHD tangent hyperbolic nanofluid with chemical reaction, viscous dissipation and Joule heating effects," *AIP advances*, 9, 025007.

[51] R. K. Tiwari and M. K. Das,(2007). "Heat transfer augmentation in a two-sided lid-driven differentially heated square cavity utilizing nanofluids," *International Journal of Heat and Mass Transfer*, 50, 9-10.

[52] M. H. Matin, M. Dehsara, and A. Abbassi, (2012). "Mixed convection MHD flow of nanofluid over a nonlinear stretching sheet with effects of viscous dissipation and variable magnetic field," *Mechanics*, 18, 415-423.

- [53] A. Z. Ghadi, M. J. Noroozi, and M. H. Esfe,(2013). "Nanofluid implementation for heat transfer augmentation of magneto hydrodynamic flows in a lid-driven cavity using experimental-based correlations," *International Journal of Applied Electromagnetics and Mechanics*, 42, 589-602.
- [54] N. Sandeep, C. Sulochana, C. Raju, M. J. Babu, and V. Sugunamma, "Unsteady boundary layer flow of thermophoretic MHD nanofluid past a stretching sheet with space and time dependent internal heat source/sink," *Applied Mathematics*, 10, 312-327, 2015.
- [55] I. Ahmad, M. Sajid, W. Awan, M. Rafique, W. Aziz, M. Ahmed, A. Abbasi, and M. Taj, ( 2014). "MHD flow of a viscous fluid over an exponentially stretching sheet in a porous medium," *Journal of Applied Mathematics*, vol. 2014.
- [56] Z. Shah, E. Bonyah, S. Islam, W. Khan, and M. Ishaq, (2018). "Radiative MHD thin film flow of Williamson fluid over an unsteady permeable stretching sheet," *Heliyon*, 10, p. 00825.
- [57] F. Mabood, S. Shateyi, M. Rashidi, E. Momoniat, and N. Freidoonimehr,(2016). "MHD stagnation point flow heat and mass transfer of nanofluids in porous medium with radiation, viscous dissipation and chemical reaction," *Advanced Powder Technology*, 27, 742-749.
- [58] Jang, J., & Lee, S. S. (2000). Theoretical and experimental study of MHD (magnetohydrodynamic) micropump. *Sensors and Actuators A: Physical*, 80(1), 84-89.
- [59] . K. B. Pavlov,(1974). Magnctohydrodynamic Bow of ao incompressible viscous fluid caused by deformation of a plane 8UhX Ma@nmya Gidmdhamiku (tUS.RJ 4,146147.

- [60] A.(1979). Chakrabarti and A. s. Gupta, Hydromagnetic flow and heat transfer over a stretching sheet. Q. OPPL kth. 37.73-78.
- [61] E. Magyari and A. J. Chamkha, (2010) .Combined effect of heat generation or absorption and first order chemical reaction on micropolar fluid flows over a uniformly stretched permeable surface," International Journal of Thermal Sciences, 49, 1821-1828.
- [62] A. J. Chamkha and A. Rashad, (2014). Unsteady heat and mass transfer by MHD mixed convection flow from a rotating vertical cone with chemical reaction and soot and dufour effects," The Canadian Journal of Chemical Engineering, vol. 92, 758-767.
- [63] K. Das, (2011).Effect of chemical reaction and thermal radiation on heat and mass transfer flow of MHD micropolar fluid in a rotating frame of reference," International Journal of Heat and Mass Transfer, vol. 54, no. 15-16, 3505-3513.
- [64] Anantha Kumar, K., Sandeep, N., Sugunamma, V., & Animasaun, I. L. (2020). Effect of irregular heat source/sink on the radiative thin film flow of MHD hybrid ferrofluid. Journal of Thermal Analysis and Calorimetry, 139(3), 2145-2153.
- [65] Khan, Z., Jawad, M., Bonyah, E., Khan, N., & Jan, R. (2022). Magnetohydrodynamic thin film flow through a porous stretching sheet with the impact of thermal radiation and viscous dissipation. 58, 452-460
- [66] Ismail, F., Qayyum, M., Ullah, I., Inayat Ali Shah, S., Mahtab Alam, M., & Aziz, A. (2022). Fractional analysis of thin-film flow in the presence of thermal conductivity and variable viscosity. Waves in Random and Complex Media, 1-19.

[67] T. Hayat, M. Awais, and M. Sajid,(2011). "Mass transfer effects on the unsteady flow of UCM fluid over a stretching sheet," International journal of modern physics, 25, 2863-2878.

[68] I. Animasaun, E. Adebile, and A. Fagbade,(2016). "Casson fluid flow with variable thermo-physical property along exponentially stretching sheet with suction and exponentially decaying internal heat generation using the homotopy analysis method," Journal of the nigerian mathematical society, 35, 1-17.

[69] M. Mustafa,(2017). "MHD nanofluid flow over a rotating disk with partial slip effects: buongiorno model," International journal of heat and mass transfer, 108, 1910-1916.

[70] M. Mustafa and J. A. Khan, (2015). "Model for flow of Casson nanofluid past a nonlinearly stretching sheet considering magnetic field effects," AIP advances, 5, 077148.

[71] S. Pramanik,(2014). "Casson fluid flow and heat transfer past an exponentially porous stretching surface in presence of thermal radiation," Ain shams engineering journal, 5, 205-212.

[72] Maleque, K.(2013). Effects of exothermic/endothermic chemical reactions with Arrhenius activation energy on MHD free convection and mass transfer flow in presence of thermal radiation. J. Thermodyn. 2013, 692-516.

[73] Merkin, J.; Mahmood, T. (1998). Convective flows on reactive surfaces in porous media. Transp. Porous Media 47, 279-293.

[74] E. M. Abo-Eldahab and M. E. Elbarbary (2001). "Hall current effect on magneto hydrodynamic free convection flow past a semiinfinite vertical plate with mass transfer". *International Journal of Engineering Science*, 60,1641-1652.

[75] E. M. Abo-Eldahab and M. A. Aziz (2004). Hall current and Ohmic heating effects on mixed convection boundary layer flow of a micropolar fluid from a rotating cone with power-law fluid at a stretching surface. *International Communications in Heat and Mass Transfer*, 31,751 -762.

[76] A. M. Salem and M. A. El-Aziz (2008). Effects of Hall current and chemical reaction on hydromagnetic flow of a stretching vertical surface with internal heat generation/absorption. *Applied Mathematical Modelling*, 55,1236-1254.

[77] Santhi, G., Rao, C. N. B., & Murthy, A. S. N. (2011). Dual solutions in mixed convection with variable physical properties. *Theoretical and Applied Mechanics Letters*, 1(2), 022-006.

[78] Subhashini, S. V., & Sumathi, R. (2014). Dual solutions of a mixed convection flow of nanofluids over a moving vertical plate. *International Journal of Heat and Mass Transfer*, 71, 117-124.

[79] M. M. Bhatti and M. M. Rashidi, (2016). "Study of heat and mass transfer with joule heating on magnetohydrodynamic(mhd) peristaltic blood flow under the influence of hall effect," *Propulsion and Power Research*.47, 675-682.

- [80] S. P. A. Devi and B. Ganga,(2009). “Effects of viscous and joules dissipation on mhd flow, heat and mass transfer past a stretching porous surface embedded in a porous medium,” *Non-linear Analysis: Modelling and Control*, 14, 303-314.
- [81] J.R. Lloyd, E.M. Sparrow,(1970). Combined forced and free-convection flow on vertical surfaces, *Int. J. Heat Mass Transfer* 13, 434-438.
- [82] Muhammad, R., Khan, M. I., Jameel, M., & Khan, N. B. (2020). Fully developed Darcy-Forchheimer mixed convective flow over a curved surface with activation energy and entropy generation. *Computer Methods and Programs in Biomedicine*, 188, 105-298.
- [83] Mukhopadhyay, S. (2011). Effects of slip on unsteady mixed convective flow and heat transfer past a porous stretching surface. *Nucl. Eng. Des.* 241(8), 2660-2665.
- [84] Hayat, T., Shehzad, S. A., Alsaedi, A. & Alhothuali, S. M. Mixed convection stagnation point flow of casson fluid with convective boundary conditions. *Chin. Phys. Lett.* 29(11), 114-704.
- [85] Turkyilmazoglu, M.(2013). The analytical solution of mixed convection heat transfer and fluid flow of a MHD viscoelastic fluid over a permeable stretching surface. *Int. J. Mech. Sci.* 77, 263-268.
- [86] C. S. K. Raju, N. Sandeep, V. Sugunamma, J. Jayachandra Babu, and J. V. Ramana Reddy, (2016).“Heat and mass transfer in magneto hydrodynamic casson fluid over an exponentially permeable stretching surface,” *Engineering Science and Technology, an International Journal*, vol. 19, 45-52.

- [87] M. A. Mansour, M. A. El-Hakiem, and S. M. El Kabeir,(2000) .“Heat and mass transfer in magnetohydrodynamic flow of micropolar fluid on a circular cylinder with uniform heat and mass flux,” *Journal of Magnetism and Magnetic Materials*, vol. 220, 259-270.
- [88] L. Howarth,(1938). “On the solution of the laminar boundary layer equations,” *Proceedings of the Royal Society of London. Series A, Mathematical and Physical Sciences*, 547-579.
- [89] [95] M. Sheikholeslami, D. D. Ganji, M. Y. Javed, and R. Ellahi, (2015).“Effect of thermal radiation on magnetohydrodynamics nanofluid flow and heat transfer by means of two phase model,” *Journal of Magnetism and Magnetic Materials*, vol. 374, 36-43.
- [90] M. Chutia and P. Deka,(2015). “Numerical study on MHD mixed convection flow in a vertical insulated square duct with strong transverse magnetic field,” *Journal of Applied Fluid Mechanics*.
- [91] N. A. Kelson and A. Desseaux,(2001). “Effect of surface conditions on flow of a micropolar fluid driven by a porous stretching sheet,” *International Journal of Engineering Science*, vol. 39, no. 16, 1881-1897.
- [92] Lee, C., & Jiang, X. (2019). Flow structures in transitional and turbulent boundary layers. *Physics of Fluids*, 31(11), 111301.
- [93] Guo, J., Li, Y., Cohen, J. B., Li, J., Chen, D., Xu, H., ... & Zhai, P. (2019). Shift in the temporal trend of boundary layer height in China using long-term (1979–2016) radiosonde data.

Geophysical Research Letters, 46(11), 6080-6089.

[94] R. W. Fox, "A. McDonald, and P. Pitchard", Introduction to Fluid Mechanics, 2006.

[95] Y. A. Cengel, "Fluid mechanics". Tata McGraw-Hill Education, 2013.

[96] R.k. Bansal, "A Textbook of Fluid Mechanics and Hydraulic Machines". Laxmi publications, 2010.

[97] R. Bansal, "A textbook of fluid mechanics". Firewall Media, 2005.

[98] J. N. Reddy and D. K. Gartling, "The Finite Element Method in Heat Transfer and Fluid Dynamics", CRC press, 2010.

[99] J. Ahmed and M. S. Rahman, "Handbook of Food Process Design", John Wiley and Sons, 2012.

[100] Cengel, Yunus A and Cimbala, John M, "Momentum Analysis of Flow Systems," Fluid Mechanics Fundamentals and Applications, Mc Graw Hill Higher Education, pp. 227-268, 2006.

[101] S. Molokov, R. Moreau, and H. K. Moffatt, "Magnetohydrodynamics historical evolution and trends", Springer, fourth edition, 2007.

- [102] F. White and I. Corfield, "Viscous Fluid Flow, vol. 3 McGraw-Hill," New York, 2006.
- [103] M. Gad-el Hak, "Frontiers in Experimental Fluid Mechanics, vol. 46." Springer Science and Business Media, 2013.
- [104] Papanastasiou, Tasos and Georgiou, Georgios and Alexandrou, Andreas N, Viscous fluid flow. CRC press, 1999.
- [105] D. Cleland, "Moisture and humidity control in refrigerated facilities, Encyclopaedia of Agricultural, Food and Biological Engineering, ed. DR Heldman, Taylor, Francis, New York, ISBN: 0-8247-0938-1 (paper) 0-8247-0937-3 (electronic)," 2005.
- [106] Senapati, M., Swain., & Parida, S.K. (2020). Numerical analysis of three-dimensional MHD flow of Casson nanofluid past an exponentially stretching sheet. *Karbala International Journal of Modern Science*, 6, 93-102.